Ab initio calculations of hadronic and electromagnetic reactions in few-body systems

Thesis submitted for the degree of
Doctor of Philosophy

by

Sergio Deflorian

to
Dipartimento di Fisica
Universitá degli Studi di Trento

April 2016

Contents

Chapter 1

Introduction

This thesis is a work in the field of nuclear few-body physics. In particular, the focus is the study of different methods which may be used to investigate hadronic scattering and electromagnetic reactions taking place in small nuclei.

During the last century, a large number of experiments have been performed and an enormous amount of data has been collected concerning nuclear reactions and interaction. Scattering experiments are amongst the most used tools devoted to the study of interactions between particles in general, and in particular the nuclear one. One of the first examples is the famous experiment of Rutherford which led to the understanding of the structure of atoms. The study of the nuclear interaction in a theoretical framework is in this sense the complementary tool to scattering experiments, and the development of techniques and methods to study and test models for the nuclear interaction is an important part of the process.

A complete understanding of the principles which govern the interaction of the fundamental constituents of matter is of the greater importance and represents one of the major goals in physics. While Quantum ChromoDynamics is commonly acknowledged as the underlying theory of interaction of fundamental particles which build nuclei, nuclear structure and low-energy interactions are better described in terms of nucleonic (and mesonic) degrees of freedom. The fundamental issue in nuclear physics is the description of

the nuclear interaction in terms of this relevant degrees of freedom. Modern realistic nucleon-nucleon (NN) potentials are fitted on the NN bound state as well as on the wealth of two-nucleon scattering observables below pion threshold. In comparison, the also necessary 3N-force is much less settled.
The reason to build a nuclear theory from nucleonic degrees of freedom starts from the fact that QCD is non-perturbative at low energies. This makes it difficult to link low-energy nuclear observables such as binding energies to the fundamental theory of particle interaction. The link is represented by effective nuclear interactions which consider nucleons (and mesons) as their degrees of freedom. Lattice QCD calculations are going in the direction of constructing nuclear theory from the fundamental theory. On the other hand, semi-phenomenological interactions and potentials derived from effective field theories (see for example review articles [1, 2]) represent the tools which are most used in the practical calculations and interpretation of data from experiments.
The methods used to produce results using this kind of interactions are also important, for two main reasons. First, interactions need testing: this means that reliable methods and calculations may be used for the production of results which can be compared with experimental data in order to determine their accuracy. The development of methods which may be used in combination with different kind of interactions are of great interest. In this sense, *ab initio* methods represent the tool which can be used to this purpose, since they do not involve in principle any approximation and their results can be considered exact, having been obtained by solving the quantum mechanical problem expressed with the relevant degrees of freedom. Secondly, the extension of ab initio techniques to more complex problems, such as calculations involving a larger number of nucleons, is an important issue, both in the study of bound states and reactions (see for example review article [3]). The realm of few-body nuclear physics has in fact extended in the last years: the construction of an overlap between few-body and many-body techniques is one of the goals of nuclear theoretical physics. The region of applicability of both approaches has recently witnessed the development of different methods and the direct application to more complex problems of already existing

techniques. The importance of such methodologies, as mentioned, lies in the fact that the study is performed taking into account all the relevant degrees of freedom (these being the nucleons in the case of nuclear interaction) without introducing approximations, or using only controlled approximations. In this sense the results depend only on the type of interaction used.
In the past years a great progress has been made in the development of ab initio methods in the study of hadronic scattering, which started in a limited range of applicability, namely two- or three-nucleons problems; also, the increasing capability of computational facilities have strongly contributed in making this development possible.
Now such techniques may be applied to the study of problems involving even $A \sim 10$ nucleons concerning bound-state, hadronic scattering and electroweak reactions observables [3]. For $A = 4$ examples of this development are the Faddeev equations method, extended to four-body problems in the Faddeev-Yakubowski formulation, Alt-Grassberger-Sandhas technique and expansion in Hyperspherical Harmonics together with the Kohn variational principle (see for example [4]). Further examples for $A \geq 4$ are Green Function Monte Carlo calculations which have been used in solving problems up to $A = 12$ [5], or the No Core Shell Model technique [6, 7]. Another example is represented by the Lorentz Integral Transform method (see for example [8]), which maps continuum problems into bound-state-like ones.

Historically, one of the most useful techniques to get information about the nuclear interaction is represented by *photonuclear reactions* with real and virtual photons. The use of electromagnetic probes to investigate nuclear structure and reactions is an important device, because it tests the nuclear interaction exploiting the electromagnetic force, which is theoretically well known. For example, electrons have been used as electromagnetic probes in the study of nuclear structure since the middle of the last century [9].
The theoretical description of these processes requires the knowledge of bound and/or continuum wave functions of the system under investigation as well as the form of the electromagnetic operators: lighter nuclei are the perfect ground to make this kind of calculations. If the system under study is small

enough, an ab initio description is possible with different approaches.
Further interest in considering photonuclear reactions arises from their direct connection with astrophysics. Many nuclear reactions taking place in stars interior directly involve real photons, and their understanding and precise description is a major goal in nuclear astrophysics.
The Sun is by far the most well known star of the universe: the amount of data on solar emissions is extremely large. The mechanism through which stars in general and the Sun in particular burn Hydrogen and other elements to sustain their emissions and structure is deeply related to nuclear fusions, and the stars are in fact nuclear factories in which a large part of the elements heavier than Helium are produced.
In particular, nowadays the most accepted description of the Sun is represented by the standard solar model (SSM). In this description, nuclear fusion reactions like the synthesis of deuterium, Helium isotopes and heavier nuclei take place, through the mechanism of the *pp* chains and the CNO cycle (see for example [10, 11]). The energy production inside the Sun is mainly due to *pp* chains, which ultimately transform protons into alpha particles, through fusions involving weak interactions and photoemissions. In particular, the three-nucleon reaction

$$^2\mathrm{H} + \mathrm{p} \rightarrow {}^3\mathrm{He} + \gamma \tag{1.1}$$

is one of the reactions belonging to the *pp* chains involving photoemission, along with the synthesis of Beryllium and Boron nuclei

$$^3\mathrm{He} + {}^4\mathrm{He} \rightarrow {}^7\mathrm{Be} + \gamma \tag{1.2}$$

$$^7\mathrm{Be} + \mathrm{p} \rightarrow {}^8\mathrm{B} + \gamma \ . \tag{1.3}$$

All the previous reactions involve two nuclei which combine giving as a product a heavier nucleus and an emitted photon.

An important development in ab initio methods has been the calculation of continuum observables with bound-state methods, which constitutes an enormous calculational reduction. The already mentioned Lorentz Integral

Transform (LIT) method for calculations of reactions with electroweak probes is already in use since about 20 years. A more recent development is the calculation of hadronic scattering observables with bound-state methods [12]. The central effort of the present work is the testing of such methodologies in the framework of wave function expansion methods, and their use to study low-energy reactions for few-nucleon systems. A particular aim is to test whether the LIT method can be used to determine the low-energy photodisintegration cross section in presence of the Coulomb barrier with a possible future application for the reactions (1.2) and (1.3). This test is made for the ^{3}He case. A further aim is the application of the bound-state method for hadronic scattering presented in [12] to calculate phase shifts for 2+1 and 4+1 scattering.
Rather than performing these calculations with a realistic nuclear force, a simpler central NN interactions is used.

The structure of the thesis is the following.

Chapter 2 presents an introduction to electromagnetic nuclear reactions and their interest in astrophysics. In particular, the derivation of the cross section for the photodisintegration processes considered in this work is presented.

In **Chapter 3** hadron scattering is discussed. A description of the techniques used for N+1 scattering is given. The two methods used in the calculations are discussed in detail. Also a brief discussion of the LIT method is given. In the formulation used in this work, both methods for hadron scattering have been proposed by the Pisa group (see for example [12]-[19]). The first method involves a description of the scattering wave function which is correct also in the region of large separation between the projectile and the target, whereas the second method uses a formulation which makes it possible to describe

the scattering wave function in the interaction region using an expansion on square-integrable functions. Both methods are based on an expansion of the wave function on a complete basis.

In **Chapter 4** the basis systems used in the different calculations are defined: Hyperspherical Harmonics basis, Nonsymmetrized Hyperspherical Harmonics basis and Laguerre Polynomials basis.

Chapter 5 presents the results obtained with the different methods.

Chapter 6 presents a summary of the work and a brief discussion of the results.

In **Appendix A** a detailed presentation of the application of the second method presented in Chapter 3 to the study of the neutron-^{4}He scattering is given.

Chapter 2

Nuclear photoabsorption

As already mentioned in the introduction there are various reactions in the *pp* chains of stars which involve the electromagnetic interaction (see [10, 11]). Before coming to the theoretical description of the electromagnetic interaction with nuclei in the next subsection, first a brief summary is given concerning the basic idea how a rate for a specific reaction in a star is calculated.

In the stellar interior the rate of a reaction involving nuclei of species a and b

$$ {}^{A_a}_{Z_a}A + {}^{A_b}_{Z_b}B \rightarrow X + X' \tag{2.1} $$

depends on the densities of the reagents, on the cross section of the reaction and on the velocity of the reagents [11]. The relative velocity v is given by a Maxwell distribution, since the interacting nuclei usually reach thermal equilibrium on a time scale which is infinitesimal compared to the typical nuclear reactions time scales. The rate can be written as

$$ r_{ab} = \frac{n_a n_b}{1+\delta_{ab}} \langle \sigma v \rangle_{ab} \quad , \tag{2.2} $$

where the Kronecker delta prevents double counting when the reagent nuclei are indistinguishable, n_a and n_b denote their densities and $\langle \sigma v \rangle_{ab}$ corresponds to the integral

$$ \langle \sigma v \rangle_{ab} = \int_0^\infty \sigma(v) v \Phi(v) dv \quad , \tag{2.3} $$

that is the average of the cross section σ multiplied by the relative velocity v of nuclei a and b, $\Phi(v)$ being the distribution of velocities. In the case of the Sun the distribution of the velocities can be assumed to be a Maxwell-Boltzmann distribution (T, μ and k_B being respectively the temperature, the reduced mass of the reaction and the Boltzmann constant)

$$\Phi(v) = \left(\frac{\mu}{2\pi k_B T}\right)^{\frac{3}{2}} \exp\left(-\frac{\mu v^2}{2k_B T}\right) 4\pi v^2 \quad . \tag{2.4}$$

Since almost each of the fusion reactions of the *pp* chains involves charged particles, the Coulomb interaction must be taken into account. This effect is considered via the tunneling penetration probability of the Coulomb barrier (as calculated by George Gamow in 1928)

$$P_{tunnel}(E) = \exp\left(-\frac{\pi\alpha Z_a Z_b \sqrt{2\mu c^2}}{\sqrt{E}}\right) \quad , \tag{2.5}$$

where α is the fine structure constant and $E = \frac{1}{2}\mu v^2$ is the relative kinetic energy of the particles. While the tunneling probability rapidly increases with increasing v, the Maxwell-Boltzmann distribution shows an opposite behaviour. The combination of this two effects gives a narrow window of energies in which the reaction rate is important, called *Gamow peak*.
However, in astrophysics it is often useful to remove the rapid dependency of the rate upon the energy due to the Coulomb barrier, introducing the so called *S-factor* $S(E)$ defined by

$$\sigma(E) = \frac{S(E)}{E} P_{tunnel}(E) \quad . \tag{2.6}$$

The S-factor varies slowly with energy: this makes the extrapolation of its value from available data to the usually low energy regions of the Gamow peaks more reliable.
Astrophysical data are usually related directly to the S-factor, which knowledge corresponds to the knowledge of the scattering cross section at low energies: as mentioned, the Gamow peak usually lies in the low-energy re-

gion well below ∼80 keV, while data for the S-factor are taken at energies typically above 100 keV [11].

One of the reactions considered in this work is the synthesis of ^{3}He of Eq. (1.1), namely radiative capture of protons on deuterium. Deuterium is produced during the first step of the *pp* chain:

$$\mathrm{p} + \mathrm{p} \rightarrow {}^2\mathrm{H} + e^+ + \nu_e \quad , \tag{2.7}$$

while ^{3}He production is the second. Since this reaction is considered in the present work using a central potential model, it is important to point out that a much more refined calculation with realistic nuclear forces has already been carried out by Marcucci et al. [20], which is in very good agreement with experimental data [11]. The precise knowledge of the rate of this reaction (and hence of its cross section) is not determining in the understanding of solar structure and energy production, because in the case of the Sun this reaction is much faster than the deuterium production of Eq. (2.7), which is induced by the weak interaction. This means that all deuterium produced is almost instantly converted in ^{3}He, and uncertainties in the rate for this production play a minor role; however, it plays an important role in protostellar evolution. In the latter case, when the collapse of the gas rise the temperature enough to begin ^{3}He production (about 10^6 K), this increases the energy production and slows down the collapse. Reliable description of the cross section for ^{3}He production in the energy region of a few keV is very important for the understanding of protostellar evolution.
Another point of interest is represented by Big Bang nucleosynthesis. When the early universe cooled to a temperature of $\sim$ 100 keV, nucleosynthesis took place, and uncertainties in the *pd* reactions (in the energy region of 25-120 keV) propagate in uncertainties in the abundances of deuterium, ^{3}He and ^{7}Li ([10, 11]).

The study of nucleon capture reactions

$$^{A-1}\mathrm{X}' + \mathrm{N} \rightarrow {}^{A}\mathrm{X} + \gamma \tag{2.8}$$

may be approached studying the inverse reaction, namely photodisintegration processes:

$$^{A}\mathrm{X} + \gamma \rightarrow {}^{A-1}\mathrm{X}' + \mathrm{N} \quad . \tag{2.9}$$

The cross sections of the two processes (respectively $\sigma_{nuc.cap.}$ and $\sigma_{ph.dis.}$) are in fact related by a simple relation connected to the different phase spaces [21]:

$$\sigma_{nuc.cap.} = \frac{q_\gamma^2}{q_N^2} \frac{2J_A + 1}{2J_{A-1} + 1} \sigma_{ph.dis.} \quad , \tag{2.10}$$

where q_γ and q_N are the momenta of the photon and the nucleon respectively, and J_A and J_{A-1} are the total angular momenta of the two nuclei involved. Knowledge of one reaction directly leads to knowledge of the other, so the study of nucleosynthesis processes may be performed through calculations on photodisintegrations. Such kind of processes have been studied in this work.

2.1 Electromagnetic reactions

The photodisintegration cross-section (at low energies) is dominated by the contribution of the electric dipole; in fact, the unretarded dipole approximation may be used. If no resonance are present, effects due to higher electric multipoles, magnetic multipoles and retardation may be neglected (see [22]), but in order to have a very accurate result it is necessary to check the importance of other multipoles, in particular the M1 contribution.
A brief overview of the multipole expansion and its connection with the study of photoabsorption reactions is given in the following.

The interaction Hamiltonian for electromagnetic interaction has the form

$$H_{em} = \int d^3x j_\mu(\mathbf{x}) A^\mu(\mathbf{x}) \quad , \tag{2.11}$$

which is the one-photon-exchange term of the electromagnetic interaction. The symbol $j_\mu(\mathbf{x})$ denotes the current, which satisfies the continuity equation

$$\partial^\mu j_\mu(\mathbf{x}) = 0 \Rightarrow \boldsymbol{\nabla} \cdot \mathbf{j}(\mathbf{x}) = -i[H, \rho(\mathbf{x})] \tag{2.12}$$

with

$$\rho(\mathbf{x}) = e \sum_i \frac{1 + \tau_i^z}{2} \delta(\mathbf{x} - \mathbf{r}_i) \tag{2.13}$$

representing the charge density operator. In the former definition, the sum on i goes over all particles and τ_i^z is the third component of the isospin; e is the fundamental charge (nucleon form factors are neglected in Eq. (2.13), since we consider only real photons).
In momentum space, the Fourier transforms of the current operator $\tilde{\mathbf{j}}(\mathbf{q})$ and of the charge density $\tilde{\rho}(\mathbf{q})$ may be defined as

$$\tilde{\rho}(\mathbf{q}) = \int d^3x \ \rho(\mathbf{x}) e^{i\mathbf{q}\cdot\mathbf{x}} \tag{2.14}$$

$$\tilde{\mathbf{j}}(\mathbf{q}) = \int d^3x \ \mathbf{j}(\mathbf{x}) e^{i\mathbf{q}\cdot\mathbf{x}} \quad . \tag{2.15}$$

The continuity equation expressed in momentum space becomes

$$\mathbf{q} \cdot \tilde{\mathbf{j}}(\mathbf{q}) = w\tilde{\rho}(\mathbf{q}) \quad , \tag{2.16}$$

where $\mathbf{q}$ and ω are respectively the photon momentum and energy.
The operator $\tilde{\mathbf{j}}(\mathbf{q})$ may be expanded (see for example [23]) in terms of the vector spherical harmonics

$$Y^\mu_{Jl1}(\hat{q}) = \sum_{m\xi} \langle l1J | m\xi\mu \rangle \, Y_l^m(\hat{q}) \mathbf{e}_\xi \quad , \tag{2.17}$$

where $Y_l^m(\hat{q})$ are the usual spherical harmonics and $\mathbf{e}_\mu$ is the set of vectors defined with respect to the spherical basis

$$\begin{aligned} \mathbf{e}_0 &= \mathbf{e}_z & (2.18)\\ \mathbf{e}_{\pm 1} &= \mp\frac{1}{\sqrt{2}}(\mathbf{e}_x \pm i\mathbf{e}_y) \quad . & (2.19) \end{aligned}$$

The expansion of the current reads

$$\tilde{\mathbf{j}}(\mathbf{q}) = 4\pi \sum_{lJ\mu} J^\mu_{Jl}(q)\mathbf{Y}^{\mu *}_{Jl1}(\hat{q}) \tag{2.20}$$

where

$$J^\mu_{Jl}(q) = \frac{1}{4\pi}\int d\hat{q}'\ \tilde{\mathbf{j}}(\mathbf{q}')\cdot\mathbf{Y}^\mu_{Jl1}(\hat{q}') \quad . \tag{2.21}$$

Using the properties of the vector spherical harmonics, the following expression for the current can be found:

$$\tilde{\mathbf{j}}(\mathbf{q}) = \sum_{J\mu}\left(\tilde{\mathbf{j}}^{el}_{J\mu}(\mathbf{q}) + \tilde{\mathbf{j}}^{mag}_{J\mu}(\mathbf{q})\right) \tag{2.22}$$

where

$$\begin{aligned} \tilde{\mathbf{j}}^{el}_{J\mu}(\mathbf{q}) &= 4\pi\left(J^\mu_{JJ-1}\mathbf{Y}^{\mu *}_{JJ-11}(\hat{q}) + J^\mu_{JJ+1}\mathbf{Y}^{\mu *}_{JJ+11}(\hat{q})\right) & (2.23)\\ \tilde{\mathbf{j}}^{mag}_{J\mu}(\mathbf{q}) &= 4\pi J^\mu_{JJ}\mathbf{Y}^{\mu *}_{JJ1}(\hat{q}) \quad . & (2.24) \end{aligned}$$

The former expression can be further manipulated to obtain

$$\begin{aligned} \tilde{\mathbf{j}}(\mathbf{q}) &= \sum_{J\mu}\sqrt{4\pi}\sqrt{2J+1}\left[L^{el}_{J\mu}(q)\mathbf{e}_0 + \mu\left\langle J1J|0\mu\mu\right\rangle T^{el}_{J\mu}(q)\mathbf{e}^*_\mu\right]\\ &\quad + \sum_{J\mu}\sqrt{4\pi}\sqrt{2J+1}\left\langle J1J|0\mu\mu\right\rangle T^{mag}_{J\mu}(q)\mathbf{e}^*_\mu \quad . \end{aligned} \tag{2.25}$$

where $L^{el}_{J\mu}(q)$, $T^{el}_{J\mu}(q)$ and $T^{mag}_{J\mu}(q)$ are respectively the longitudinal electric multipole, the transverse electric multipole and the magnetic multipole, de-

fined by

$$L^{el}_{J\mu}(q) = \frac{1}{4\pi}\int d\hat{q}' \left(\frac{1}{q'}\mathbf{q}'\cdot\tilde{\mathbf{j}}(\mathbf{q})\right) Y^{\mu}_{J}(\hat{q}') \quad (2.26)$$

$$T^{el}_{J\mu}(q) = \frac{i}{4\pi}\int d\hat{q}' \left(\frac{1}{q'}\mathbf{q}'\times\mathbf{Y}^{\mu}_{JJ1}(\hat{q}')\right)\cdot\tilde{\mathbf{j}}(\mathbf{q}) \quad (2.27)$$

$$T^{mag}_{J\mu}(q) = \frac{1}{4\pi}\int d\hat{q}'\ \tilde{\mathbf{j}}(\mathbf{q})\cdot\mathbf{Y}^{\mu}_{JJ1}(\hat{q}') = J^{\mu}_{JJ}(q) \quad . \quad (2.28)$$

It can be shown using Siegert's theorem that for low momentum $\mathbf{q}$ the only important contribution is given by the electric dipole, while all other contributions are negligible with respect to it:

$$\tilde{\mathbf{j}}(\mathbf{q}) \xrightarrow{qr\ll 1} \sum_{\mu}\sqrt{4\pi}\sqrt{3}\left[\mu\,\langle 111|0\mu\mu\rangle\left(-2\omega i\int d^3x\rho(\mathbf{x})\frac{r}{3}Y^{\mu}_{1}(\hat{x})\right)\mathbf{e}^{*}_{\mu}\right] \quad . \quad (2.29)$$

The electric dipole is defined in fact by

$$\mathbf{D} = \int d^3x\rho(\mathbf{x})\mathbf{x} \quad , \quad (2.30)$$

which corresponds to the integral in Eq. (2.29).
A photoabsorption reaction involves a photon (a real photon, in contrast with what happens in the case of electron scattering, where a virtual photon is exchanged) being absorbed by a nucleus. Being the photon real, only the transverse part of the nuclear current is involved.
The total cross section for photodisintegration can be expressed in general as following (see for example [24]):

$$\sigma(\omega) = \omega R(\omega)\frac{4\pi^2\alpha}{2J_0+1} \quad . \quad (2.31)$$

Here $\alpha = \frac{e^2}{\hbar c}$ is the fine structure constant, J_0 is the total angular momentum of the nucleus ω is the photon energy and $R(\omega)$ is the response function of

the reaction

$$R(\omega) = \sum_{\mu=\pm1} \frac{1}{2J_i+1} \sum_{M_i} \sum_{M_f} \int df \left| \langle \Psi_f | \hat{\mathbf{J}}(\mathbf{r}) \cdot \boldsymbol{\epsilon}_\mu e^{i\mathbf{q}\cdot\mathbf{r}} | \Psi_0 \rangle \right|^2 \delta(\omega - E_f + E_0 - \frac{\omega^2}{2M_{tot}}) \quad . \tag{2.32}$$

In the latter equation, $\mathbf{q}$ is the photon momentum, Ψ_0 is the nucleus bound state with energy E_0, Ψ_f is the final scattering state with energy E_f and the integral runs over the final states indicated by the subscript f; the final and initial states have total momentum J_f and J_i respectively, with projections M_f and M_i. The small contribution $\frac{\omega^2}{2M_{tot}}$ that appears in Eq. (2.32) is due to the recoil of the nucleus that appear inside the delta function can be neglected, being much smaller than all other energies involved:

$$R(\omega) = \sum_{\mu=\pm1} \frac{1}{2J_i+1} \sum_{M_i} \sum_{M_f} \int df \, |T_{f0,\mu} \boldsymbol{\epsilon}_\mu|^2 \, \delta(\omega - E_f + E_0) \quad . \tag{2.33}$$

The expression

$$T_{f0,\mu} = \langle \Psi_f | \hat{\mathbf{J}}(\mathbf{r}) e^{i\mathbf{q}\cdot\mathbf{r}} | \Psi_0 \rangle \tag{2.34}$$

denotes the transition matrix element between initial and final states, and $\hat{\mathbf{J}}(\mathbf{r})$ is the nuclear current operator. The symbol $\boldsymbol{\epsilon}_\mu$ denotes the polarization of the photon with momentum $\mathbf{q}$. Being the photon real, only transverse polarization is possible ($\mu = \pm 1$).

Using the previous expressions for the current, the total cross section in unretarded dipole approximation can be expressed as

$$\sigma(\omega) = R_{\mathbf{D}}(\omega) \omega 4\pi^2 \frac{e^2}{\hbar c} \quad , \tag{2.35}$$

with

$$R_{\mathbf{D}}(\omega) = \int df \, |\langle \Psi_f | \mathbf{D} | \Psi_0 \rangle|^2 \, \delta(\omega - E_f + E_0) \quad . \tag{2.36}$$

The unretarded dipole approximation is rather good even at higher energies, and quite precise for $\omega < 40$ MeV (see for example [22]). In the present work the energies considered for the photon are well below 20 MeV, and then all

calculations have been performed within this framework.

Chapter 3

Hadron scattering

In this work two main methods have been used to perform the calculation of scattering parameters like phase-shifts and scattering wave functions. Both have been presented by the group of Pisa in recent works (see for example [13]-[18]). The methods used to tackle the problem of nuclear scattering are based on the Kohn variational principle [25] for scattering.
In the framework of an Hyperspherical Harmonics basis expansion, the method has been proposed by Zakharyev et al. (see [26] or later work by Permyakov et al. [27]) already in the '60s, and has been further used and improved in the years. The present work follows the outline presented in various articles by the Pisa group. In particular, two different ways of application of the Kohn variational principle are considered. The first method is a direct application of such principle in the study of the scattering of a nucleon off a nucleus ([13]-[18]). The second technique makes use of integral relations derived from the Kohn variational principle in order to derive the quantities of interest ([19, 12]). The methods are described in sections 3.2 and 3.3, whereas in section 3.1 a brief review of the theory of hadronic scattering is given.

3.1 S-matrix parameters

The study of hadronic scattering reactions and the investigation of a nuclear interaction through scattering is a problem which can be formulated in a con-

venient way using the concept of *phase shifts* and *mixing parameters*, which parametrize the S-matrix and can be determined from scattering observables. The formalism of this concept is based on the well known decomposition into partial waves. A brief outline of the method is given here (for a more complete description, see for example [28]).

In the case of elastic scattering of a projectile off a target, for large values of the coordinate r corresponding to their relative distance, the interaction between the projectile itself and the target is zero and the Schrödinger equation takes its asymptotic form

$$(H_{as} - E)\Psi(r, \theta, \phi) = (T - E)\Psi(r, \theta, \phi) \quad , \tag{3.1}$$

with Ψ representing the scattering wave function, H_{as} the asymptotic Hamiltonian operator, E the energy of the projectile and

$$T = -\frac{\hbar^2}{2\mu}\nabla^2 \tag{3.2}$$

the kinetic energy operator (μ being the reduced mass). Here only the degrees of freedom relevant to scattering are considered, assuming the projectile and the target not to have internal structure.
By means of the separation

$$\Psi(r, \theta, \phi) = \sum_{l=0}^{\infty} \frac{u_l(r)}{r} Y_l^m(\theta, \phi) \tag{3.3}$$

of the wave function into a radial and an angular part (where $Y_l^m(\theta, \phi)$ is a spherical harmonic function), Eq. (3.1) reduces to its radial form

$$-\frac{\hbar^2}{2\mu}\left(\frac{\partial^2}{\partial r^2} + \frac{2}{r}\frac{\partial^2}{\partial r^2} - \frac{l(l+1)}{r^2}\right) u_l(r) = E u_l(r) \quad . \tag{3.4}$$

The solution of the equation is known to be represented by regular and irregular Bessel functions, respectively denoted as $F_l(qr)$ and $G_l(qr)$. The

function $G_l(qr)$ is irregular in the origin:

$$G_l(qr) \xrightarrow{r\to 0} \infty \quad . \tag{3.5}$$

This means that, if the potential is 0 everywhere, the radial wave function reduces to the regular Bessel function $F_l(qr)$. The presence of the potential reduces the applicability of Eq. (3.4) to the asymptotic region, so in general the radial wave function takes the form

$$u_l(r) \xrightarrow{r\to\infty} A(F_l(qr) + \tan\delta_l G_l(qr)) \quad , \tag{3.6}$$

where δ_l is the value of the phase shift for a given partial wave identified by its momentum l, and q is the relative momentum of the projectile, defined by

$$E = -\frac{\hbar^2 q^2}{2\mu} \quad . \tag{3.7}$$

The meaning of the phase shift becomes clear if we look at the asymptotic form of the Bessel functions:

$$F_l(qr) + \tan\delta_l G_l(qr) \sim \sin\left(qr - \frac{1}{2}l\pi + \delta_l\right) \quad . \tag{3.8}$$

The phase shift represents the change in phase of the wave function of the projectile caused by the presence of the potential. In this sense the knowledge of the phase shifts for any value of the angular momentum l corresponds to the knowledge of the potential itself.
Another useful observable is represented by the *scattering length* a, which is defined as

$$a = -\lim_{q\to 0}\frac{\tan\delta_0}{q} \quad ; \tag{3.9}$$

in the effective range expansion scheme, the scattering length is the observable which gives information on scattering at very low energy.
The general case of nuclear scattering is of course more complex. In the case of charged projectiles and targets, the Bessel functions have to be substituted by Coulomb functions. If projectiles and targets have a structure and

spin, they have to be taken into account. Also, when dealing with interaction which are non-central, the wave function takes a more general form which mixes states with equal total angular momentum j but have different values of the orbital angular momentum l. For the description of the wave function in this case not only the phase shifts, but also the mixing parameters (which are related to the mixing between different solutions with the same value of j) are needed.
In this work the main aim was to develop and consolidate tools for the calculation of scattering observables, and so the focus was not on the interaction used but on the methods themselves. Therefore, the potential chosen to perform the calculations is a central one, leading to substantial simplification in the formulation of the problem but without any loss of generality.

3.2 Solution with explicit continuum wave function

The first method (method I), as already mentioned, is a direct application of the Kohn variational principle to the determination of the scattering wave function. This method has been described extensively by Kievsky et al. (see [13]-[18]) in the study of few-body scattering reactions in nuclear physics.
To describe such a method, we first present it in the simple case of two-body scattering and then expand the formalism to include the general case.
In general, considering the scattering wave function Ψ of a particular reaction, we can decompose it in an asymptotic and a core part:

$$\Psi = \Psi_{as} + \Psi_{core} \quad . \tag{3.10}$$

The asymptotic part Ψ_{as} is defined as the function which solves the Schrödinger equation

$$(T + V_{Coul})\Psi_{as} = E\Psi_{as} \tag{3.11}$$

between the fragments, without strong interaction (T here represents the kinetic energy operator and V_{Coul} is the Coulomb potential that may be

acting between the fragments; E is the energy of the projectile relative to the target). This means Ψ_{as} is a Bessel or Coulomb function, depending on the charge of the two particles (or of the two fragments in the general A-body case).
First we consider the two-body case: this makes it possible to describe the main method outline in a simpler way. As we will see, the generalization to more complex cases is straightforward.

3.2.1 The two-body case

Let us first consider the simple case of just two particles. The only relevant coordinate is the relative Jacobi coordinate

$$\boldsymbol{\eta} = \frac{1}{\sqrt{2}} (\mathbf{r}_1 - \mathbf{r}_2) \tag{3.12}$$

between the particles. The asymptotic wave function Ψ_{as} is defined by the following relation:

$$T\Psi_{as}(\boldsymbol{\eta}) + \alpha \frac{(e_1 e_2)\hbar c}{\sqrt{2}\eta} \Psi_{as}(\boldsymbol{\eta}) = E\Psi_{as}(\boldsymbol{\eta}) \quad , \tag{3.13}$$

where T is the kinetic energy operator

$$T = -\frac{\hbar^2}{2m}\nabla^2 = -\frac{\hbar^2}{2m}\left(\frac{d^2}{d\eta^2} + \frac{2}{\eta}\frac{d}{d\eta} - \frac{\hat{L}^2}{\eta^2}\right) \tag{3.14}$$

and E is the scattering energy

$$E = \frac{\hbar^2 q^2}{2m} \quad . \tag{3.15}$$

In the equation above q is the relative momentum between the particles, m denotes the nucleon mass, $\hat{L}$ is the orbital angular momentum operator, and e_1 and e_2 are the electric charges of the fragments. If one of the charges vanishes, the former is a Bessel equation, while in the other case we have a Coulomb equation.

We may write Ψ_{as} (with L, S, J, M indicating respectively the total orbital angular momentum, the total spin, the total angular momentum and its projection along the z axis) as

$$\Psi_{as}^{LSJM}(\boldsymbol{\eta}) = \Omega_{LSJM}^{R}(\eta) + F_{LSJM,L'S'}\Omega_{L'S'JM}^{I}(\eta) \quad , \tag{3.16}$$

where Ω_{LSJM}^{R} and Ω_{LSJM}^{I} are the regular and irregular parts of the asymptotic wave function, while $F_{LSJM,L'S'}$ represents the matrix containing the tangents of the phase-shifts and the mixing parameters for the channel in consideration.
In the case of central potentials, such as the Malfliet-Tjon [29] potential, the former definition becomes simpler due to the conservation of the orbital angular momentum L: in this case the quantum numbers L and S are conserved separately, and the matrix $F_{LSJM,L'S'}$ reduces to a single number for each value of J and M. For simplicity, we will consider implicitly the quantum numbers as simple parameters, and drop them in the formulas. It has to be noticed that the same simplification could have been introduced considering separately each element of the matrix $F_{LSJM,L'S'}$, so this reduction in notation does not affect the generality of the formalism. From now on, we consider then

$$\Psi_{as}(\boldsymbol{\eta}) = \Omega^{R}(\eta) + F\Omega^{I}(\eta) \quad . \tag{3.17}$$

The functions $\Omega^{\lambda}(\eta)$ ($\lambda = R, I$) are defined as follows:

$$\Omega^{\lambda}(\eta) = G_{L}^{\lambda}(q\eta)Y_{L}^{M}(\hat{\eta}) \tag{3.18}$$

where $Y_{L}^{M}(\hat{\eta})$ is a spherical harmonic and $G_{L}^{R}(q\eta)$ and $G_{L}^{I}(q\eta)$ are defined as follows (see for example [30]):

$$G_{L}^{R}(q\eta) = \mathcal{N}\mathcal{G}_{L}^{R}(q\eta) \tag{3.19}$$

$$G_{L}^{I}(q\eta) = \mathcal{N}g_{reg}(\eta)\mathcal{G}_{L}^{I}(q\eta) \quad . \tag{3.20}$$

The functions $\mathcal{G}_{L}^{R}$ and $\mathcal{G}_{L}^{I}$ are, as mentioned, the regular and irregular Bessel (Coulomb) functions respectively, and $\mathcal{N}$ is a normalization factor. The nor-

malization is chosen so that

$$\langle\Omega^R|H-E|\Omega^I\rangle - \langle\Omega^I|H-E|\Omega^R\rangle = 1 \quad , \tag{3.21}$$

where here H includes the strong interaction potential:

$$H = T + V_{Coul} + V_{strong} \quad . \tag{3.22}$$

It has to be noted that the operator $H-E$ is not hermitian in this case. In fact, the effect of multiplicative operators in Eq. (3.21) is the same when acting on the right or on the left, and we are left with

$$\langle\Omega^R|H-E|\Omega^I\rangle - \langle\Omega^I|H-E|\Omega^R\rangle = \langle\Omega^R|T|\Omega^I\rangle - \langle\Omega^I|T|\Omega^R\rangle \quad . \tag{3.23}$$

The kinetic energy operator is Hermitian only when acting on functions which go to zero fast enough, so that integrating twice by parts the Laplacian can be made to act on the left function. With the asymptotic functions, surface terms appear and this is not anymore possible. The reason for the normalization given above is the following: the integral involved in the above calculation is of the kind

$$\int dz z^2 \mathcal{G}_L^R(z)\frac{\partial^2}{\partial z}\mathcal{G}_L^I(z) - \int dz z^2 \mathcal{G}_L^I(z)\frac{\partial^2}{\partial z}\mathcal{G}_L^R(z) = 1 \quad ; \tag{3.24}$$

the above relation also fixes the normalization coefficient to

$$\mathcal{N} = \sqrt{q}\sqrt{\frac{2m}{\hbar^2}} \quad . \tag{3.25}$$

It has to be noticed that the irregular function $\mathcal{G}_L^I(\eta)$ has to be regularized, since it diverges for $\eta \to 0$. Anyway, since this problem arises in the core region, where the complete wave function is given by the sum of Ψ_{as} and Ψ_{core}, we may regularize $G_L(q\eta)$ multiplying it by a function $g_{reg}(\eta)$ which is

zero at the origin and is equal to 1 for η going to infinity, that is:

$$g_{reg}(\eta) \xrightarrow{\eta\to 0} 0 \tag{3.26}$$

$$g_{reg}(\eta) \xrightarrow{\eta\to\infty} 1 \ ; \tag{3.27}$$

the normalization $\mathcal{N}$ does not depend on the explicit form of g_{reg}.
The core part of the wave function may be expanded on a basis. Of course, in the 2-body case HH functions are not needed, but here we consider in general an expansion on a basis of N functions ϕ_i:

$$\Psi_{core}(\boldsymbol{\eta}) = \sum_{i=1}^{N} c_i \phi_i(\boldsymbol{\eta}) \quad . \tag{3.28}$$

The functions ϕ_i are square integrable functions, and are antisymmetric, so an expansion on such a basis will yield a function which is antisymmetric with respect to the exchange of any two particles. When the former expressions are taken into account, the wave function is given by

$$\Psi(\boldsymbol{\eta}) = \mathcal{N}\left(G_L^R(q\eta) + F g_{reg}(\eta) G_L^I(q\eta)\right) Y_L^M(\hat{\eta}) + \sum_{i=1}^{N} c_i \phi_i(\boldsymbol{\eta}) \quad . \tag{3.29}$$

Let's now consider the functional Z given by

$$Z[\Psi_t] = F - \langle \Psi_t | H - E | \Psi_t \rangle \quad . \tag{3.30}$$

Here Ψ_t is a trial wave function obtained varying the $N+1$ parameters F and c_i in Ψ. The Kohn variational principle states that the functional Z is stationary with respect to the variation of these parameters. The variations with respect to F and c_i gives the following $N+1$ equations:

$$\frac{\delta Z}{\delta F} = -\langle \Omega^I | H - E | \Psi_t \rangle = 0 \tag{3.31}$$

$$\frac{\delta Z}{\delta c_i} = -\langle \phi_i | H - E | \Psi_t \rangle = 0 \quad , \tag{3.32}$$

which explicitly read:

$$\langle\Omega^I|H-E|\Omega^R\rangle + F\,\langle\Omega^I|H-E|\Omega^I\rangle + \sum_j c_j\,\langle\Omega^I|H-E|\psi_j\rangle \;=\; 0 \quad (3.33)$$

$$\langle\psi_i|H-E|\Omega^R\rangle + F\,\langle\psi_i|H-E|\Omega^I\rangle + \sum_j c_j\,\langle\psi_i|H-E|\psi_j\rangle \;=\; 0 \quad (3.34)$$

To derive Eq. (3.33) it has been made use of the normalization relation of Eq. (3.21).
It has also to be noted that the former system of equations is consistent with the request that the scattering wave function solves the Schrödinger equation:

$$(H-E)\,|\Psi\rangle = 0 \quad . \quad (3.35)$$

The former is a linear system which can be solved by any means in principle. The method chosen (following [17]) is the following. First we define

$$D_j^\lambda = \langle\Omega^\lambda|H-E|\Psi_j\rangle \quad , \quad j=1,\ldots,N \quad , \quad \lambda,\lambda'=R,I \quad (3.36)$$

$$Q^{\lambda\lambda'} = \langle\Omega^\lambda|H-E|\Omega^{\lambda'}\rangle \quad , \quad \lambda=R,I \quad (3.37)$$

$$L_{ij} = \langle\Psi_i|H-E|\Psi_j\rangle \quad , \quad i,j=1,\ldots,N \quad , \quad (3.38)$$

so that the system to be solved reads

$$Q^{IR} + FQ^{II} + \sum_j c_j D_j^I \;=\; 0 \quad (3.39)$$

$$D_i^R + FD_i^I + \sum_j c_j L_{ij} \;=\; 0 \quad . \quad (3.40)$$

Then we define the coefficients c_j^λ as the coefficients satisfying

$$\sum_{j=1}^{N} L_{ij}c_j^\lambda = -D_i^\lambda \quad , \quad \lambda=R,I \quad , \quad i=1,\ldots,N \quad . \quad (3.41)$$

If the latter equations are fulfilled for both $\lambda = R$ and $\lambda = I$, it is easy to check that also Eq. (3.40) is satisfied, provided that

$$c_i = c_i^R + F c_i^I \quad , \quad i = 1, \ldots, N \quad . \tag{3.42}$$

The last condition leads, thanks to Eq. (3.39), to the following equation in the variable F:

$$Q^{IR} + \sum_{i=1}^{N} c_i^R D_i^I + F \left(Q^{II} + \sum_{i=1}^{N} c_i^I D_i^I \right) = 0 \quad . \tag{3.43}$$

Then,

$$F_{1st} = -\frac{B}{A} \tag{3.44}$$

is a first order estimate of the parameter $F = \tan\delta$, where

$$\begin{aligned} B &= Q^{IR} + \sum_{i=1}^{N} c_i^R D_i^I \\ A &= Q^{II} + \sum_{i=1}^{N} c_i^I D_i^I \quad . \end{aligned}$$

A second order estimate of F may be obtained substituting F_{1st} in the functional Z:

$$F_{2nd} = F_{1st} - \langle \Psi_{1st} | H - E | \Psi_{1st} \rangle \quad , \tag{3.45}$$

where Ψ_{1st} here is the scattering wave function with values for the parameters $F = F_{1st}$ and the $c_{i,1st}$ obtained in the solution of the linear system.
In some cases (for example, when we want to calculate electroweak cross sections) we are not only interested in the reaction phase-shifts, but we need to have the whole scattering wave function. To this aim, we note that in general the second order estimate for F leads to a value for the phase shift which is much better then the first order one. Then we can use F_{2nd} as a constraint in our scattering w.f., and solve for the remaining parameters c_i.

The equations to be solved are the following:

$$\sum_{j_1}^{N} L_{ij} c_j = -\left(D_i^R + F_{2nd} D_i^I\right) \quad . \tag{3.46}$$

They give as result new values of the parameters c_j, which give a better estimate of the wave function with a better value of the phase-shift. It has however to be underlined that these, differently from what happens with the parameter F itself, are not second order estimates of the parameters, but they represent just an improvement in the estimate of the scattering wave function, given a particular value for the phase shift.

3.2.2 N+1 scattering

The procedure when more than two particles are involved is perfectly analogous to the two-body case. The main differences lie in the definition of the various parts of the scattering wave function, which now takes into account the fact that one of the fragment is a composite system.
Let A be the number of particles, and $N = A - 1$. First of all, to get rid of the center of mass motion, we define A sets of Jacobi coordinates

$$\boldsymbol{\eta}_{i,p} = \sqrt{\frac{i}{i+1}} \left(\mathbf{r}_{p+i+1} - \frac{1}{i} \sum_{j=1}^{i} \mathbf{r}_{p+j} \right) \quad , \quad i = 1, \ldots, N \quad , \quad p = 1, \ldots, A \quad . \tag{3.47}$$

The index p identifies a particular circular permutation of the particles, and all indexes are defined accordingly with the definition $\mathbf{r}_{A+k} = \mathbf{r}_k$.
As an example, let us take a look explicitly at the three-body case. There are just two Jacobi coordinates that can be arranged in three different sets

corresponding to $p = 1, 2, 3$:

$$\boldsymbol{\eta}_{1,p=3} = \sqrt{\frac{1}{2}}\left(\mathbf{r}_2 - \mathbf{r}_1\right) \tag{3.48}$$

$$\boldsymbol{\eta}_{2,p=3} = \sqrt{\frac{2}{3}}\left(\mathbf{r}_3 - \frac{1}{2}\left(\mathbf{r}_1 + \mathbf{r}_2\right)\right) \tag{3.49}$$

$$\boldsymbol{\eta}_{1,p=1} = \sqrt{\frac{1}{2}}\left(\mathbf{r}_3 - \mathbf{r}_2\right) \tag{3.50}$$

$$\boldsymbol{\eta}_{2,p=1} = \sqrt{\frac{2}{3}}\left(\mathbf{r}_1 - \frac{1}{2}\left(\mathbf{r}_2 + \mathbf{r}_3\right)\right) \tag{3.51}$$

$$\boldsymbol{\eta}_{1,p=2} = \sqrt{\frac{1}{2}}\left(\mathbf{r}_1 - \mathbf{r}_3\right) \tag{3.52}$$

$$\boldsymbol{\eta}_{2,p=2} = \sqrt{\frac{2}{3}}\left(\mathbf{r}_2 - \frac{1}{2}\left(\mathbf{r}_3 + \mathbf{r}_1\right)\right) \quad . \tag{3.53}$$

To make the notation simpler, it is useful to define a particular set p as the principal one, and drop the index p only for that particular set (resuming it only if it is useful to understand the notation). To this purpose, the set $p = A$ is chosen, so that

$$\boldsymbol{\eta}_i = \boldsymbol{\eta}_{i,A} \quad , \quad i = 1, \ldots, N \quad . \tag{3.54}$$

Using set p, the last particle to be coupled with the others is particle p. The vector $\eta_{N,p}$ turns out to be the most convenient in the description of the scattering of particle p off the nucleus composed by particles $p+1, \ldots, A, 1, \ldots, p-1$, since it is proportional to the position of particle p with respect to the center of mass of the others.
The asymptotic wave function Ω can be expressed as a sum of Faddeev-like amplitudes Ω_p, where each of the amplitudes pertains to the situation of the corresponding particle being scattered off the bulk:

$$\Omega^\lambda = \frac{1}{\sqrt{A}} \sum_{p=1}^{A} \sigma_p \Omega_p^\lambda(\boldsymbol{\eta}_{1,p}, \ldots, \boldsymbol{\eta}_{N,p}) \quad , \quad \lambda = R, I \quad , \tag{3.55}$$

where

$$\Omega_p^\lambda = \left[\Phi^{nucleus}(\boldsymbol{\eta}_{1,p},\ldots,\boldsymbol{\eta}_{N-1,p})G_L^\lambda(q\eta_{N,p})Y_L^M(\hat{\eta}_{N,p})\chi_{s_p}\chi_{t_p}\right]_{JJ_zTT_z} \tag{3.56}$$

with $\lambda = R, I$. The symbol $\Phi^{nucleus}$ denotes the $(A-1)$-nucleus wave function (with quantum numbers $J_{A-1}, M_{A-1}, T_{A-1}, T^z_{A-1}$) and χ_{s_A} and χ_{t_A} are respectively the spin and isospin wave functions of the p-th particle. The coefficients σ_p are defined as

$$\sigma_p = 1 \quad \forall p = 1,\ldots,A \quad \text{for } A \text{ odd} \tag{3.57}$$

$$\sigma_p = (-1)^{p+1} \quad \forall p = 1,\ldots,A \quad \text{for } A \text{ even} \quad . \tag{3.58}$$

The latter definition ensures the antisymmetry of Ω_{as} for the exchange of any two particles, provided that the wave function of the $(A-1)$-nucleus is itself antisymmetric. All the angular momenta of the nucleus and of the free particle are coupled accordingly to the values of the total momenta J, J^z, T, T^z (or analogously, in the case of central potentials, L, L^z, S, S^z, T, T^z).
The basis used in the expansion in the core region is now an A-body basis:

$$\Psi_{core}(\boldsymbol{\eta}_1,\ldots\boldsymbol{\eta}_N) = \sum_{i=1}^{N} c_i\phi_i(\boldsymbol{\eta}_1,\ldots\boldsymbol{\eta}_N) \quad . \tag{3.59}$$

The algebraic equations and the method itself remain exactly the same as in the simple two-body case.

3.3 Solution with bound-state methods

The second method (method II) considered, differently from the former, involves a separation of the wave function in an asymptotic part and a core part only for the derivation of the integral equation, while during the actual calculation the scattering wave function in the interaction region is entirely described through an expansion on a basis set.
As it has been done for the previous method, let us consider first the two-body problem, in which only the coordinate $\boldsymbol{\eta} = \frac{1}{\sqrt{2}}(\mathbf{r}_1 - \mathbf{r}_2)$ is relevant.

Let

$$\Psi = \Psi_{as} + \Psi_{core} \tag{3.60}$$

represent the scattering wave function, while Ψ_{as} is its asymptotic form and the correction Ψ_{core} is square-integrable. The asymptotic behaviour of Ψ is known:

$$\Psi \xrightarrow{\eta\to\infty} A\Omega^R + B\Omega^I \quad , \tag{3.61}$$

where functions Ω^λ are defined as in (3.55). Again, we choose their normalization to be

$$\langle\Omega^R|H-E|\Omega^I\rangle - \langle\Omega^I|H-E|\Omega^R\rangle = 1 \quad . \tag{3.62}$$

Then, the Wronskian theorem can be used to derive the following expression for the coefficients A and B:

$$A = \langle\Psi|H-E|\Omega^I\rangle - \langle\Omega^I|H-E|\Psi\rangle \tag{3.63}$$

$$B = \langle\Omega^R|H-E|\Psi\rangle - \langle\Psi|H-E|\Omega^R\rangle \quad . \tag{3.64}$$

A simple derivation (which does not involve the Wronskian theorem) of the previous relations is presented here. We note that the operator $(H-E)$ is hermitian if the functions inside the integrals do not lead to non-zero surface terms; in particular, if a function which goes to zero fast enough for large separation of the particles is present, all surface contributions to the integral coming from the derivatives in the kinetic energy operator vanish and $(H-E)$ is hermitian. This means that

$$\langle\Psi_{core}|H-E|\Omega^\lambda\rangle = \langle\Omega^\lambda|H-E|\Psi_{core}\rangle \quad , \quad \lambda = R, I \quad . \tag{3.65}$$

Then starting from the normalization relations for Ω^R, Ω^I, we may write

$$\begin{aligned} A &= A\,\langle\Omega^R|H-E|\Omega^I\rangle - \langle\Omega^I|H-E|\Omega^R\rangle\,A \\ &= A\,\langle\Omega^R|H-E|\Omega^I\rangle + B\,\langle\Omega^I|H-E|\Omega^I\rangle + \langle\Psi_{core}|H-E|\Omega^I\rangle \\ &\quad - \langle\Omega^I|H-E|\Omega^R\rangle\,A - \langle\Omega^I|H-E|\Omega^I\rangle\,B - \langle\Omega^I|H-E|\Psi_{core}\rangle \\ &= \langle\Psi|H-E|\Omega^I\rangle - \langle\Omega^I|H-E|\Psi\rangle \end{aligned} \tag{3.66}$$

and analogously

$$\begin{aligned} B &= \langle\Omega^R|H-E|\Omega^I\rangle\, B - B\,\langle\Omega^I|H-E|\Omega^R\rangle \\ &= \langle\Omega^R|H-E|\Omega^I\rangle\, B + \langle\Omega^R|H-E|\Omega^R\rangle\, A + \langle\Omega^R|H-E|\Psi_{core}\rangle \\ &\quad -B\,\langle\Omega^I|H-E|\Omega^R\rangle - A\,\langle\Omega^R|H-E|\Omega^R\rangle - \langle\Psi_{core}|H-E|\Omega^I\rangle \\ &= \langle\Omega^R|H-E|\Psi\rangle - \langle\Psi|H-E|\Omega^R\rangle \quad , \end{aligned} \tag{3.67}$$

which are exactly corresponding to Eq. (3.63) and (3.64). If Ψ satisfies the Schrödinger equation

$$(H-E)\Psi = 0 \quad , \tag{3.68}$$

we find the expressions for A and B:

$$A = \langle\Psi|H-E|\Omega^I\rangle \tag{3.69}$$

$$B = -\langle\Psi|H-E|\Omega^R\rangle \quad . \tag{3.70}$$

The value of the phase-shift can then be obtained as

$$F = \tan\delta = \frac{B}{A} \quad . \tag{3.71}$$

The generalization to the A-body case is straightforward and perfectly agrees with what has been done in the previous section for the first method.
Let us consider now the trial wave function Ψ_t. Then, according to the Kohn variational principle, the functional

$$Z = F - \frac{1}{A}\,\langle\Psi_t|H-E|\Psi_t\rangle \tag{3.72}$$

is stationary with respect to variations of each of the parameters of Ψ_t. If, like in the previous method presented, we expand the trial wave function as

$$\Psi_t = A\Omega^R + B\Omega^I + \sum_{i=1}^{N} c_i\phi_i \quad , \tag{3.73}$$

the variation of Z yields the equations

$$\langle \Omega^I | H - E | \Psi_t \rangle = 0 \tag{3.74}$$

$$\langle \phi_i | H - E | \Psi_t \rangle = 0 \quad . \tag{3.75}$$

Equation (3.75) implies that

$$\langle \Psi_{core} | H - E | \Psi_t \rangle = \sum_{i=1}^{N} c_i \langle \phi_i | H - E | \Psi_t \rangle = 0 \quad , \tag{3.76}$$

while if we substitute Eq. (3.74) in Eq. (3.63) we get

$$\langle \Psi_t | H - E | \Omega^I \rangle = A \quad . \tag{3.77}$$

A first order estimate of the phase-shift can be obtained substituting Ψ with Ψ_t in Eq. (3.64): (3.64):

$$B_{1st} = \langle \Omega^R | H - E | \Psi_t \rangle - \langle \Psi_t | H - E | \Omega^R \rangle \quad . \tag{3.78}$$

A second order estimate of the phase shift can then be obtained substituting the previous expression in the functional Z:

$$AZ = A\frac{B}{A} - \frac{1}{A} \langle \Psi_t | H - E | \Psi_t \rangle \tag{3.79}$$

$$\begin{aligned} \Rightarrow B_{2nd} &= B_{1st} - \frac{1}{A} \langle \Psi_t | H - E | \Psi_t \rangle \\ &= \langle \Omega^R | H - E | \Psi_t \rangle - \langle \Psi_t | H - E | \Omega^R \rangle - \langle \Omega^R | H - E | \Psi_t \rangle \\ &\quad - \frac{B}{A} \langle \Omega^I | H - E | \Psi_t \rangle - \frac{1}{A} \langle \Psi_{core} | H - E | \Psi_t \rangle \\ &= - \langle \Psi_t | H - E | \Omega^R \rangle \quad . \end{aligned} \tag{3.80}$$

So, the second order estimate for F is given by

$$F_{2nd} = \tan \delta_{2nd} = \frac{B_{2nd}}{A} = -\frac{\langle \Psi_t | H - E | \Omega^R \rangle}{\langle \Psi_t | H - E | \Omega^I \rangle} \quad . \tag{3.81}$$

The biggest difference with respect with the previous method presented is that we choose now to represent the trial wave function Ψ_t only by means of an expansion on a basis set. In the technique presented in Section 3.2, the trial wave function is explicitly represented as a sum of an asymptotic part and a core part, the latter one corresponding to a linear combination of square integrable basis functions. In this case instead, the trial wave function can be expressed as a linear combination of such basis states, not involving explicitly the asymptotic functions.
Let us consider such an expansion:

$$\Psi_t = \sum_{i=1}^{N} c_i \psi_i \quad . \tag{3.82}$$

Of course, since the functions ψ_i are square-integrable, this expansion cannot represent fully the scattering wave function. Anyway, all the integrals needed in the calculation of the second order estimate of the phase-shift involve functions which are limited. In fact, consider the explicit form of the operator $(H - E)$:

$$H - E = T + V_{strong} + V_{Coul} - E \quad . \tag{3.83}$$

When acting on the right on Ω^R, the only surviving term is

$$(H - E) \left|\Omega^R\right\rangle = V_{strong} \left|\Omega^R\right\rangle \quad . \tag{3.84}$$

and when acting on Ω^I, which contains the regularizing function g_{reg}, we are left with

$$(H - E) \left|\Omega^I\right\rangle = \mathcal{T}[g'_{reg}, g''_{reg}] + V_{strong} \left|\Omega^I\right\rangle \quad , \tag{3.85}$$

where $\mathcal{T}[g'_{reg}, g''_{reg}]$ is a functional of the derivatives of g_{reg} which vanishes for $\eta \to \infty$. Also the strong interaction potential is short-ranged, so all the integrals to be calculated are in fact limited to the interacting region. This is the reason Ψ_t may be expressed in the interaction region as a linear combination of square integrable functions.
In order to find Ψ_t, we simply solve the Schrödinger equation for states above the ground state, diagonalizing the Hamiltonian matrix in the basis ϕ_i. With

this diagonalization, we find the following eigenvalues:

$$H\Phi_i = E_i\Phi_i \quad . \tag{3.86}$$

If the system has one or more bound states, the lowest energies will represent these bound states, while higher energies will be related to scattering states. In the two-body case, negative and positive energies, respectively, identify bound and scattering states. In the A-body case, the energy region of interest is in general the one above the energy of the $(A-1)$-body nucleus E_{A-1}. The upper limit depends on the scattering process under consideration. For example, let us consider the three-body case, the process under study being the scattering of a neutron off a deuteron. The lowest energy eigenvalue will be the energy of triton $E_{^3H} < 0$. If the potential allows excited bound states for the three-body state, there will be other energies eigenvalues $E_{^3H} < E_{exc} < E_d$ where $E_d < 0$ is the deuteron energy. Since the only other configuration possible is the one with three free particles, the energy region in which only the $2+1$ scattering is possible is $E_d < E_i < E_0$. For each of this values of the energy, the phase-shift can be determined with the presented procedure.

A further discussion is worth concerning the Coulomb potential, when the case of more than two particles is studied. If the scattered nucleon is a proton, the long-range Coulomb interaction is present. It may be pointed out that this has already been taken into account, since the asymptotic wave functions Ω^λ solve the complete Coulomb equation. However, the Coulomb potential present in the Schrödinger equation represents the Coulomb interaction between the nucleus as a whole and the scattering proton, while the true Coulomb potential involves particle-to-particle interaction between the proton and each of the particles which form the $(A-1)$-nucleus. Outside the core region, anyway, the two potentials coincide, so the eventual correction can be taken into account in a short-range potential.

3.4 The Lorentz Integral Transform method

In this section a brief outline of the Lorentz Integral Transform (LIT) method is given.
The LIT method is a way to solve a continuum problem (like the photodisintegration one) using bound-state-like methods. Let us consider the inclusive response function $R_{\mathcal{O}}(E)$ for the operator $\mathcal{O}$

$$R_{\mathcal{O}}(E) = \int df \, |\langle \Psi_0 | \mathcal{O} | \Psi_f \rangle|^2 \, \delta(E - E_f) \quad . \tag{3.87}$$

Its transform is defined as

$$\Phi(\sigma) = \int dE R_{\mathcal{O}}(E) K(\sigma, E) \quad , \tag{3.88}$$

where $K(\sigma, E)$ is a smooth kernel. Substituting for $R_{\mathcal{O}}(E)$ leads to the expression

$$\Phi(\sigma) = \int df \, \langle \Psi_0 | \mathcal{O}^\dagger K(\sigma, E) | \Psi_f \rangle \, \langle \Psi_f | \mathcal{O} | \Psi_0 \rangle \quad . \tag{3.89}$$

The closure property of the Hamiltonian eigenstates can then be used:

$$\int df \, |\Psi_f\rangle \, \langle \Psi_f| = 1 \quad , \tag{3.90}$$

leading to the equation

$$\Phi(\sigma) = \langle \Psi_0 | \mathcal{O}^\dagger K(\sigma, E) \mathcal{O} | \Psi_0 \rangle \quad . \tag{3.91}$$

The transform $\Phi(\sigma)$ can be calculated and then the response function is retrieved via an inversion of $\Phi(\sigma)$. The kernel used is a Lorentzian

$$\begin{aligned} K(\sigma, E) &= \frac{1}{(E - \sigma_R)^2 + \sigma_I^2} \\ &= \frac{1}{E - \sigma_R - i\sigma_I} \frac{1}{E - \sigma_R + i\sigma_I} \quad , \end{aligned} \tag{3.92}$$

with $\sigma = \sigma_R + i\sigma_I$.
The transform can be expressed as

$$\Phi(\sigma) = \langle \tilde{\Psi} | \tilde{\Psi} \rangle \tag{3.93}$$

in terms of the functions $\tilde{\Psi}$ defined by the equation

$$(H - \sigma_R - i\sigma_I) \, |\tilde{\Psi}\rangle = \mathcal{O} \, |\Psi_0\rangle \quad . \tag{3.94}$$

It has to be noted that the functions $\tilde{\Psi}$ are localized for any value of σ. Then the latter is a bound-state-like equation, and hence can be solved applying bound-state methods: in particular, if an expansion on a basis is performed, Eq. (3.94) represent a linear system to be solved.
A finite expansion can be performed for the states $\mathcal{O} \, |\Psi_0\rangle$ on the eigenstates of the Hamiltonian H

$$H\phi_i = E_i \phi_i \quad . \tag{3.95}$$

The expression for the transform becomes then

$$\Phi(\sigma) = \sum_i \langle \tilde{\Psi} | \phi_i \rangle \, \langle \phi_i | \tilde{\Psi} \rangle \tag{3.96}$$

$$= \sum_i \frac{S_i}{(E_i - \sigma_R)^2 + \sigma_I^2} \quad , \tag{3.97}$$

with

$$S_i = |\langle \phi_i | \mathcal{O} \, |\Psi_0\rangle\rangle|^2 \quad . \tag{3.98}$$

In the former expressions E_i, S_i and σ_I represent respectively the position, strength and width of each Lorentzian (LIT state) considered.
In order to obtain the response function $R_{\mathcal{O}}(E)$ one needs to invert the LIT [31]. Since this constitutes a so called ill-posed problem one has to work with an inversion where a regularization method is implemented. The standard LIT inversion method involves an expansion of the response function on an

appropriate basis set of functions:

$$R_{\mathcal{O}}(E) = \sum_{i=1}^{N} c_i f_i(E) \quad , \tag{3.99}$$

where the correct behaviour of the response function at the reaction threshold is implemented. After a LIT of these basis functions is calculated, the coefficients c_i are determined via a fit to the calculated LIT. The regularization consists in the use of a limited number of basis functions in such an expansion, to avoid the appearance of high-frequency modes in the obtained response function.
The advantage of using a Lorentzian lies in the controllable resolution σ_I of the transform [32]. In fact, the Lorentzian kernel is identified by its position σ_R and width σ_I: calculations with smaller values for σ_I lead to finer resolutions. Anyway, in order to construct a precise transform of the response function, a sufficiently high number of LIT states is required. Given a basis and its representation of the Hamiltonian, its eigenvalues correspond to the positions of the Lorentzian functions that define the transform: if the density of the eigenstates of the Hamiltonian is too low, the transform function may be not accurate. The resolution cannot be infinitely high (which would correspond to $\sigma_I = 0$ and to the Lorentzian kernel becoming a delta function), thus defining a controlled resolution technique.

In the case of low-energy ^{3}He photodisintegration, the cross section is very low due to the Coulomb barrier between the fragments. In this energy range the precision of the LIT may not be sufficient (see for example calculations of the isoscalar monopole resonance of ^{4}He calculated with a Hyperspherical harmonics expansion in [33]), if the framework used is an Hyperspherical Harmonics expansion to find the Hamiltonian eigenstates ϕ_i. A high density of LIT states is indeed needed because the resolution σ_I must be small enough to allow the low-energy part of the transform not to get too strong contributions from other parts of the cross section.

In Chapter 5 it is shown how a sufficiently high density of LIT states is obtained.

Chapter 4

The basis systems

The attempt to solve both bound and scattering problems in few-body physics using an expansion of wave functions on a suitable basis is a well established methodology in nuclear and atomic physics. Different basis sets may be most suitable for different purposes, and different problems may be treated more easily or more efficiently with different choices of the basis set used.
In the case of bound state problem, the expansion of the Hamiltonian operator on a basis and its diagonalization is a useful ab initio technique in the case of few-body nuclear physics (up to a number of particles $A \simeq 10$). When the problem involves too many particles, other methods are needed in order to get a solution (ab initio techniques like Auxiliary Field Diffusion Monte Carlo [34] and Coupled Cluster [35] or mean field approximations methods). The interest in ab initio calculations lies in the fact that the problem is solved starting from the microscopic Hamiltonian, and solving the relevant equations without approximations, and so results are in principle correct. This provides a tool in the developing of potentials and in the study of interaction itself.
In general the expansion method is, regardless of the basis used, a method which may give both binding energies and complete wave functions, which may be used to calculate expectations values of other operators.
In particular, the basis used in the present work are Hyperspherical Harmonics (HH) and a Laguerre basis.

A basis of Hyperspherical Harmonic functions is a natural choice in the study of problems where three or more particles are involved, HHs being the natural extension to more than two particles of the eigenfunctions of the angular momentum operator, the usual spherical harmonics. The usual framework of the Hyperspherical Harmonic basis expansion is its use with the Jacobi coordinates. This makes possible to get rid of the center of mass problem from the beginning.

4.1 Jacobi coordinates

As mentioned, Jacobi coordinates are often used in physics calculations when it is useful to express the problem in its center of mass frame. This set of coordinates separates the motion of the center of mass from the motion of the particles with respect to it, thus making possible a treatment of the problem where the center of mass does not contribute at all.
Various different definitions of the Jacobi coordinates may be used. In particular the mass-weighted Jacobi coordinates are useful, because they let the kinetic energy operator take a particularly simple form. They are defined as following:

$$\boldsymbol{\eta}_i = \sqrt{\frac{m_i M_i}{\mu M_{i+1}}} \left(\mathbf{r}_{i+1} - \frac{1}{M_i} \sum_{j=1}^{i} m_j \mathbf{r}_j \right) \quad , \tag{4.1}$$

where $\mathbf{r}_i$ is the position of particle i, m_i is its mass, and

$$M_i = \sum_{j=1}^{i} m_j \quad , \tag{4.2}$$

so that each Jacobi coordinate η_i is proportional to the position of particle i with respect to the center of mass of the preceding ones. The symbol μ corresponds to a reference mass, to be arbitrarily chosen.
As noted, being A the number of particles, we pass from having $3A$ coordi-

nates to $3(A-1) = 3N$, since we can disregard the center of mass coordinate

$$\mathbf{R} = \frac{1}{M_A}\sum_{i=1}^{A} m_i \mathbf{r}_i \quad . \tag{4.3}$$

The Hamiltonian of a system can in general be expressed as

$$H = T + V = -\sum_{i=1}^{A} \frac{\hbar^2}{2m_i}\nabla^2_{\mathbf{r}_i} + V \quad , \tag{4.4}$$

with T and V denoting respectively kinetic energy and potential operators, while $\nabla^2_{\mathbf{r}_i}$ is the Laplacian operator calculated with respect on the coordinate $\mathbf{r}_i$. The kinetic energy expression becomes simple when transformed in the set of Jacobi coordinates:

$$T = -\sum_{i=1}^{A} \frac{\hbar^2}{2m_i}\nabla^2_{\mathbf{r}_i} \tag{4.5}$$

$$= -\sum_{i=1}^{A-1} \frac{\hbar^2}{2\mu}\nabla^2_{\boldsymbol{\eta}_i} - \frac{\hbar^2}{2M_A}\nabla^2_{\mathbf{R}} \quad , \tag{4.6}$$

where the last term representing the center of mass motion can be disregarded to study only the internal motion.
In nuclear physics often the problem treated deals with just one kind of particles, namely nucleons; in this case the Jacobi coordinates take the simpler form:

$$\boldsymbol{\eta}_i = \sqrt{\frac{i}{i+1}}\left(\mathbf{r}_{i+1} - \frac{1}{i}\sum_{j=1}^{i}\mathbf{r}_j\right) \quad , \tag{4.7}$$

where the particular choice of the reference mass being the nucleon mass $\mu = m_{nucleon}$ has been made. In this case the kinetic energy operator takes the form

$$T = -\frac{\hbar^2}{2m_{nucleon}}\sum_{i=1}^{A-1}\nabla^2_{\boldsymbol{\eta}_i} \quad . \tag{4.8}$$

It has to be noted that the previous is just one of the possibilities to construct a set of Jacobi coordinates, the difference between different sets lying in the

order by which particles positions are taken into account. If, for example, the problem taken into consideration involves clusters of particles, it may be useful to define Jacobi coordinate sets for each cluster and then define the relative coordinates between clusters. Another useful definition is the one of *reversed order* Jacobi coordinates, where the order of the particles is reversed:

$$\boldsymbol{\eta}_{A-i} = \sqrt{\frac{i}{i+1}} \left(\mathbf{r}_{i+1} - \frac{1}{i} \sum_{j=1}^{i} \mathbf{r}_j \right) \quad . \tag{4.9}$$

The latter definition is useful in the use of Nonsymmetrized Hyperspherical Harmonics, as will be seen.
The set of the $3(A-1)$ Jacobi Cartesian coordinates may be converted in another set of coordinates, namely hyperspherical coordinates, substituting linear coordinates with spherical ones:

$$\{\boldsymbol{\eta}_1, \dots \boldsymbol{\eta}_N\} \to \{\eta_1, \hat{\eta}_1, \dots \eta_N, \hat{\eta}_N\} \quad , \tag{4.10}$$

where $\hat{\eta}_i = \{\theta_i, \phi_i\}$ denotes the angles of $\boldsymbol{\eta}_i$ in spherical coordinates and $N = A - 1$ is the number of Jacobi vectors $\boldsymbol{\eta}_i$. The values $\{\eta_1, \dots \eta_N\}$ may also be substituted with *hyperangular* coordinates:

$$\{\eta_1, \dots \eta_N\} \to \{\rho, \alpha_2, \dots, \alpha_N\} \quad . \tag{4.11}$$

The *hyperangles* α_i are defined as follows:

$$\rho_1 = \eta_1 \tag{4.12}$$

$$\rho_i = \sqrt{\rho_{i-1}^2 + \eta_i^2} = \sqrt{\sum_{j=1}^{i} \eta_j^2} \quad ; \quad i = 2, N \tag{4.13}$$

$$\rho = \rho_N = \sqrt{\sum_{j=1}^{N} \eta_j^2} \tag{4.14}$$

$$\sin \alpha_i = \frac{\eta_i}{\rho_i} \quad ; \quad i = 2, N \tag{4.15}$$

$$\cos \alpha_2 = \frac{\eta_1}{\rho_2} \quad . \tag{4.16}$$

The $3N$ Jacobi coordinates set expressed in angular and hyperangular form becomes then

$$\{\rho, \alpha_2, \ldots, \alpha_N, \hat{\eta}_1, \ldots, \hat{\eta}_N\} \quad . \tag{4.17}$$

The *hyperradius* ρ measures the global size of the system, while all the angular and hyperangular variables pertain to the relative disposition and distances of the particles.
The expression of the Laplacian operator relative to a single Jacobi coordinate in spherical coordinates is:

$$\nabla^2_{\boldsymbol{\eta}_i} = \nabla^2_{\eta_i} - \frac{1}{\eta_i^2}\hat{l}_i^2 \quad , \tag{4.18}$$

where $\hat{l}_i$ denotes the orbital angular momentum operator relative to $\boldsymbol{\eta}_i$, and $\nabla^2_{\eta_i}$ the radial part of the Laplacian operator:

$$\nabla^2_{\eta_i} = \frac{\partial^2}{\partial \eta_i^2} + \frac{2}{\eta_i}\frac{\partial}{\partial \eta_i} \quad . \tag{4.19}$$

As already stated in Eq. (4.8), the kinetic energy operator is proportional to the sum of each Laplacian operator $\nabla^2_{\boldsymbol{\eta}_i}$. We may define partial Laplacian operators in the following way:

$$\nabla^2_{(i)} = \sum_{j=1}^{i} \nabla^2_{\boldsymbol{\eta}_j} = \sum_{j=1}^{i} \left(\nabla^2_{\eta_j} - \frac{1}{\eta_j^2}\hat{l}_j^2 \right) \quad , \tag{4.20}$$

so that

$$\nabla^2_{(N)} = \sum_{j=1}^{N} \nabla^2_{\boldsymbol{\eta}_j} \tag{4.21}$$

is the total Laplacian operator appearing in Eq. (4.8). The partial Laplacian operators may be expressed making use of the following recurrence relation:

$$\nabla^2_{(i+1)} = \nabla^2_{(i)} + \nabla^2_{\boldsymbol{\eta}_{i+1}} \quad . \tag{4.22}$$

In terms of the hyperangular variables, they may be expressed as

$$\nabla^2_{(i)} = \nabla^2_{\rho_i} - \frac{1}{\rho_i^2}\hat{K}_i^2 \quad , \tag{4.23}$$

where $\hat{K}_i$ is the *hyperangular momentum* (or *grand angular momentum*) operator, the generalization for more than one coordinate of the orbital angular momentum operator:

$$\hat{K}_i^2 = -\frac{\partial^2}{\partial\alpha_i^2} + \frac{3i-6+(3i-2)\cos(2\alpha_i)}{\sin(2\alpha_i)} + \frac{1}{\cos^2(2\alpha_i)}\hat{K}_{i-1}^2 + \frac{1}{\sin^2(2\alpha_i)}\hat{l}_i^2 \quad , \tag{4.24}$$

where

$$\hat{K}_1 = \hat{l}_1 \quad , \tag{4.25}$$

while $\nabla^2_{\rho_i}$ is

$$\nabla^2_{\rho_i} = \frac{\partial^2}{\partial\rho_i^2} + \frac{3N-1}{\rho_i}\frac{\partial}{\partial\rho_i} \quad . \tag{4.26}$$

The kinetic energy operator reads then

$$T = -\frac{\hbar^2}{2m_{nucleon}}\nabla_{(N)} = -\frac{\hbar^2}{2m_{nucleon}}\left(\nabla_\rho - \frac{1}{\rho^2}\hat{K}_N^2\right) \quad . \tag{4.27}$$

The operator $\hat{K}_N$ is the total hyperangular momentum. Its eigenstates are the Hyperspherical Harmonics, in analogy with the usual orbital angular momentum and the spherical harmonics.
The volume element associated with the N Jacobi coordinates $\boldsymbol{\eta}_1, \ldots, \boldsymbol{\eta}_N$ is the following:

$$dV_{3N} = \rho^{3N-1} d\rho dS_{3N-1} \tag{4.28}$$

where dS_{3N-1} is the volume element associated with the $(3N-1)$-dimensional hypersphere. It is defined recursively:

$$dS_{3i-1} = \sin^2\alpha_i \cos^{3i-4}\alpha_i d\alpha_i d\Omega_i dS_{3i-4} \quad , \tag{4.29}$$

where, for $i = 1$,

$$dS_{3-1} = d\Omega_1 \tag{4.30}$$

and

$$d\Omega_i = d\hat{\eta}_i = d\cos\theta_i d\phi_i \quad . \tag{4.31}$$

The value of the hyperangles α_i runs between 0 and $\frac{\pi}{2}$.

4.2 Hyperspherical Harmonics

As mentioned in the preceding section, Hyperspherical Harmonics are the eigenstates of the hyperangular momentum operator $\hat{K}_N$. In this sense they are a natural extension for the case of more than two particles of the ordinary spherical harmonics.
The usual spherical harmonics Y_l^m are identified by their quantum numbers l and m representing the eigenvalues of operators $\hat{l}$ and $\hat{l}_z$. In the case of $A \geq 3$, more quantum numbers are needed to specify the eigenstate of hyperangular momentum. With reference to Eq. (4.24), let the total internal angular momentum operator of the particles described by Jacobi coordinates $\boldsymbol{\eta}_1, \ldots, \boldsymbol{\eta}_i$ be

$$\hat{L}_i = \hat{L}_{i-1} + \hat{l}_i \quad . \tag{4.32}$$

The operators $\hat{K}_{i-1}^2$, $\hat{l}_i^2$, $\hat{K}_i^2$, $\hat{L}_i^2$ and $\hat{L}_{iz}$ all commute with each other, so each hyperspherical harmonic function may be labeled by the set of $3N-1$ quantum numbers

$$\{l_1, \ldots, l_N, L_2, \ldots, L_N, M_N, K_2, \ldots, K_N\} \quad , \tag{4.33}$$

representing the eigenvalues of the operators

$$\left\{\hat{l}_1^2, \ldots, \hat{l}_N^2, \hat{L}_2^2, \ldots, \hat{L}_N^2, \hat{L_{Nz}}, \hat{K}_2^2, \ldots, \hat{K}_N^2\right\} \quad . \tag{4.34}$$

The definition of the hyperangular momentum eigenvalues is the following:

$$\left[\hat{K}_i^2(\Omega_N) - K_i(K_i + 3i - 2)\right] \mathcal{Y}_{[K]}(\Omega_N) = 0 \tag{4.35}$$

where the symbol Ω_N here denotes the collection of all angular and hyperangular variables

$$\Omega_N = \{\alpha_2, \ldots, \alpha_i, \hat{\eta}_1, \ldots, \hat{\eta}_N\} \quad . \tag{4.36}$$

The symbol $[K]$ denotes the collection of all quantum numbers identifying the Hyperspherical Harmonic functions $\mathcal{Y}_{[K]}(\Omega_N)$.
The explicit form of the Hyperspherical Harmonics functions is:

$$\begin{aligned}
\mathcal{Y}_{[K]}\left(\Omega_N\right) \quad = \quad & \left[\sum_{m_1,\ldots,m_N} \langle l_1 m_1 l_2 m_2 | L_2 M_2 \rangle \, \langle L_2 M_2 l_3 m_3 | L_3 M_3 \rangle \cdot \ldots \right. \\
& \left. \cdot \, \langle L_{N-1} M_{N-1} l_N m_N | L_N M_N \rangle \prod_{j=1}^{N} Y_{l_j m_j}\left(\hat{\eta}_j\right) \right] \\
& \cdot \left[\prod_{j=2}^{N} \mathcal{N}(K_j; l_j K_{j-1}) (\sin\alpha_j)^{l_j} (\cos\alpha_j)^{K_{j-1}} \right. \\
& \left. \cdot P_{\mu_j}^{[l_j+1/2],[K_{j-1}+(3j-5)/2]}\left(cos\left(2\alpha_j\right)\right) \right] \quad ,
\end{aligned} \tag{4.37}$$

where $\mathcal{N}_j(K_j; l_j K_{j-1})$ are normalization coefficients given by

$$\mathcal{N}_j(K_j; l_j K_{j-1}) = \left[\frac{(2K_j + 3j - 2)\mu_j! \Gamma[\mu_j + K_{j-1} + l_j + (3j-2)/2]}{\Gamma\left[\mu_j + l_j + 3/2\right] \Gamma[\mu_j + K_{j-1} + (3j-2)/2]} \right]^{1/2} \tag{4.38}$$

with μ_j being integer non-negative numbers, and $K_j = K_{j-1} + 2\mu_j + l_j$.
The Hyperspherical Harmonics defined are identified by quantum numbers

$$\{l_1, \ldots, l_N, L_2, \ldots, L_N, M_N, \mu_2, \ldots, \mu_N\} \quad , \tag{4.39}$$

or, as said before,

$$\{l_1, \ldots, l_N, L_2, \ldots, L_N, M_N, K_2, \ldots, K_N\} \quad . \tag{4.40}$$

The previous is just one of the possible schemes for the construction of the Hyperspherical Harmonic functions.

Hyperspherical Harmonics obey the orthonormal relation

$$\int dS_{3N-1}\mathcal{Y}_{[K]}(\Omega_N)\mathcal{Y}_{[K']}(\Omega_N) = \delta_{[K][K']} \quad , \tag{4.41}$$

where the Kronecker delta represents a delta for each pair of correspondent quantum numbers represented by $[K]$ and $[K']$.

4.3 Hyperspherical Harmonics basis

A basis for the wave function of a system of A nucleons may be constructed using Hyperspherical Harmonic functions. The spatial part of the wave function may be expanded on a basis composed for the angular and hyperangular part of Hyperspherical Harmonics, and for the hyperradial part of other polynomials:

$$\Psi_i = \mathcal{Y}_{[K]_i}(\Omega_N)\mathcal{R}_{r_i}(\rho) \quad , \tag{4.42}$$

the index r_i identifying the hyperradial functions. A typical choice for the hyperradial functions is represented by associated Laguerre polynomials

$$\mathcal{R}_r(\rho) = \sqrt{\frac{r!}{(r+k)!}} L_r^k(\frac{\rho}{b}) e^{-\frac{\rho}{2b}} \left(\frac{\rho}{b}\right)^{\frac{k-3N+1}{2}} b^{-\frac{3N}{2}} \tag{4.43}$$

$$L_r^k(x) = \frac{e^x x^{-k}}{r!}\frac{d^r}{dx^r}\left(e^{-x}x^{r+k}\right) \quad , \tag{4.44}$$

with b a parameter to be chosen arbitrarily and k an integer number. The normalization is chosen so that

$$\int_0^\infty \rho^k \mathcal{R}_r(\rho)\mathcal{R}_{r'}(\rho)d\rho = \delta_{rr'} \tag{4.45}$$

The value of k is usually chosen to be $k = 3N-1 = 3A-4$, since the volume element of the integration in the space of Jacobi coordinates gives a factor ρ^{3N-1}, as seen in Eq. (4.28), but in principle the value of k may be chosen arbitrarily.

The spin wave χ^S functions are determined by quantum numbers

$$\{s_1, \ldots, s_A, S_1, \ldots, S_A\} \quad , \tag{4.46}$$

representing respectively spins of particles $1, \ldots, A$ and total spins up to the A-th particle:

$$\Big[\big[[s_1, s_2]_{S_2}, s_3\big]_{S_3}, \ldots, s_A\Big]_{S_A} \quad . \tag{4.47}$$

An analogous definition is made for the isospin wave function:

$$\Big[\big[[t_1, t_2]_{T_2}, t_3\big]_{T_3}, \ldots, t_A\Big]_{T_A} \quad , \tag{4.48}$$

where $t_1, \ldots, t_A$ and $T_1, \ldots, T_A$ are single particle and cluster isospins respectively. The total basis function is then identified by

$$|\Psi_i\rangle = \mathcal{R}_{r_i}(\rho)\, |\mathcal{Y}_{[K]_i}\rangle\, |\chi^S\rangle\, |\chi^T\rangle \quad , \tag{4.49}$$

where i identifies the basis function, with total orbital angular momentum L_N, total spin S_A, total isospin T_A and total angular momentum J given by $\hat{J} = \hat{L}_N + \hat{S}_A$.

One of the issues that has to be faced when using Hyperspherical Harmonics is that they do not have well-defined permutational symmetry. If an operator $\hat{P}_{jk}$ (which exchanges particles j and k) acts on the function Ψ_i, the result of its action is in general different from a simple sign. Since in nuclear physics calculations one has to deal with identical fermions, an antisymmetric wave function is needed. There are in principle two different ways to obtain that. The first and most natural way is to apply an antisymmetrizer operator to each basis function, thus constructing an antisymmetric basis, so that any linear combination of basis functions is itself antisymmetric. This means a Symmetrized Hyperspherical Harmonics basis is used. The second way is to use the Hyperspherical Harmonics basis as it is, requiring only the antisymmetry of the linear combinations which solve the Schrödinger equation. The latter method involves the use of a Nonsymmetrized Hyperspherical Harmon-

ics basis.

4.3.1 Symmetrized Hyperspherical Harmonics

The procedure to symmetrize the Hyperspherical Harmonics basis is in general rather complicated, and becomes more complicated increasing the number of particles A [36]. Since this kind of basis has been used in the present work only in the three-body case, only the $A = 3$ symmetrized basis will be discussed here.
In order to achieve the complete antisymmetrization of the basis states, it is necessary to make sure that each permutation operator ($\hat{P}_{12}$, $\hat{P}_{13}$ and $\hat{P}_{23}$) has the effect to change the sign of the functions of the basis. The procedure is in general cumbersome, and for the three-body case it is simpler to first describe the basis functions and then check that they are antisymmetric with respect to the permutation operators.
To introduce the antisymmetric basis states, four different sets of coordinates will be needed. According to the definition of Jacobi coordinates given, we may label the particles with numbers $1, 2, 3$, and define a first set (a) of Jacobi coordinates as

$$\boldsymbol{\eta}_1^{(a)} = \sqrt{\frac{1}{2}}\,(\mathbf{r}_2 - \mathbf{r}_1) \tag{4.50}$$

$$\boldsymbol{\eta}_2^{(a)} = \sqrt{\frac{2}{3}}\left(\mathbf{r}_3 - \frac{\mathbf{r}_1 + \mathbf{r}_2}{2}\right) \quad . \tag{4.51}$$

where $\mathbf{r}_1$, $\mathbf{r}_2$ and $\mathbf{r}_3$ are the positions of particles 1, 2 and 3 respectively. Then the other sets of Jacobi vectors correspond to various permutations of the particles. Set (b) is obtained exchanging particles 1 and 2:

$$\boldsymbol{\eta}_1^{(b)} = \sqrt{\frac{1}{2}}\,(\mathbf{r}_1 - \mathbf{r}_2) = -\boldsymbol{\eta}_1^{(a)} \tag{4.52}$$

$$\boldsymbol{\eta}_2^{(b)} = \sqrt{\frac{2}{3}}\left(\mathbf{r}_3 - \frac{\mathbf{r}_2 + \mathbf{r}_1}{2}\right) = \boldsymbol{\eta}_2^{(a)} \quad ; \tag{4.53}$$

set (c) is obtained exchanging particles 1 and 3:

$$\boldsymbol{\eta}_1^{(c)} = \sqrt{\frac{1}{2}}\,(\mathbf{r}_2 - \mathbf{r}_3) \tag{4.54}$$

$$\boldsymbol{\eta}_2^{(c)} = \sqrt{\frac{2}{3}}\left(\mathbf{r}_1 - \frac{\mathbf{r}_3 + \mathbf{r}_2}{2}\right) \quad ; \tag{4.55}$$

while set (d) is obtained from set (c) exchanging particles 1 and 2:

$$\boldsymbol{\eta}_1^{(d)} = \sqrt{\frac{1}{2}}\,(\mathbf{r}_1 - \mathbf{r}_3) \tag{4.56}$$

$$\boldsymbol{\eta}_2^{(d)} = \sqrt{\frac{2}{3}}\left(\mathbf{r}_2 - \frac{\mathbf{r}_3 + \mathbf{r}_1}{2}\right) \quad . \tag{4.57}$$

The meaning of the former definition can be better understood with the use of permutation operators: starting from set (a), the other coordinates sets may be obtained in the following way:

$$(a) \xrightarrow{\hat{P}_{12}} (b) \tag{4.58}$$

$$(a) \xrightarrow{\hat{P}_{13}} (c) \tag{4.59}$$

$$(a) \xrightarrow{\hat{P}_{12}\hat{P}_{13}} (d) \quad . \tag{4.60}$$

A set of angular and hyperangular variables $\Omega^{(a,b,c,d)}$ and a corresponding Hyperspherical Harmonic function can be associated to each coordinate set:

$$\mathcal{Y}_{[K]}^{(a)} = \mathcal{Y}_{[K]}(\Omega^{(a)}) \quad , \tag{4.61}$$

where the symbol $\Omega^{(a)} = \left\{\theta_1^{(a)}, \phi_1^{(a)}, \theta_2^{(a)}, \phi_s^{(a)}, \alpha_2^{(a)}\right\}$ denotes here the collection of all angles and hyperangles pertaining to set (a), and analogously for all sets (a), (b), (c), (d).
In this sense the different permutations act of the Hyperspherical Harmonics

in the following way:

$$\hat{P}_{12}\mathcal{Y}^{(a)}_{[K]} = \mathcal{Y}^{(b)}_{[K]} \quad (4.62)$$
$$\hat{P}_{13}\mathcal{Y}^{(a)}_{[K]} = \mathcal{Y}^{(c)}_{[K]} \quad (4.63)$$
$$\hat{P}_{12}\hat{P}_{13}\mathcal{Y}^{(a)}_{[K]} = \mathcal{Y}^{(d)}_{[K]} \ . \quad (4.64)$$

The spatial part of each basis state is then calculated in the following way: three possibilities corresponding to symmetric ($\mathcal{Y}^{S}_{[K]}$), mixed ($\mathcal{Y}'_{[K]}$ and $\mathcal{Y}''_{[K]}$) and antisymmetric spatial states ($\mathcal{Y}^{A}_{[K]}$) are given. The construction is presented here. For symmetric and antisymmetric states, only states with l_1 even and odd respectively are possible, because the spatial symmetry for the exchange of the particles associated with $\eta_1^{(a,b,c,d)}$ is equal to $(-1)^{l_1}$:

$$\mathcal{Y}^{S}_{[K]} = \frac{1}{6}\left(\mathcal{Y}^{(a)}_{[K]} + \mathcal{Y}^{(b)}_{[K]}\right) + \frac{1}{3}\left(\mathcal{Y}^{(c)}_{[K]} + \mathcal{Y}^{(d)}_{[K]}\right) \qquad \text{with } l_1 \text{ even} \quad (4.65)$$
$$\mathcal{Y}^{A}_{[K]} = \frac{1}{6}\left(\mathcal{Y}^{(a)}_{[K]} - \mathcal{Y}^{(b)}_{[K]}\right) + \frac{1}{3}\left(-\mathcal{Y}^{(c)}_{[K]} + \mathcal{Y}^{(d)}_{[K]}\right) \qquad \text{with } l_1 \text{ odd} \ . \quad (4.66)$$

It can be verified that the action of each permutation operator is the expected one, remembering the value of l_1 for each case:

$$\hat{P}_{12}\mathcal{Y}^{S}_{[K]} = \mathcal{Y}^{S}_{[K]} \ ; \quad \hat{P}_{13}\mathcal{Y}^{S}_{[K]} = \mathcal{Y}^{S}_{[K]} \ ; \quad \hat{P}_{23}\mathcal{Y}^{S}_{[K]} = \mathcal{Y}^{S}_{[K]} \ ; \quad (4.67)$$
$$\hat{P}_{12}\mathcal{Y}^{A}_{[K]} = -\mathcal{Y}^{A}_{[K]} \ ; \quad \hat{P}_{13}\mathcal{Y}^{A}_{[K]} = -\mathcal{Y}^{A}_{[K]} \ ; \quad \hat{P}_{23}\mathcal{Y}^{A}_{[K]} = -\mathcal{Y}^{A}_{[K]} \ . \quad (4.68)$$

Mixed symmetry states can be of two different kinds: states which are symmetric with respect to particles 1 and 2 ($\mathcal{Y}''_{[K]}$) and states which are antisymmetric for the same exchange ($\mathcal{Y}'_{[K]}$). The construction of the states is different for l_1 even or odd:

$$\mathcal{Y}'_{[K]} = \frac{1}{\sqrt{3}}\left(\mathcal{Y}^{(a)}_{[K]} - \mathcal{Y}^{(b)}_{[K]} - \mathcal{Y}^{(c)}_{[K]} + \mathcal{Y}^{(d)}_{[K]}\right) \qquad \text{with } l_1 \text{ even} \quad (4.69)$$
$$\mathcal{Y}''_{[K]} = \frac{1}{3}\left(\mathcal{Y}^{(a)}_{[K]} + \mathcal{Y}^{(b)}_{[K]} - \mathcal{Y}^{(c)}_{[K]} - \mathcal{Y}^{(d)}_{[K]}\right) \qquad \text{with } l_1 \text{ even} \quad (4.70)$$
$$\mathcal{Y}'_{[K]} = \frac{1}{3}\left(\mathcal{Y}^{(a)}_{[K]} - \mathcal{Y}^{(b)}_{[K]} + \mathcal{Y}^{(c)}_{[K]} + \mathcal{Y}^{(d)}_{[K]}\right) \qquad \text{with } l_1 \text{ odd} \quad (4.71)$$
$$\mathcal{Y}''_{[K]} = \frac{1}{\sqrt{3}}\left(\mathcal{Y}^{(a)}_{[K]} + \mathcal{Y}^{(b)}_{[K]} - \mathcal{Y}^{(c)}_{[K]} - \mathcal{Y}^{(d)}_{[K]}\right) \qquad \text{with } l_1 \text{ odd} \ . \quad (4.72)$$

Again, the symmetry requirements may be verified by direct application of the permutation operators:

$$\hat{P}_{12}\mathcal{Y}''_{[K]} = \mathcal{Y}''_{[K]} \ ; \tag{4.73}$$

$$\hat{P}_{12}\mathcal{Y}'_{[K]} = -\mathcal{Y}'_{[K]} \ . \tag{4.74}$$

To construct a completely antisymmetric function, also spin-isospin functions must be constructed to have proper symmetries.
We consider only tritium and ^{3}He, which ground states have isospin $T = \frac{1}{2}$, and third component of isospin $T^z = -\frac{1}{2}$ and $T^z = +\frac{1}{2}$ for ^{3}H and ^{3}He respectively. The isospin functions may have then only mixed symmetry, and are defined by

$$\tau' = \frac{1}{\sqrt{2}}\left|(\downarrow_1\uparrow_2 - \uparrow_1\downarrow_2)\uparrow_3\right\rangle = \frac{1}{\sqrt{2}}\left|\downarrow_1\uparrow_2\uparrow_3\right\rangle - \frac{1}{\sqrt{2}}\left|\uparrow_1\downarrow_2\uparrow_3\right\rangle \tag{4.75}$$

$$\tau'' = -\sqrt{\frac{2}{3}}\left|\uparrow_1\uparrow_2\downarrow_3\right\rangle + \sqrt{\frac{1}{6}}\left|\uparrow_1\downarrow_2\uparrow_3\right\rangle + \sqrt{\frac{1}{6}}\left|\downarrow_1\uparrow_2\uparrow_3\right\rangle \tag{4.76}$$

for $T_z = +\frac{1}{2}$, and

$$\tau' = \frac{1}{\sqrt{2}}\left|(\downarrow_1\uparrow_2 - \uparrow_1\downarrow_2)\downarrow_3\right\rangle = \frac{1}{\sqrt{2}}\left|\downarrow_1\uparrow_2\downarrow_3\right\rangle - \frac{1}{\sqrt{2}}\left|\uparrow_1\downarrow_2\downarrow_3\right\rangle \tag{4.77}$$

$$\tau'' = \sqrt{\frac{2}{3}}\left|\downarrow_1\downarrow_2\uparrow_3\right\rangle - \sqrt{\frac{1}{6}}\left|\downarrow_1\uparrow_2\downarrow_3\right\rangle - \sqrt{\frac{1}{6}}\left|\uparrow_1\downarrow_2\downarrow_3\right\rangle \tag{4.78}$$

for $T_z = -\frac{1}{2}$.
The spin functions are defined in a similar way, taking into account the possibility to have total spin $S = \frac{3}{2}$ and therefore symmetric spin functions. For $S = \frac{1}{2}$ and $S_z = +\frac{1}{2}$ we have:

$$\sigma' = \frac{1}{\sqrt{2}}\left|(\downarrow_1\uparrow_2 - \uparrow_1\downarrow_2)\uparrow_3\right\rangle = \frac{1}{\sqrt{2}}\left|\downarrow_1\uparrow_2\uparrow_3\right\rangle - \frac{1}{\sqrt{2}}\left|\uparrow_1\downarrow_2\uparrow_3\right\rangle \tag{4.79}$$

$$\sigma'' = -\sqrt{\frac{2}{3}}\left|\uparrow_1\uparrow_2\downarrow_3\right\rangle + \sqrt{\frac{1}{6}}\left|\uparrow_1\downarrow_2\uparrow_3\right\rangle + \sqrt{\frac{1}{6}}\left|\downarrow_1\uparrow_2\uparrow_3\right\rangle \ ; \tag{4.80}$$

for $S = \frac{1}{2}$ and $S_z = -\frac{1}{2}$:

$$\sigma' = \frac{1}{\sqrt{2}} |(\downarrow_1\uparrow_2 - \uparrow_1\downarrow_2)\downarrow_3\rangle = \frac{1}{\sqrt{2}} |\downarrow_1\uparrow_2\downarrow_3\rangle - \frac{1}{\sqrt{2}} |\uparrow_1\downarrow_2\downarrow_3\rangle \quad (4.81)$$

$$\sigma'' = \sqrt{\frac{2}{3}} |\downarrow_1\downarrow_2\uparrow_3\rangle - \sqrt{\frac{1}{6}} |\downarrow_1\uparrow_2\downarrow_3\rangle - \sqrt{\frac{1}{6}} |\uparrow_1\downarrow_2\downarrow_3\rangle \quad ; \quad (4.82)$$

for $S = \frac{3}{2}$ and $S_z = +\frac{3}{2}$:

$$\sigma^S = |\uparrow_1\uparrow_2\uparrow_3\rangle \quad ; \quad (4.83)$$

for $S = \frac{3}{2}$ and $S_z = +\frac{1}{2}$:

$$\sigma^S = \sqrt{\frac{1}{3}} |\uparrow_1\uparrow_2\downarrow_3\rangle + \sqrt{\frac{1}{3}} |\uparrow_1\downarrow_2\uparrow_3\rangle + \sqrt{\frac{1}{3}} |\downarrow_1\uparrow_2\uparrow_3\rangle \quad ; \quad (4.84)$$

for $S = \frac{3}{2}$ and $S_z = -\frac{1}{2}$:

$$\sigma^S = \sqrt{\frac{1}{3}} |\downarrow_1\downarrow_2\uparrow_3\rangle + \sqrt{\frac{1}{3}} |\downarrow_1\uparrow_2\downarrow_3\rangle + \sqrt{\frac{1}{3}} |\uparrow_1\downarrow_2\downarrow_3\rangle \quad ; \quad (4.85)$$

for $S = \frac{3}{2}$ and $S_z = +\frac{3}{2}$:

$$\sigma^S = |\downarrow_1\downarrow_2\downarrow_3\rangle \quad . \quad (4.86)$$

Like in the case of spatial functions, all spin and isospin functions obey the following symmetry relations:

$$\hat{P}_{12}\sigma^S = \sigma^S \quad (4.87)$$

$$\hat{P}_{13}\sigma^S = \sigma^S \quad (4.88)$$

$$\hat{P}_{23}\sigma^S = \sigma^S \quad (4.89)$$

$$\hat{P}_{12}\sigma' = -\sigma' \quad (4.90)$$

$$\hat{P}_{12}\sigma'' = \sigma'' \quad (4.91)$$

$$\hat{P}_{12}\tau' = -\tau' \quad (4.92)$$

$$\hat{P}_{12}\tau'' = \tau'' \quad . \quad (4.93)$$

Spin and isospin functions are combined into functions of the required symmetry as follows in the case of $S = \frac{1}{2}$:

$$\begin{aligned}
\theta^A &= \frac{1}{\sqrt{2}}(\sigma''\tau' - \sigma'\tau'') \\
\theta' &= \frac{1}{\sqrt{2}}(\sigma''\tau' + \sigma'\tau'') \\
\theta'' &= \frac{1}{\sqrt{2}}(\sigma'\tau' - \sigma''\tau'') \\
\theta^S &= \frac{1}{\sqrt{2}}(\sigma'\tau' + \sigma''\tau'') \quad ;
\end{aligned}$$

and for $S = \frac{3}{2}$:

$$\begin{aligned}
\theta' &= \sigma^S\tau' \\
\theta'' &= \sigma^S\tau'' \quad .
\end{aligned}$$

Finally, for the spin doublet all symmetries are allowed:

$$\begin{aligned}
|\Psi_i^S\rangle &= \mathcal{R}_{r_i}(\rho)\,|\mathcal{Y}^S_{[K]_i}\theta^A\rangle \\
|\Psi_i^M\rangle &= \mathcal{R}_{r_i}(\rho)\,|\mathcal{Y}'_{[K]_i}\theta'' - \mathcal{Y}''_{[K]_i}\theta'\rangle \\
|\Psi_i^A\rangle &= \mathcal{R}_{r_i}(\rho)\,|\mathcal{Y}^A_{[K]_i}\theta^S\rangle \quad ,
\end{aligned}$$

while for the spin triplet only mixed symmetry states are allowed:

$$|\Psi_i^M\rangle = \mathcal{R}_{r_i}(\rho)\,|\mathcal{Y}'_{[K]_i}\theta'' - \mathcal{Y}''_{[K]_i}\theta'\rangle \tag{4.94}$$

In the former definitions, $\mathcal{R}_{r_i}(\rho)$ identifies the hyperradial function associated with the total state $|\Psi_i^X\rangle$, where X identifies the different spatial symmetries $X = S, M, A$.

It can be verified that the complete states $|\Psi_i^X\rangle$ are antisymmetric for exchanges of any two particles.

The basis constructed has two main advantages. Any linear combination of the basis functions is itself antisymmetric, so any calculation which involves an expansion of the wave function on this basis will yield automatically an

antisymmetric result. Secondly, the use of antisymmetrized basis functions makes the calculation of the matrix elements of some operators easier. Let us consider a two-body potential

$$V = \frac{1}{2}\sum_{i,j=1}^{A} V_{ij} \quad , \tag{4.95}$$

with index i, j identifying particle pairs. The calculation of its matrix elements expressed in an antisymmetrized basis may be performed exploiting the symmetry:

$$\langle \Psi_a | V | \Psi_b \rangle = \frac{1}{2}\sum_{i,j=1}^{A} \langle \Psi_a | V_{ij} | \Psi_b \rangle = \frac{A(A-1)}{2} \langle \Psi_a | V_{12} | \Psi_b \rangle \tag{4.96}$$

where Ψ_a and Ψ_b are two states of the antisymmetrized basis.
Anyway, the construction of antisymmetric states starting from functions without defined permutational symmetry becomes more difficult increasing the number of particles. An alternative to this procedure is represented by the use of a nonsymmetrized basis, as explained in the next section.

4.3.2 Nonsymmetrized Hyperspherical Harmonics

As mentioned, the cost of the construction of an antisymmetrized Hyperspherical Harmonics basis is heavier the more particles are involved. The use of a Nonsymmetrized Hyperspherical Harmonics (NSHH) basis avoids this inconvenience; however the procedure to construct antisymmetric wave functions out of nonsymmetrized basis states needs some explanation.
In the following procedure, a set of reversed order mass weighted Jacobi coordinates like the one described in Eq. (4.9) will be considered. The definition of the hyperradial and hyperangular variables is the same as in Eq. (4.12). Also the definition of the spatial part of each basis state follows directly the general definition for Hyperspherical Harmonic functions exposed in Eq. (4.37).
The spin-isospin part of the basis functions are defined, accordingly to the

Jacobi coordinates chosen, in reversed order. The relevant quantum numbers for the spin function are the single particle spins $\{s_1, \ldots, s_A\}$, coupled in reversed order in the following way:

$$|\chi^S\rangle = |\Big[\big[[s_A, s_{A-1}]_{S_2}, s_{A-2}\big]_{S_3}, \ldots, s_1\Big]_{S_A}\rangle \quad , \tag{4.97}$$

so that the spin function is identified by the quantum numbers

$$\{s_1, \ldots, s_A, S_2, \ldots, S_A\} \quad . \tag{4.98}$$

Analogously, the isospin functions are identified by quantum numbers

$$\{t_1, \ldots, t_A, T_2, \ldots, T_A, T_A^z\} \quad , \tag{4.99}$$

where T_A^z is the third projection of the total isospin, coupled as

$$|\chi^T\rangle = |\Big[\big[[t_A, t_{A-1}]_{T_2}, t_{A-2}\big]_{T_3}, \ldots, t_1\Big]_{T_A, T_A^z}\rangle \quad . \tag{4.100}$$

The reason for this choice of ordering lies in the calculation of the Hamiltonian operator matrix elements. A basis state Ψ_i is defined as

$$|\Psi_i\rangle = \mathcal{R}_{r_i}(\rho) \left[\mathcal{Y}_{[K]_i}(\Omega_N) \, |\chi_i^S\rangle\right]_J |\chi^T\rangle \tag{4.101}$$

where $\mathcal{R}_{r_i}(\rho)$ is as usual the hyperradial function, defined as in Eq. (4.43). The collection of quantum numbers specifying a basis function Ψ_i is (omitting all single spin and isospin quantum number which are known to be equal to $\frac{1}{2}$):

$$\begin{aligned} \{r_i, \{l_1, \ldots, l_N\}, \{L_2, \ldots, L_N\}, \{K_2, \ldots, K_N\}, \\ \{S_2, \ldots, S_A\}, J, \{T_2, \ldots, T_A, T_A^z\}\} \quad . \end{aligned} \tag{4.102}$$

As specified before, these functions have no well-defined permutational symmetries: acting with a permutation operator on such functions does not yield a simple sign as a result. It is thus useful to analyze the properties of Hyperspherical Harmonics under the action of permutation operators $\hat{P}_{ij}$.

First, let us note that any permutation operator $\hat{P}_{ij}$ exchanging two particles can be expressed as a product of permutation operators of the kind $\hat{P}_{i,i+1} = \hat{P}_i$. When acting with $\hat{P}_i$, the only interested coordinates are $\boldsymbol{\eta}_{A-1}$ and $\boldsymbol{\eta}_{A-i+1}$. The only quantum numbers affected are then l_{A-i}, l_{A-i+1}, L_{A-i} and K_{A-i}. L_{A-i+1} and K_{A-i+1} are not influenced (like instead l_{A-i+1}) because they are cumulative quantum numbers. In the particular case $i = 1$, $\hat{P}_1$ exchanges particles 1 and 2, the only Jacobi vector influenced being $\boldsymbol{\eta}_N$, which is reversed, and in this case all quantum numbers are conserved. In the case $i = A - 1$, $\hat{P}_{A-1}$ exchanges particles $A - 1$ and A, affecting only $\boldsymbol{\eta}_1$ and $\boldsymbol{\eta}_2$; the only involved quantum numbers are then l_1 e l_2.
The matrix elements of the permutation operators $\hat{P}_i$ on the hyperspherical part of the basis are known and are related to the Raynal-Revai [37] and Tree-recoupling coefficients (see for example [38]). Since the only quantum numbers affected are the ones mentioned, for each operator $\hat{P}_i$ we have

$$\begin{aligned}\hat{P}_i \mathcal{Y}_{[K]_a} = & \sum_{l_{A-i_a} l_{A-i+1_a} L_{A-i_a} K_{A-i_a}} c_{l_{A-i_a} l_{A-i+1_a} L_{A-i_a} K_{A-i_a}, l_{A-i_b} l_{A-i+1_b} L_{A-i_b} K_{A-i_b}} \\ & \mathcal{Y}_{[K]_b} \prod_{j \neq A-i, A-i+1} \delta_{l_{j_a} l_{j_b}} \prod_{m \neq A-i} \delta_{L_{m_a} L_{m_b}} \delta_{K_{m_a} K_{m_b}} \end{aligned} \tag{4.103}$$

where the product of deltas runs over all values of j and m allowed. The former expression of the matrix elements for the permutations shows that each matrix representing an operator $\hat{P}_i$ is *block diagonal* if a proper ordering is chosen for the basis functions: the ordering is simply found by the grouping the basis states which have the same values of the conserved quantum numbers.
The action of permutations of consecutive particles on the spin-isospin functions can be calculated by means of 6-j symbols; the hyperradial function is not affected.
Also the recoupling of the various angular moments can be performed by means of 6-j and 9-j symbols.
The use of a nonsymmetrized basis in calculations is explained in the following section.

Use of Nonsymmetrized Hyperspherical Harmonics

The formalism developed to work with nonsymmetrized basis has been developed in the last years (see for example [39, 40]).
In general, it is necessary to calculate matrix elements of the kind

$$\langle\Psi_a|\hat{H}|\Psi_b\rangle = \langle\Psi_a|\hat{T}|\Psi_b\rangle + \langle\Psi_a|\hat{V}|\Psi_b\rangle \tag{4.104}$$

where $|\Psi_a\rangle$ and $|\Psi_b\rangle$ are defined by Eq. (4.101). The calculation of the matrix elements of the kinetic energy is quite simple, thanks to the properties of the Hyperspherical Harmonics and Laguerre polynomials. Since the reversed order Jacobi coordinates are used, the most convenient expression for a two-body potential matrix element is

$$\langle\Psi_a|\hat{V}^{2-b}|\Psi_b\rangle = \sum_{i<j}\langle\Psi_a|\hat{V}_{ij}|\Psi_b\rangle = \sum_{i<j}\langle\Psi_a|\hat{P}^\dagger_{1i}\hat{P}^\dagger_{2j}\hat{V}_{12}\hat{P}_{2j}\hat{P}_{1i}|\Psi_b\rangle \quad , \tag{4.105}$$

since the coordinate $\boldsymbol{\eta}_N$ is proportional to the relative distance of particles 1 and 2, and all quantum numbers relative to the couple $l_{12} = l_N$, S_{12}, J_{12} and T_{12} are easily obtainable via 6-j and 9-j symbols. The permutations $\hat{P}_{1i}$ and $\hat{P}_{2j}$ which exchange particles 1 with i and 2 with j respectively may be expressed as a product of permutations of consecutive particles, which, as said, can be represented by block diagonals matrices. An analogous expression holds for three-body potentials

$$\langle\Psi_a|\hat{V}^{3-b}|\Psi_b\rangle = \sum_{i<j<k}\langle\Psi_a|\hat{V}_{ijk}|\Psi_b\rangle = \sum_{i<j<k}\langle\Psi_a|\hat{P}^\dagger_{1i}\hat{P}^\dagger_{2j}\hat{P}^\dagger_{3k}\hat{V}_{123}\hat{P}_{3k}\hat{P}_{2j}\hat{P}_{1i}|\Psi_b\rangle \quad , \tag{4.106}$$

where coordinates $\boldsymbol{\eta}_N$ and $\boldsymbol{\eta}_{N-1}$ are this time involved in the calculation. The procedure can in principle be extended to any many-body potential.
The former procedure describes the construction of the Hamiltonian matrix in terms of a nonsymmetrized basis. The procedure to ensure the construction of antisymmetric wave functions is presented for example in [41] or [42]. It

involves the Casimir operator of the permutation group for A particles

$$\hat{C}(A) = \sum_{j>i=1}^{A} \hat{P}_{ij} \quad , \tag{4.107}$$

which is a sum of permutation operators over all couples of particles. This operator commutes with the Hamiltonian, since all permutations do:

$$\left[\hat{H}, \hat{P}_{ij}\right] = 0 \Rightarrow \left[\hat{H}, \hat{C}(A)\right] \quad , \tag{4.108}$$

and so the eigenstates of the Hamiltonian (the states solving the Schrödinger equation) are also eigenstates of $\hat{C}(A)$.
The eigenvalues $\lambda_S, \lambda_M, \lambda_A$ of the Casimir operator are

$$\hat{C}(A)\,|S\rangle = \sum_{j>i=1}^{A} \hat{P}_{ij}\,|S\rangle = (1 + \ldots + 1)\,|S\rangle = \frac{A(A-1)}{2}\,|S\rangle = \lambda_S\,|S\rangle \quad ; \tag{4.109}$$

$$\hat{C}(A)\,|M\rangle = \sum_{j>i=1}^{A} \hat{P}_{ij}\,|M\rangle = \lambda_M\,|M\rangle \quad ; \tag{4.110}$$

$$\hat{C}(A)\,|A\rangle = \sum_{j>i=1}^{A} \hat{P}_{ij}\,|A\rangle = (-1 + \ldots - 1)\,|A\rangle = -\frac{A(A-1)}{2}\,|A\rangle = \lambda_A\,|A\rangle \quad ; \tag{4.111}$$

where $|S\rangle$ denotes fully symmetric states, $|M\rangle$ states of mixed symmetry and $|A\rangle$ antisymmetric states. Of course

$$-\frac{A(A-1)}{2} = \lambda_A < \lambda_M < \lambda_S = \frac{A(A-1)}{2} \quad . \tag{4.112}$$

Then the diagonalization of the operator

$$\hat{H}' = \hat{H} + \gamma \hat{C}(A) \tag{4.113}$$

yields eigenvalues

$$E'_{n,X} = E_{n,X} + \gamma \lambda_X \quad , \tag{4.114}$$

where $X = S, M, A$ indicates the possible symmetry of the eigenstate correspondent to $E_{n,X}$ and $E'_{n,X}$, with $\gamma > 0$ a parameter. If the value of γ is chosen to be large enough, the lowest eigenstates will be antisymmetric states, corresponding to $\lambda_A = -\frac{A(A-1)}{2}$. If the states of interest are the lowest k antisymmetric states, the following relation must hold:

$$E'_{i,A} = E_{i,A} + \gamma\lambda_A < E_{n,X} + \gamma\lambda_X \quad \forall n, \quad \forall i \leq k, \quad \forall X = S, M \quad , \tag{4.115}$$

which means

$$\gamma > \frac{E_{k,A} - E_{0,X}}{\lambda_X - \lambda_A} \quad \forall X = S, M \quad , \tag{4.116}$$

where $E_{0,X}$ is the lowest state which is not antisymmetric. The symmetry of the states may be checked after the calculation by the application of the Casimir operator, or each permutation operators (for the wave function to be antisymmetric, it is sufficient for the state to be antisymmetric with respect to each permutation of consecutive particles).

It has to be noted that the discussion so far is valid for a complete basis $\{|\Psi_a\rangle\}$, $a = 1, \ldots, \infty$; in practical applications, a subspace of the one generated by the complete basis is used: $\{|\Psi_a\rangle\}$, $a = 1, \ldots, N_{basis}$. Each operator $\hat{O}$ (in particular $\hat{C}(A)$, $\hat{H}$ and the identity $\hat{1}$) is then substituted by its projected $\hat{P}\hat{O}\hat{P}$, $\hat{P} = \sum_{a=1}^{N} |\Psi_a\rangle \langle\Psi_a|$ being the projection operator on the subspace generated by the truncated basis. Also in this case

$$\left[\hat{C}(A), \hat{P}\hat{H}\hat{P}\right] = 0 \tag{4.117}$$

because the basis functions are eigenfunctions of the operators $\hat{K}^2$, $\hat{L}^2$, $\hat{S}^2$, $\hat{J}^2$, $\hat{T}^2$, which all commute with $\hat{C}(A)$; so λ is a good quantum number also for the eigenstates of $\hat{P}\hat{H}\hat{P}$.

The presented procedure shows how to find antisymmetric eigenstates of the Hamiltonian on a nonsymmetrized Hyperspherical Harmonics basis. The method is particularly well-suited for the use in combination with the Lanczos algorithm, which fastens the extraction of the lowest eigenstates of a matrix avoiding the complete diagonalization of the matrix itself.

4.4 Laguerre polynomials basis

The last basis used in this work is a Laguerre polynomial basis. Again, its use is limited to the three-body case; also in this case more than one coordinate system is considered, with the definitions of Eq. (4.50-4.57). Instead of constructing hyperspherical coordinates, the Jacobi vectors will be used directly. The spatial part of basis chosen is defined by means of the following functions:

$$\begin{aligned}\psi^{(a)}_{spatial} &= \mathcal{R}^{[1]}_{n_1}\left(\eta^{(a)}_1\right) Y^{m_1}_{l_1}\left(\theta^{(a)}_1,\phi^{(a)}_1\right) \\ &\quad \mathcal{R}^{[2]}_{n_2}\left(\eta^{(a)}_2\right) Y^{m_2}_{l_2}\left(\theta^{(a)}_2,\phi^{(a)}_2\right) \langle LM|l_1m_1l_2m_2\rangle \qquad (4.118)\end{aligned}$$

and analogous definitions for $\psi^{spatial}_{(c)}$ and $\psi^{spatial}_{(d)}$. The symbol $\langle LM|l_1m_1l_2m_2\rangle$ denotes a Clebsch-Gordan coefficient.
The radial functions $\mathcal{R}^{[1,2]}_n(\eta)$ are defined analogously to what is done in Eq. (4.43):

$$\mathcal{R}^{[1]}_{n_1}(\eta) = \sqrt{\frac{n_1!}{(n_1+2)!}} L^2_{n_1}(\frac{\eta}{b_1}) e^{-\frac{\eta}{2b_1}} b_1^{-\frac{3}{2}} \qquad (4.119)$$

$$\mathcal{R}^{[2]}_{n_2}(\eta) = \sqrt{\frac{n_2!}{(n_2+2)!}} L^2_{n_2}(\frac{\eta}{b_2}) e^{-\frac{\eta}{2b_2}} b_2^{-\frac{3}{2}} \quad . \qquad (4.120)$$

Then we define

$$\psi^{(a)} = \psi^{(a)}_{spatial}\chi^S_{(a)}\chi^T_{(a)} \quad , \qquad (4.121)$$

where the spin and isospin functions are defined to have spin and isospin equal to 1 or 0 for the first two particles (the particles identified by $\boldsymbol{\eta}^{(a)}_1$), and total spin and isospin S and $T = \frac{1}{2}$. The total antisymmetric wave function is given by

$$\Psi_i = \psi^{(a)}_i + \psi^{(c)}_i + \psi^{(d)}_i \quad , \qquad (4.122)$$

where $\psi^{(c)}_i$ and $\psi^{(d)}_i$ corresponds to the respective sets of coordinates, as defined in Eq. (4.50-4.57). The advantage in the former definition of the basis lies in the explicit description of the relative coordinate between the

third particle and the center of mass of the pair, the dynamical coordinate for calculations in the case of 2+1 scattering.

Chapter 5

Discussion of results

In this chapter the results obtained for the three-nucleon photodisintegration as well for 2+1 and 4+1 scattering are discussed. The calculations presented in the following have been performed using the central two-body Malfliet-Tjon [29] I/III (MT-I/III) potential. The MT-I/III potential is a sum of Yukawa terms, with different parameters depending on the total spin $S = 0, 1$ and total isospin $T = 0, 1$ of the couple of nucleons. Its explicit definition is the following:

$$V^{S,T}(r) = V_A \frac{e^{-\mu_A r}}{r} - V_B \frac{e^{-\mu_B r}}{r} \quad , \tag{5.1}$$

with parameters given in Table 5.1. It has to be precised that, whereas usually

Table 5.1: Parameters for the MT-I/III potential

	V_A (MeV)	μ_A (fm^{-1})	V_B (MeV)	μ_B (fm^{-1})
$S = 0, T = 0$	0		0	
$S = 0, T = 1$	1458.258	3.110	520.948	1.555
$S = 1, T = 0$	1458.258	3.110	635.398	1.555
$S = 1, T = 1$	0		0	

the MT-I/III potential is chosen to be active only when the two nucleons have relative angular momentum $L = 0$ (s-wave potential), in this parametrization the potential is active in all partial waves.

5.1 The ^{3}He photodisintegration cross section

An important aim of this work is to investigate the precision of LIT calculations for the photodisintegration cross section of the ^{3}He nucleus:

$$^3\mathrm{He} + \gamma \rightarrow {}^2\mathrm{H} + p \quad . \tag{5.2}$$

It is of great interest to check whether such a LIT calculation is able to reproduce the correct low-energy cross section in presence of the Coulomb barrier. The LIT calculations, as described in Chapter 3.4, are based on the expression of the transform of the response function as a sum of Lorentzians. The position of the peak of each Lorentzian is given by the eigenvalues of the Hamiltonian expressed in the basis chosen: the main ingredients of the LIT method are the eigenstates and eigenvalues of the Hamiltonian. If the density of such LIT states is low in a certain energy region, then in this region there is not sufficient information for a very detailed distribution of strength. Moreover, if the response function is very small, contributions coming from Lorentzians corresponding to other energies may be present if the density of LIT states is not high enough to allow a higher accuracy (namely a smaller width of these Lorentzians). In fact such a tiny cross section is found for the reaction considered close to the breakup threshold. This is due to the Coulomb barrier between the two fragments.
In the following, the LIT results for the response function of the ^{3}He photodisintegration with the MT-I/III potential in unretarded dipole approximation are discussed (see Chapter 2.1).
It may be difficult in a LIT calculation to obtain a high enough number of states in the energy region of interest. This is needed in order to perform a reliable inversion of the LIT and thus to obtain proper response functions. The usual approach to few-body problems with the LIT method relies on an expansion of the states on a Hyperspherical Harmonics basis. A symmetrized basis (see Chapter 4.3.1) with a Jastrow correlation factor consisting of proper two-nucleon correlation functions $f_{corr}(r)$ (see for example [43]) has been used for the calculations shown in Figures 5.1 and 5.2, with dif-

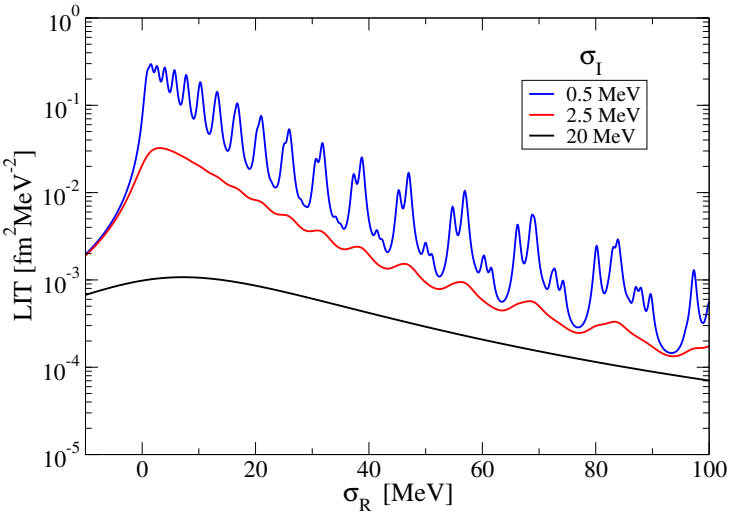

Figure 5.1: LIT for ^{3}He photodisintegration with HH basis: the basis is composed of 30 hyperspherical states and 31 hyperradial states, for a total of 930 states. The value of the hyperradial parameter is $b = 0.3$ fm. LIT functions for the values of $\sigma_I = 20$, 2.5 and 0.25 MeV are shown.

ferent values for the parameter b which defines the range of the hyperradial functions of Eq. (4.43). The single peaks which can be observed in the LIT functions when a small value of σ_I is used correspond to contributions of single Lorentzian functions: in fact the Lorentz kernel of Eq. (3.88) tends to a delta function in the limit $\sigma_I \to 0$. If the limit is reached, only single peaks located at energies

$$\sigma_R = E_i \tag{5.3}$$

would be present, E_i being the eigenvalues of the Hamiltonian in the basis chosen.

Figure 5.1 shows the LIT function for an HH basis of 30 states and an hyperradial basis of 31 states, with the value for the hyperradial parameter of $b = 0.3$ fm. The plot shows that in this case $\sigma_I = 2.5$ MeV is already critical at higher energies, whereas for $\sigma_I = 0.5$ MeV the single Lorentzians are even very pronounced at low energies. The appearance of visible single peaks is the signature of a low density of LIT states.

In general an increase in the value of b shifts the lowest LIT states to lower energy values, while increasing the size of the basis increments the number of

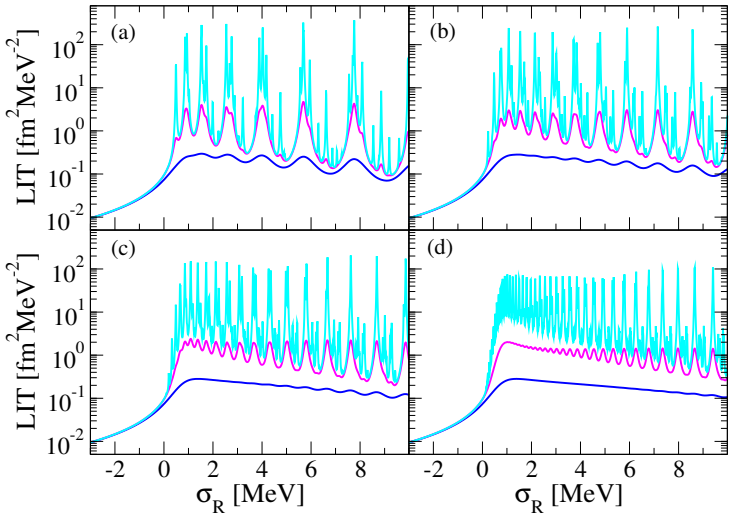

Figure 5.2: LIT for ^{3}He photodisintegration with HH basis and different sets of parameters. Results for the values of $\sigma_I = 0.5$ (blue lines), 0.1 (magenta lines) and 0.01 MeV (cyan lines) are shown. Panel (a): 30 hyperspherical states and 31 hyperradial states, for a total of 930 states; the hyperradial parameter is $b = 0.3$ fm. Panel (b): 40 hyperspherical states and 51 hyperradial states, for a total of 2040 states; $b = 0.3$ fm. Panel (c): as in (b), but with $b = 0.5$ fm. Panel (d): 40 hyperspherical states and 76 hyperradial states, for a total of 3040 states; $b = 1.0$ fm.

eigenstates of the Hamiltonian (note that $\sigma_R = 0$ MeV represents the three-body breakup threshold). Figure 5.2 shows the LIT for different basis sets and small σ_I values of 0.5, 0.1 and 0.01 MeV. In panel (a) the results for the same basis sets as the one in Figure 5.1 is shown, but for $\sigma_R \leq 10$ MeV and smaller values of σ_I. In panels (b), (c) and (d) the number of basis states and the value of the parameter b is increased, leading to a higher density of states. One sees that even with rather long-ranged hyperradial functions ($b = 1.0$ fm) and 3040 basis states (panel (d) of Figure 5.2) no LIT state is present below $\sigma_R = 0$ MeV.

To overcome this problem, the Laguerre basis defined in Chapter 4.4 has been used in the calculation of the LIT. This kind of basis presents various eigenstates of the Hamiltonian in the energy region under the three-body breakup threshold already with a relatively small number of basis states. The parameters for this basis are the number of Laguerre functions for the couple and

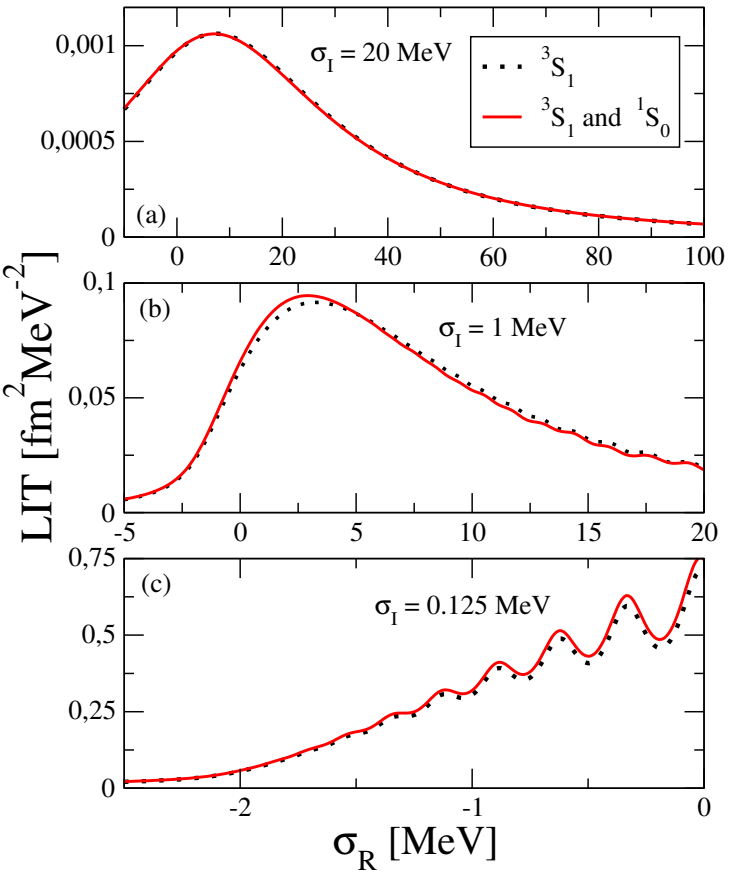

Figure 5.3: LIT for ^{3}He photodisintegration with the Laguerre (new) basis. Parameters: $N_2 = 18$, $N_3 = 70$ for $^3S_1$ states, $N_2 = 6$ and $N_3 = 20$ for $^1S_0$ states; $b_1 = 0.75$ fm and $b_2 = 0.5$ fm.

for the third particle N_2 and N_3 ($n_1 = 0, \ldots, N_2 - 1$ and $n_2 = 0, \ldots, N_3 - 1$) and the values of b_1 and b_2 entering Eq. (4.119) and (4.120). In Figure 5.3 LIT results for this new basis are shown. In this basis only states with $l_1 = 0$ (meaning that the particle pair described by the coordinate η_1 are in an s-wave state, while the orbital angular momentum of the third particle with respect to the pair is $l_2 = 1$) are taken into account. In principle all different possibilities for the momenta should be considered, but later it is pointed out that the contributions for $l_1 \geq 1$ are negligible (see discussion of Figure 5.5). The HH basis, on the other hand, in principle includes all possible values of orbital angular momenta between the particles, their number being limited only by the maximum value of the hyperangular quantum number K_2. The

basis taken for the results in Figure 5.3 consists of two types of functions: in the first ("triplet" states) the nucleon pair described by coordinate η_1 is in a $^3S_1$ state, while in the second ("singlet" states) it is in a $^1S_0$ state. The number of basis states used for the results in Figure 5.3 are $N_2 = 18$ and $N_3 = 70$ for the triplet states, and $N_2 = 6$ and $N_3 = 20$ for the singlet (the radial range parameters are $b_1 = 0.75$ fm and $b_2 = 0.5$ fm). The convergence for the singlet states is in fact much faster and a small number of states is sufficient, since, as Figure 5.3 shows, the by far dominant contribution to the LIT comes from the triplet states of the basis (it has to be noted that all couples of particles are considered and that the basis states are antisymmetric, so all channels of the interaction can be active).

In Figure 5.4 the convergence of the LIT function is shown in the energy range below the three-body breakup threshold with respect to the number of basis states for the pair coordinate (N_2) and the third particle Jacobi coordinate (N_3). One observes that with $N_3 = 70$ a sufficient convergence is

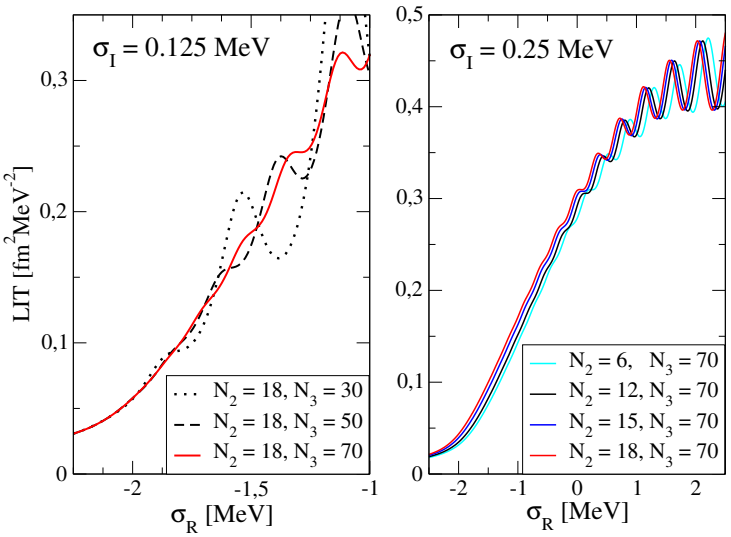

Figure 5.4: Convergence of the LIT for ^{3}He photodisintegration with Laguerre (new) basis. Left panel: convergence pattern for N_3 with $\sigma_I = 0.125$ MeV. Right panel: convergence pattern for N_2 with the value $\sigma_I = 0.25$ MeV ($b_1 = 0.75$ fm and $b_2 = 0.5$ fm).

obtained, especially at low energies. On the contrary for increasing values of N_2 one notes a tiny shift of the LIT towards smaller σ_R and higher values for

N_2 have to be used in order to reach a complete convergence for the transform.

A comparison between the LIT obtained with the HH basis and the Laguerre basis is shown in Figure 5.5. For $\sigma_I = 20$ MeV the two transforms are in very

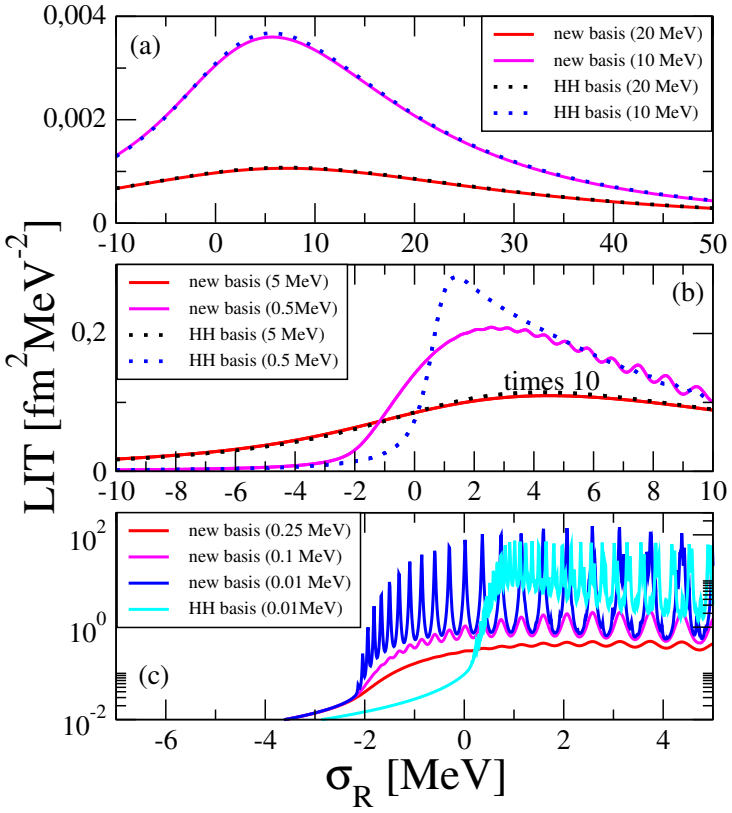

Figure 5.5: Comparison between the LIT with HH and Laguerre (new) basis (the value σ_I is given in parenthesis). In panel (a) the results for large values of σ_I (see text). In panels (b) and (c) the differences between the two basis sets with small σ_I in the breakup threshold region are shown.

good agreement, showing that $l_1 \geq 1$ values are not important for the new basis in this case. The figure also illustrates that, with decreasing σ_I the agreement between the results with HH and new basis worsens more and more. In particular it is evident that the transform with the HH basis has too little strength in the energy region below the three-body breakup threshold ($\sigma_R < 0$ MeV). Contrary to the HH basis (compare results of $\sigma_I = 0.01$ MeV in panel (c) of Figure 5.5), the new basis has quite a number of LIT

states close to the two-body breakup threshold at $\sigma_R = -2.2$ MeV which corresponds to the deuteron ground state energy with the MT-I/III potential. In fact a smooth result for the LIT is found at very low energies for quite small σ_I values of 0.25 MeV and 0.125 MeV (see also Figure 5.4). One also notices (see results for $\sigma_I = 0.5$ MeV in panel (b) of Figure 5.5) that, due to the lack of low-energy LIT states in case of the HH basis, strength is artificially shifted from the low-energy region to the region above the three-body breakup threshold (as already mentioned total strength in both calculations coincides rather well, as seen from the very good agreement for $\sigma_I = 20$ MeV).

In order to obtain the ^{3}He photodisintegration cross section one needs to invert the LIT (see Chapter 3.4). The following set of functions is used for the inversion:

$$f_i(E) = P_{tunnel}(E) e^{-\alpha \frac{E}{i}} \quad , \tag{5.4}$$

where $P_{tunnel}(E)$ is the Gamow factor defined in Eq. (2.5) and α is a nonlinear fit parameter. The quality of the inversion of the LIT is of course affected by the precision of the calculated LIT function. Structures in the response function with a size smaller than the distance between two LIT states cannot be resolved, thus a not sufficient density of LIT states may result in a poor response function after the inversion. On the other hand, if the density of LIT states is high enough, a smaller value of σ_I leads to a sufficiently convergent LIT. In the case of the HH basis, the inversion of the transform with values of $\sigma_I \leq 10$ MeV already presents the signature of the fact that the LIT is not correct at low σ_R, leading to unstable inversion results, whereas with $\sigma_I = 20$ MeV rather stable inversion results are obtained. On the contrary, for the new basis the density of LIT states is sufficiently high that very stable inversion results are obtained even with $\sigma_I = 0.125$ MeV. Figure 5.6 presents the cross section for the photodisintegration reaction, obtained via such inversions of the LIT function. As seen in panel (a) one finds a very good agreement for both basis sets in the whole energy range considered. The incorrect LIT for the HH basis leads mainly to a small shift of the peak to higher energies, whereas the peak height is the same as for the new basis. In panel (b) of

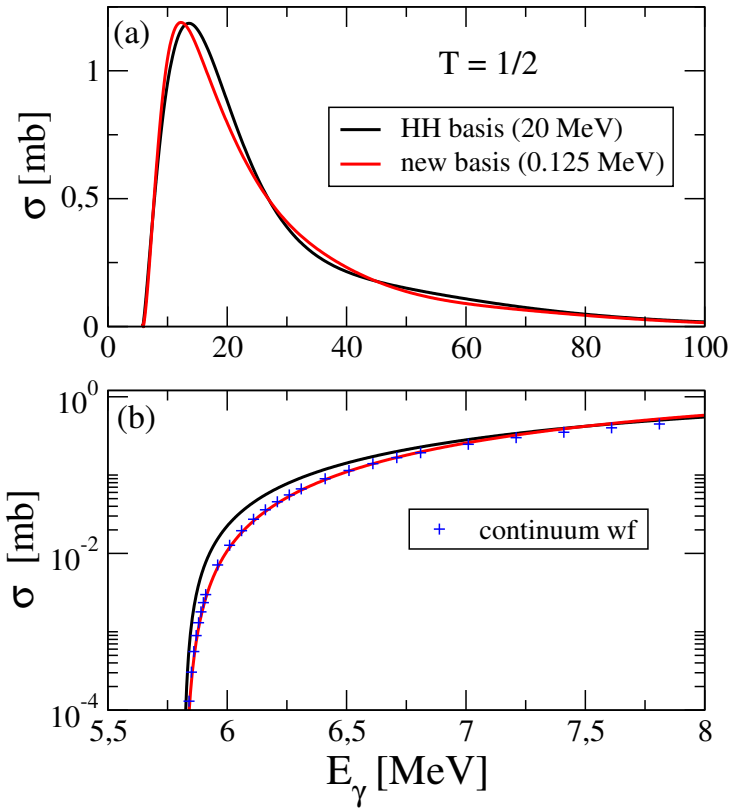

Figure 5.6: ^{3}He photodisintegration cross section in function the photon energy E_γ obtained via LIT with HH and Laguerre (new) basis. The new basis allows the use of small values of σ_I (see text). In panel (b), a comparison with the direct calculation (continuum wf, with maximum values of $K = 19$ and $N = 10$, further details in section 5.2.1) obtained with method I (see Chapter 3.2) is shown.

Figure 5.6 the low-energy cross section is shown. One sees that there is a not negligible difference between results of the HH and the new basis (note the logarithmic scale). A comparison of these results is made with the result of a direct calculation, where the Schrödinger equation is solved for a continuum state (method I described in Chapter 3.2 is used). The Kohn Variational Principle is used to calculate the second order estimate of the phase shift for the scattering wave function of Eq. (5.2), and then this second order value is used as a parameter to recalculate the coefficients of the expansion of the core part of the wave function. This does not represent a second order estimate for all the parameters which determine the scattering wave function, but it

ensures that it has a better estimate of the phase shift value and that it solves the Schr̈odinger equation. The scattering wave function so obtained is used to calculate the transition matrix element of the dipole operator between the ground state of ^{3}He and the scattering state

$$\langle \Psi_f | \mathbf{D} | \Psi_0 \rangle \quad , \tag{5.5}$$

(see discussion in Chapter 2.1). Results for such a calculation, performed with a symmetrized HH basis (in combination with Jastrow two-body correlation functions), are shown in panel (b) of Figure 5.6, as well as the same LIT results of panel (a) in the low-energy region. As already mentioned, the density of LIT states is much higher in the case of the Laguerre basis, allowing a value of $\sigma_I = 0.125$ MeV for the inversion. This higher precision in the transform influences strongly the value of the cross section at low energies. The very good agreement of the direct calculation with the LIT results obtained with the Laguerre basis confirms that this basis is more suited for low-energy calculations than the HH basis.
In Figure 5.7 also the calculation of the S-factor for the capture reaction ^{2}H+p (related to the photodisintegration as explained in Eq. (2.10)) is given for the direct calculation and the LIT with the Laguerre basis. Since the main energy dependence of the photodisintegration cross section (Gamow factor) is taken out in the S-factor, a more precise comparison between the results can be made. In fact here one notices still some differences between the LIT result and the result of the direct calculation. It is shown in the figure how increasing the size (from $N_2 = 15$ to $N_2 = 18$) of the Laguerre basis the result for the S-factor moves towards the one of the direct calculation. In fact already in the discussion of Figure 5.4 it is noted that the complete convergence with respect to N_2 is not reached. New calculations (with N_2 up to the value of 25) are in progress, in the aim to reach full agreement also for the calculation of the S-factor.

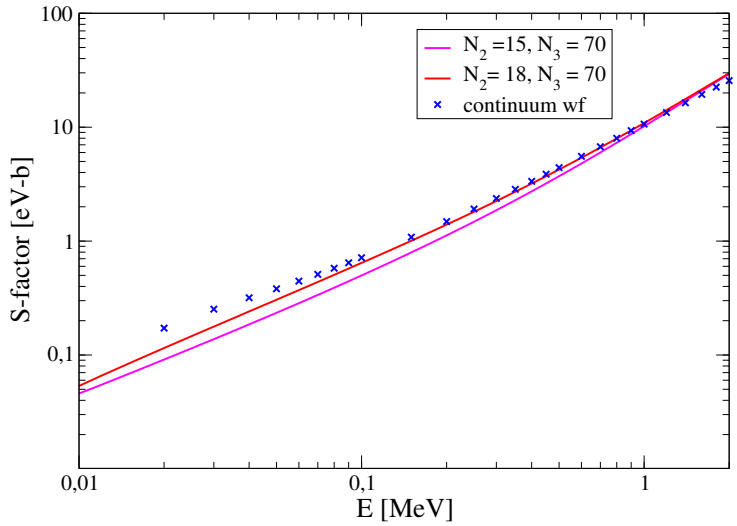

Figure 5.7: S-factor for the capture reaction ^{2}H+p. Results of the direct calculation (continuum wf, as in Figure 5.6), and with the LIT using the Laguerre basis with $N_2 = 15, 18$ and $N_3 = 70$ are shown.

5.2 2+1 and 4+1 scattering

In the following the results for the phase shifts are discussed. The various methods of calculation discussed in Chapter 3 are applied. The discussion starts with the p-wave phase shift of proton-deuteron scattering. Note that the corresponding continuum wave functions are used in the preceding section to calculate the ^{3}He photodisintegration cross section.
In a following section the discussion is turned to s-wave scattering for neutron-deuteron and proton-deuteron scattering (doublet and quadruplet cases).
The third section is devoted to s-wave phase shifts in neutron-^{4}He scattering. Differently from the nucleon-deuteron scattering case, for the five-body problem a very simplistic NN potential is used, namely the Volkov potential [44].

5.2.1 p-wave phase shifts for p-^{2}H scattering

Method I (see Chapter 3.2) used in the calculation of the photodisintegration cross section also provides results for the phase shifts of the associated scattering state. The basis used is the same as for the photodisintegration cal-

Table 5.2: Phase shifts for the p-wave p-^{2}H scattering, in the channel $S = \frac{1}{2}$, obtained with method I with HH basis (maximum values of the hyperspherical quantum number $K = 19$ and number of hyperradial functions $N = 11$).

E (MeV)	δ (degrees)	E (MeV)	δ (degrees)
0.01	$-1.09 \cdot 10^{-3}$	0.5	-2.40
0.02	$-3.32 \cdot 10^{-3}$	0.6	-2.96
0.03	$-9.53 \cdot 10^{-3}$	0.7	-3.48
0.04	$-2.04 \cdot 10^{-2}$	0.8	-3.96
0.05	$-3.58 \cdot 10^{-2}$	0.9	-4.32
0.06	$-5.56 \cdot 10^{-2}$	1.0	-4.79
0.07	$-7.95 \cdot 10^{-2}$	1.2	-5.45
0.08	-0.107	1.4	-5.96
0.09	-0.138	1.6	-6.32
0.1	-0.172	1.8	-6.55
0.2	-0.635	2.0	-6.67
0.3	-1.21	2.2	-6.68
0.4	-1.81		

culation, namely a HH basis (including proper two-body Jastrow correlation functions), with maximum values of $K = 19$ (definining the Hyperspherical functions) and $N = 11$ (for the hyperradial part, where the parameter $r = 0, \ldots, N-1$, is the one of Eq. (4.43)), for a total of 803 functions in the basis. The following form for the regularization function (see Eq. (3.26)) has been chosen in the case of p-wave scattering:

$$g_{reg}(\eta_2) = (1 - e^{-b_{reg}\eta_2})^3 \quad , \tag{5.6}$$

where η_2 denotes the Jacobi coordinate which represents the position of the scattering nucleon relative to the deuteron. In table 5.2 the results for p-^{2}H scattering for the $S = \frac{1}{2}$ channel are given. The presented results have a good convergence (estimated error being less than about 1%). A little variation of the results with the regularization parameter b_{reg} is within the accuracy of the calculations, but results could be further improved, at least partially, by a still higher precision for the matrix elements to be calculated. Table 5.3 shows as a typical example the convergence pattern for increasing values of K

Table 5.3: Convergence in the hyperangular quantum number K for the phase shift for the p-wave p-^{2}H scattering, in the channel $S = \frac{1}{2}$, obtained with method I with HH basis (maximum values of $K = 19$ and $N = 11$). The value of energy is $E = 0.4$ MeV and $b_{reg} = 0.2$, 0.3 and 0.5 fm^{-1}.

K	δ (degrees)		
	$b_{reg} = 0.2$ fm^{-1}	$b_{reg} = 0.3$ fm^{-1}	$b_{reg} = 0.5$ fm^{-1}
1	-1.868	-1.871	-1.907
11	-1.820	-1.810	-1.813
15	-1.815	-1.804	-1.802
17	-1.813	-1.802	-1.798
19	-1.812	-1.800	-1.794

in the case of energy of the projectile (in the center of mass system) $E = 0.4$ MeV and values of $b_{reg} = 0.2$, 0.3 and 0.5 fm^{-1}. A comparison between this results and other techniques is given further below.

Another attempt to study the p-wave scattering problem of a proton off a deuteron is made with method II presented in Chapter 3.3. This method relies on the diagonalization of the Hamiltonian on the basis used to find the values of energy suitable for the calculation. As mentioned, for the HH

Table 5.4: Phase shifts for the p-wave p-^{2}H scattering, in the channel $S = \frac{1}{2}$, obtained with method II in the Laguerre basis, with parameters $N_2 = 15$, $N_3 = 70$, $b_1 = 0.75$ fm, $b_2 = 0.3$ fm. Results for different values of b_{reg} are shown.

E (MeV)	δ (degrees)		
	$b_{reg} = 0.5$ fm^{-1}	$b_{reg} = 1.0$ fm^{-1}	$b_{reg} = 2.0$ fm^{-1}
$6.982 \cdot 10^{-2}$	$-8.88 \cdot 10^{-2}$	$-8.96 \cdot 10^{-2}$	$-9.02 \cdot 10^{-2}$
0.2148	-0.794	-0.800	-0.804
0.3909	-1.93	-1.95	-1.96
0.6197	-3.36	-3.39	-3.40
0.9055	-4.82	-4.87	-4.89
1.250	-6.13	-6.19	-6.22
1.654	-7.11	-7.18	-7.22
2.118	-7.67	-7.73	-7.78

Table 5.5: Phase shifts for the p-wave p-^{2}H scattering, in the channel $S = \frac{1}{2}$, obtained with method II in the Laguerre basis, with parameters $N_2 = 15$, $N_3 = 70$, $b_1 = 0.75$ fm, $b_2 = 0.5$ fm.

only triplet states		triplet + singlet states	
E (MeV)	δ (degrees)	E (MeV)	δ (degrees)
$2.412 \cdot 10^{-2}$	$-5.75 \cdot 10^{-3}$	$2.412 \cdot 10^{-2}$	$-5.74 \cdot 10^{-3}$
0.1132	-0.25	0.1132	-0.25
0.2025	-0.73	0.2025	-0.72
0.3064	-1.40	0.3064	-1.38
0.4298	-2.21	0.4298	-2.18
0.5749	-3.13	0.5748	-3.07
0.7431	-4.08	0.7430	-3.98
0.9342	-5.01	0.9339	-4.84
1.149	-5.86	1.149	-5.60
1.389	-6.60	1.388	-6.21
1.654	-7.18	1.653	-6.63
1.945	-7.60	1.943	-6.82

basis it is difficult to find eigenstates of the Hamiltonian in the energy region below the three-body breakup threshold. On the contrary, a Laguerre basis, the same as used in the LIT calculations, can be taken to calculate the phase shifts. Using different values of the parameters b_1 and b_2 appearing in the definition of the basis in Eq. (4.119) and Eq. (4.120), different eigenenergies can be obtained. As a first step, only the triplet basis states (see discussion of Figure 5.3) are used, and values for the basis parameters are $N_2 = 15$, $N_3 = 70$, $b_1 = 0.75$ fm, $b_2 = 0.3$ fm. The regularization function is the same as in Eq. (5.6). Also in this case, as shown in detail in Table 5.4, results present some variation for different values of the parameter b_{reg}; anyway, in this case increasing the value of b_{reg} leads to a rather stable result. It has to be noted that the Laguerre basis presents a direct relation between the asymptotic functions, the regularization functions and the basis functions themselves: all these functions are defined explicitly by means of the same coordinates, whereas this is not the case for the HH basis, where the hyperradial and hyperangular coordinates are chosen.

A different set of parameters can be used in order to increase the number of

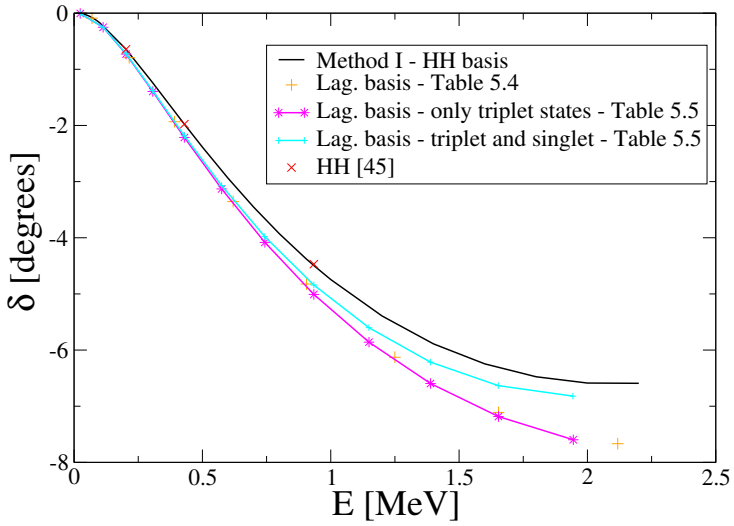

Figure 5.8: Phase shifts calculated with the different methods. Results for method I with the HH basis and method II referring to Tables 5.4 and 5.5 with and without the inclusion of singlet states, as well as the reference [45], are shown.

states in the energy region of interest. Table 5.5 presents the results for the basis obtained varying the value of b_2 from $b_2 = 0.3$ fm to $b_2 = 0.5$ fm. The inclusion of the singlet states in the basis is also considered here. Inspecting the table, one sees that the inclusion of singlet states has almost no effect on the values of the eigenenergies, while the phase shifts are more evidently influenced, especially at higher energies, moving towards the results of Table 5.2, as is also shown in Figure 5.8. On the other hand, the variation in the

Table 5.6: Comparison between the results for p-wave scattering obtained with the different techniques: method I with the HH basis, method II with the Laguerre basis (including both singlet and triplet states), and a HH method [45].

E (MeV)	δ (degrees)		
	method I, HH basis	method II, Laguerre basis	HH [45]
0.203	-0.645	-0.724	-0.644
0.430	-1.98	-2.18	-1.976
0.934	-4.49	-4.84	-4.47

parameters of the Laguerre basis has almost no effect on the results when considering only the triplet states. In principle the influence of more singlet states, as well as those of other partial waves, has to be investigated to get a result comparable with the one obtained with method I and the HH basis.
A comparison between the various results and with a reference value (with Hyperspherical Harmonics, or HH, method [45]) is given in Table 5.6. The results obtained with method I and the HH basis are far more accurate than the one obtained with the Laguerre basis, suggesting, as mentioned, that this basis is not yet large enough to provide precise results, whereas the HH basis is in good convergence already for a relatively small number of functions.

5.2.2 s-wave phase shifts for N-^{2}H scattering

Method I, in combination with the symmetrized HH basis, has also been used to calculate phase shifts for s-wave scattering, for both cases of n-^{2}H scattering and p-^{2}H scattering, and for the doublet and quadruplet cases ($S = \frac{1}{2}$ and $S = \frac{3}{2}$ respectively).
For the s-wave scattering the regularization function has been chosen to be

$$g_{reg}(\eta_2) = 1 - e^{-b_{reg}\eta_2} \quad , \tag{5.7}$$

in fact in general following reference [17] for l-wave scattering one has

$$g_{reg}(\eta_2) = (1 - e^{-b_{reg}\eta_2})^{2l+1} \quad . \tag{5.8}$$

In this case a rather large basis (maximum values of $K = 50$, $N = 21$, leading to a total number of 4914 basis functions for the doublet and 2457 functions for the quadruplet respectively) has been taken. Even with such a large basis, complete convergence is still not obtained, as shown in Table 5.7. This is different from the p-wave case where a rather good convergence is reached for a much smaller basis.
The results of the calculations are presented in Table 5.8 and Table 5.9. In the case of the neutron-deuteron doublet scattering, the results are compared with reference [45]: the rather large difference between the two results is

Table 5.7: Convergence in the hyperangular quantum number K for the phase shift for the s-wave n-^{2}H and p-^{2}H scattering, obtained with method I with HH basis (maximum values of $K = 50$ and $N = 21$). The value of energy is $E = 1.0$ MeV and $b_{reg} = 1.0$ fm^{-1}.

	δ (degrees)			
K	n+^{2}H		p+^{2}H	
	$S = \frac{3}{2}$	$S = \frac{1}{2}$	$S = \frac{3}{2}$	$S = \frac{1}{2}$
20	-61.01	-22.47	-53.46	-18.98
44	-57.19	-20.89	-49.29	-15.54
50	-56.81	-20.56	-48.17	-16.29

Table 5.8: Results for n-^{2}H s-wave scattering, for the doublet and quadruplet cases, for method I with a HH basis, with maximum values for the parameters $K = 50$, $N = 21$.

E (MeV)	δ (degrees)		
	$S = \frac{3}{2}$	$S = \frac{1}{2}$	$S = \frac{1}{2}$ (HH [45])
0.001	-2.13	-0.227	
0.1	-20.6	-3.03	-2.792
0.5	-43.3	-12.3	-11.29
1.0	-56.8	-20.6	-19.68
1.633	-67.6	-28.3	
2.18	-74.5	-33.2	

very likely due to the lack of complete convergence (compare phase shifts in Tables 5.7 and 5.8). The difference to the case of p-wave scattering may be related to the nature of s-wave scattering: the projectile and the target nucleus have a larger superposition in the wave function than in the case of p-wave scattering, which translates in a need for higher detail in the description of the short-range part of the scattering wave function which is expanded on the HH basis.

Table 5.9: Results for p-^{2}H s-wave scattering, for the doublet and quadruplet cases, for method I with a HH basis, with maximum values for the parameters $K = 50$, $N = 21$.

E (MeV)	δ (degrees)	
	$S = \frac{3}{2}$	$S = \frac{1}{2}$
0.1	-7.71	-0.398
0.667	-38.7	-10.3
1.0	-48.2	-16.3
1.333	-55.1	-20.6
2.0	-65.4	-28.2

5.3 Preliminary results for 4+1 scattering

One of the goals of this work is the extension of the presented few-body techniques to more complicated problems, involving more than 3 nucleons. Such an attempt is done for the five-body problem, in particular in the case of the s-wave scattering of a neutron off the ^{4}He nucleus:

$$^4\mathrm{He} + \mathrm{n} \rightarrow {}^4\mathrm{He} + \mathrm{n} \quad . \tag{5.9}$$

This reaction represents a general $N+1$ scattering problem, and it is tackled with the NSHH method described in Chapter 4.3.2. In particular, a NSHH basis is used to find the wave function of the ^{4}He nucleus and of the ^{4}He+n scattering states, according to method II described in Chapter 3.3. The search for such states is performed via a Lanczos algorithm applied to the Hamiltonian expressed in such a basis. Despite the four-body problem may be solved with good convergence with ordinary computational effort, the search for the five-body states can prove to be quite expensive in this sense: anyway as it turns out, when this steps are accomplished, only rather simple calculations (namely two-dimensional integrals) need to be performed in order to find the estimates for the phase shifts, as explained in detail in Appendix A.
Method II allows the calculation of phase shifts corresponding to the energy values given by the diagonalization of the $(N+1)$-nucleon Hamiltonian in the basis considered. For the NSHH basis, no such states appear for the five-body

calculation for the Malfliet-Tjon potential used for the three-body problem, using the maximum value for the hyperangular quantum number $K_4 = 14$. This value has been chosen to limit the basis in the preliminary calculations due to the rather good convergence of the ^{4}He energy in the four-body case. The energy range for the 4+1 scattering is defined by

$$-30 \text{ MeV} \simeq E_{^4\text{He}} < E < E_{^3\text{H}} + E_{^2\text{H}} \simeq -11 \text{ MeV} \quad . \tag{5.10}$$

To test the methodology, the Volkov potential [44] has been used, because it presents, for the same basis, one eigenstate of the energy for ^{4}He+n in the energy region where only the 4+1 channel is open, namely at a scattering energy (in the center of mass system) for the neutron of 10.05 MeV (corresponding to an energy of the system $E \simeq -20$ MeV).
It is found that the value for the phase shift strongly varies with the regularization parameter b_{reg} (for values of b_{reg} from 0.1 fm^{-1} to 10.0 fm^{-1} the phase shift takes values that range from ~ -10 to ~ -50 degrees), probably due to a lack of convergence in the five-body basis, and thus it is not comparable with the experimental data (based on R-matrix analysis) of about -80 degrees shown in [46].
These results are only preliminary, and further studies are needed in order to provide reliable calculations for this problem. Increasing the size of the five-body basis in the calculations could lead to more reliable results. This preliminary calculations have been performed for the five-body basis with a maximum value of $K = 14$ and $N = 30$ hyperradial functions, which lead already to 8415000 states in the NSHH basis, resulting in a quite heavy calculation for the scattering state, compared with the 63360 states sufficient for the bound state of ^{4}He, with the same value of $K = 14$, and $N = 20$. While the calculation of the ground state of ^{4}He can be carried out quite easily, the increasing in the size of the HH basis for five nucleons represents a challenge in the application of the methodology to such systems.

Chapter 6

Summary

The work presented in this thesis is a study of few-body methods in the field of nuclear physics. The main aim of the work has been to provide a direct calculation of the cross section for the photodisintegration of the ^{3}He nucleus, and to make possible a comparison with Lorentz Integral Transform (LIT) calculations. In particular for the latter it is checked whether the inversion of the LIT leads to sufficiently precise results in presence of a tiny cross section due to a Coulomb barrier between two charged fragments.
The reaction mentioned is the inverse reaction of the proton capture by deuteron, the precise knowledge of which is of interest in astrophysics (particularly in the study of protostellar evolution). The focus is on the low-energy part of the cross section, far below the deuteron breakup threshold, which is the region of interest in astrophysics due to the contribution of the Gamow peak, which suppresses contributions from higher energies in the rates of reaction for typical stellar conditions. It has to be pointed out that for the reaction under investigation already rather precise experimental data at low energy as well as a high precision calculation with a realistic nuclear force down to the zero-energy limit exist (see [10, 11, 20]). In fact one finds a nice agreement of the experimental and theoretical S-factor. The present study is not made to get new insights into this specific reaction, but serves merely for a precision test of the LIT calculation for such an astrophysical reaction with two charged fragments. This is very interesting because a positive outcome

would allow to apply the LIT method for those astrophysical reactions, where somewhat larger nucleon systems are involved (for example the synthesis of Beryllium and Boron nuclei). Therefore the present calculation is not made with a realistic nuclear force but with a central MT-I/III NN potential. This potential has a rather strong short-range repulsion which leads to similar problems one could encounter using more realistic nuclear forces.

A necessary condition for LIT calculations to be precise is the presence of eigenstates of the Hamiltonian in the energy region of interest. A poor density of such LIT states limits the accuracy of the transform and of its inversion preventing the correct description of the cross section. It is shown that it is difficult to find LIT states below the three-body breakup threshold with the usual Hyperspherical Harmonics basis. A new Laguerre polynomial basis, where the relative coordinate between the free proton and the deuteron is explicitly taken into account (differently from the HH basis) provides a higher density of LIT states at low energy and improves the calculation of the cross section as well as that of the astronomical S-factor.

The direct calculation which has also been performed is based on the calculation of the nucleon-deuteron scattering wave function, and it uses the Kohn Variational principle (KVP) applied to the HH basis expansion formalism taking into account explicitly the asymptotic part of the scattering wave function. The wave function itself is expressed as a sum of an asymptotic (which analytic form is known) and a core part (which is expanded on a HH basis set). The KVP states that the variation of a particular functional with respect to the coefficient of the expansion and to the tangent of the phase shift is zero: this defines a system of linear equations to be solved. This method provides a second order estimate for the phase shift, which in turn is used as a parameter to find the values of the coefficients of the expansion of the core part of the scattering wave function, thus providing a better estimate of the wave function itself. Such a wave function has been used in the calculation of the photodisintegration cross section, in the unretarded dipole approximation (which is justified for the energy range considered).

The comparison of these results with the LIT calculations shows how the use of the Laguerre basis for the LIT calculations represents a strong improve-

ment for the calculation of low-energy cross sections, confirming the density of states as a crucial point in the use of the LIT method. The agreement of the direct and the LIT calculations for the S-factor needs more investigation, since it is shown (i) that an increase of the number of basis states of the Laguerre basis leads to an improved agreement of both results and (ii) that the LIT itself is not completely convergent. Therefore LIT results with a further increase of the number of basis states are presently calculated.

Since the formalism developed for the calculation of the cross section provides also the estimates for the phase shifts, such calculations have been performed for the p-^{2}H scattering in p-wave and for both p-^{2}H and n-^{2}H in the s-wave case. The agreement of the calculated values with references is good already when a rather small basis is used in the case of p-wave scattering, while complete convergence is not yet reached in the s-wave case. As shown, this problem is at least partly due to the need for a more precise description of the core part of the wave function for s-wave scattering.

Also a second method based on the KVP is used to calculate phase shifts for the p-wave p-^{2}H scattering. The difference with the first method lies in the fact that this method uses an expansion of the whole scattering wave function on a basis set, without the explicit inclusion of the asymptotic wave function, and provides phase shifts for the energies corresponding to the eigenvalues of the Hamiltonian. Since in the low-energy region the HH basis does not easily provide energy eigenstates, the same Laguerre basis used for the LIT has been used with this formalism. The calculations show how this basis (which provides very good results in the LIT calculations) is not yet sufficient for a convergent calculation of the phase shifts within this approach. The effect of the increase of the basis in the already considered nucleon pair partial waves (s-waves), as well as the inclusion of higher partial waves, has to be further investigated.

This second technique has been applied also to the study of the more complicated problem of the scattering of a nucleon off a ^{4}He nucleus. The formalism used is that of the Nonsymmetrized Hyperspherical Harmonics, which in combination with the Lanczos algorithm makes it possible to find the antisymmetric low-energy eigenfunctions of the nuclear Hamiltonian. The

formalism developed in order to apply the technique to the study of scattering problems is presented in detail, and can provide results with relatively simple calculations. Although the results for this study are just preliminary, the method could represent a useful ab initio technique to face complicated and computationally expensive scattering problems involving five or more nucleons. Anyway further effort is needed in order to refine and effectively use this method.

Appendix A

Scattering of a nucleon off the α particle

In this chapter a detailed analysis of the technique used to investigate the five-body scattering problem using method II (described in 3.3) is given.
Method II uses a diagonalization of the Hamiltonian matrix to find eigenstates and eigenvalues in the correct energy range so that the scattering wave function can be approximated in a short-range part. For this purpose the Nonsymmetrized Hyperspherical Harmonics basis method has been used.

The reaction under study is

$$^4\mathrm{He} + N \rightarrow ^4\mathrm{He} + N \quad . \tag{A.1}$$

The ^{4}He ground state wave function is found with the application of the NSHH method (as described in Chapter 4.3.2). This wave function, despite the fact that it is expanded on a base of nonsymmetrized HHs, is antisymmetric (see Chapter 4.3.2).
The same technique with the NSHH basis can be used also to find the low-energy spectrum of the five-body problem, in a similar way to the one used to find the ground state of the α particle. The description of the procedure is kept as general as possible, and it is explicitly mentioned when the particular case of a five-nucleon calculation is assumed. In general a system of A

nucleons, involving $N = A - 1$ Jacobi coordinates, is considered.

A.1 Definition of the coordinates

The coordinate set used for the five-body calculation is a reversed order mass weighted Jacobi coordinates set, as defined in Eq. (4.9). Explicitly, in the case of 4+1 scattering, the coordinates are defined as

$$\boldsymbol{\eta}_4 = \sqrt{\frac{1}{2}}\,(\mathbf{r}_2 - \mathbf{r}_1) \tag{A.2}$$

$$\boldsymbol{\eta}_3 = \sqrt{\frac{2}{3}}\left(\mathbf{r}_3 - \frac{\mathbf{r}_1 + \mathbf{r}_2}{2}\right) \tag{A.3}$$

$$\boldsymbol{\eta}_2 = \sqrt{\frac{3}{4}}\left(\mathbf{r}_4 - \frac{\mathbf{r}_1 + \mathbf{r}_2 + \mathbf{r}_3}{3}\right) \tag{A.4}$$

$$\boldsymbol{\eta}_1 = \sqrt{\frac{4}{5}}\left(\mathbf{r}_5 - \frac{\mathbf{r}_1 + \mathbf{r}_2 + \mathbf{r}_3 + \mathbf{r}_4}{4}\right) \quad , \tag{A.5}$$

where $\boldsymbol{\eta}_1$ represent the most convenient choice for the relative coordinate for the fragments, while $\boldsymbol{\eta}_2, \boldsymbol{\eta}_3, \boldsymbol{\eta}_4$ describe the four-body nucleus (in general, an $(A-1)$-body nucleus is described by coordinates $\boldsymbol{\eta}_2, \ldots, \boldsymbol{\eta}_N$).
It is also useful to define alternative coordinates pertaining the $(A-1)$ nucleus:

$$\boldsymbol{\eta}_i^{(A-1)} = \boldsymbol{\eta}_{i+1} \quad . \tag{A.6}$$

Explicitly, for the ^{4}He in the five-body case:

$$\boldsymbol{\eta}_3^{\mathrm{He}} = \boldsymbol{\eta}_4 \;\; ; \;\; \boldsymbol{\eta}_2^{\mathrm{He}} = \boldsymbol{\eta}_3 \;\; ; \;\; \boldsymbol{\eta}_1^{\mathrm{He}} = \boldsymbol{\eta}_2 \;\; ; \;\; \boldsymbol{\eta}_0^{\mathrm{He}} = \boldsymbol{\eta}_1 \quad . \tag{A.7}$$

The label He denotes the Helium nucleus and the (4+1) configuration of the particles.
The hyperradius and the angular (and hyperangular) variables are defined starting from the Jacobi coordinates, following the scheme of Eq. (4.12). In

the specific case of five nucleons, again, such definitions become:

$$\begin{aligned}
\rho &= \sqrt{{\eta_1}^2 + {\eta_2}^2 + {\eta_3}^2 + {\eta_4}^2} && \text{(A.8)}\\
X_i &= \cos 2\alpha_i && \text{(A.9)}\\
\cos\alpha_i &= \left(\frac{1+X_i}{2}\right)^{1/2} && \text{(A.10)}\\
\sin\alpha_i &= \left(\frac{1-X_i}{2}\right)^{1/2} && \text{(A.11)}\\
\eta_1 &= \rho\cos\alpha_2\cos\alpha_3\cos\alpha_4 && \text{(A.12)}\\
\eta_2 &= \rho\sin\alpha_2\cos\alpha_3\cos\alpha_4 && \text{(A.13)}\\
\eta_3 &= \rho\sin\alpha_3\cos\alpha_4 && \text{(A.14)}\\
\eta_4 &= \rho\sin\alpha_4 && \text{(A.15)}\\
\rho^{\mathrm{He}} &= \sqrt{\left(\eta_1^{\mathrm{He}}\right)^2 + \left(\eta_2^{\mathrm{He}}\right)^2 + \left(\eta_3^{\mathrm{He}}\right)^2} = \sqrt{{\eta_2}^2 + {\eta_3}^2 + {\eta_4}^2} && \text{(A.16)}\\
X_i^{\mathrm{He}} &= \cos 2\alpha_i^{\mathrm{He}} && \text{(A.17)}\\
\cos\alpha_i^{\mathrm{He}} &= \left(\frac{1+X_i^{\mathrm{He}}}{2}\right)^{1/2} && \text{(A.18)}\\
\sin\alpha_i^{\mathrm{He}} &= \left(\frac{1-X_i^{\mathrm{He}}}{2}\right)^{1/2} && \text{(A.19)}\\
\eta_0^{\mathrm{He}} &= \eta_1 = \rho\cos\alpha_4^{\mathrm{He}} && \text{(A.20)}\\
\eta_1^{\mathrm{He}} &= \eta_2 = \rho^{\mathrm{He}}\cos\alpha_2^{\mathrm{He}}\cos\alpha_3^{\mathrm{He}} && \text{(A.21)}\\
\eta_2^{\mathrm{He}} &= \eta_3 = \rho^{\mathrm{He}}\sin\alpha_2^{\mathrm{He}}\cos\alpha_3^{\mathrm{He}} && \text{(A.22)}\\
\eta_3^{\mathrm{He}} &= \eta_4 = \rho^{\mathrm{He}}\sin\alpha_3^{\mathrm{He}} \quad , && \text{(A.23)}
\end{aligned}$$

where the label He identifies, as before, the 4-nucleons variables in the $A = 5$ case.

The integration volume $d\tau$ is given by

$$\begin{aligned}
d\tau &= d^3\eta_1 d^3\eta_2 d^3\eta_3 d^3\eta_4 = \prod_{i=1}^{N} \eta_i^2 d\eta_i d\phi_i d\cos\theta_i \\
&= \rho^{3N-1} d\rho d\phi_1 d\cos\theta_1 \prod_{i=2}^{N} d\phi_i d\cos\theta_i \cos^{3i-4}\alpha_i \sin^2\alpha_i d\alpha_i \quad , \text{(A.24)}
\end{aligned}$$

which becomes, in the five-body case,

$$d\tau = \rho^{11} d\rho \left(\prod_{i=1}^{4} d\phi_i d\cos\theta_i \right) d\alpha_2 d\alpha_3 d\alpha_4 \cos^2\alpha_2 \sin^2\alpha_2 \cos^5\alpha_3 \sin^2\alpha_3 \cos^8\alpha_4 \sin^2\alpha_4 \quad . \tag{A.25}$$

A.2 Wave functions and recoupling coefficients

The hyperspherical coordinates and the couplings of the momenta can be easily represented in a so-called *tree* diagram. In the following diagram, each "leaf" corresponds to a Jacobi coordinate and to the associated orbital angular momentum l_i, while each "node" is associated with a hyperangle α_i and with its corresponding value of K_i. Also, a value of the total orbital angular momentum L_i is related to each node. It follows from the definition of the Jacobi coordinates that a factor $\cos\alpha_i$ is associated with the right branch starting at node i, while a factor $\sin\alpha_i$ is associated with each left branch. The tree diagram for the five-body Hyperspherical Harmonics can be visualized easily:

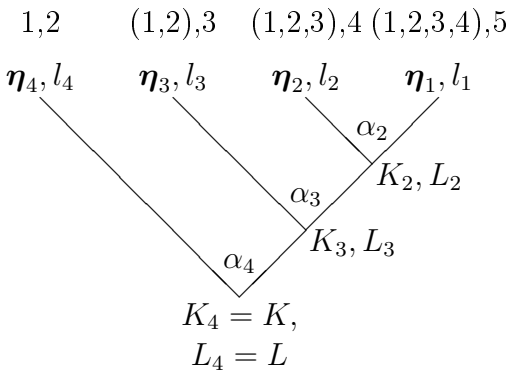

In the last diagrams, above each jacobi coordinate a representation of the corresponding clusters and particles is given.
For spin and isospin, diagrams for the couplings take the following form:

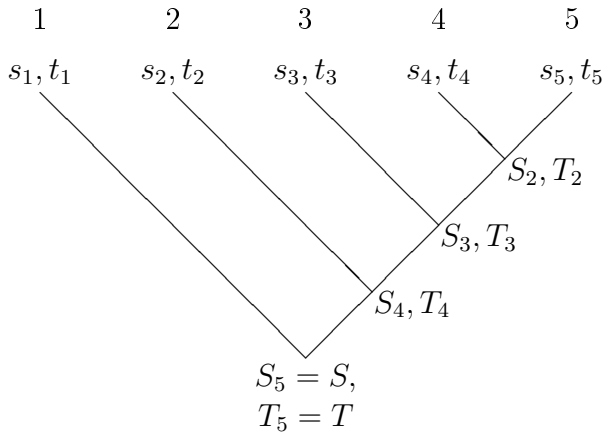

In the case of $N + 1$ scattering, and in particular for $A = 5$, it is easier to deal with a coupling scheme where the scattering coordinate $\boldsymbol{\eta}_1$ is coupled to the $(A-1)$-particle cluster as in the following diagram (explicit for five nucleons):

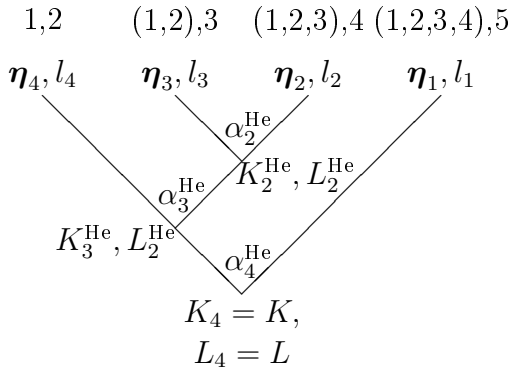

and similarly for spin and isospin:

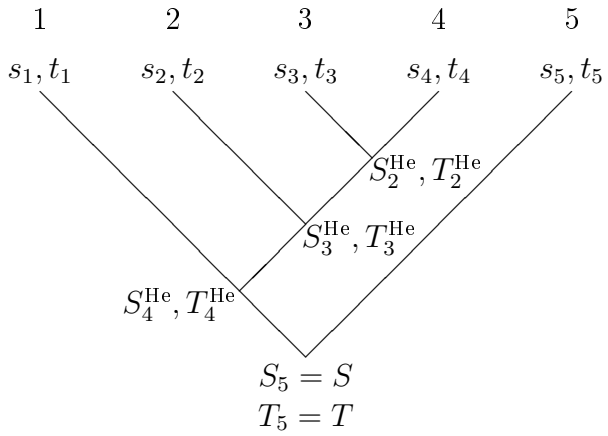

where, again, the label He represents the scheme and the coordinates pertaining the $(A-1)$-nucleus plus the projectile particle.
It is possible to pass from a basis constructed in the (A)-body representation to the one in the $(A-1)$-body representation using 6-j and the so-called *tree* coefficients. The tree coefficients are the generalization of the 6-j coefficients for hyperangular momenta. In general, for an A-nucleon problem, $A-3$ coefficients are needed for the recoupling of orbital angular momenta, as well as $A-3$ tree coefficients for the hyperangular recoupling. The spin and isospin functions need $A-2$ recoupling coefficients each.

For the spatial part of the wave function, two contributions arise: one from the recoupling of the orbital angular momenta L_i and one from the hyperspherical recoupling. The tree-coefficients change the coupling of the hyperspherical coordinates. The usual definition of the HH functions is the one of Eq. (4.37):

$$\begin{aligned}\mathcal{Y}_{[K]}\left(\Omega_N\right) \;=\; & \left[\sum_{m_1,\ldots,m_N} \langle l_1 m_1 l_2 m_2 | L_2 M_2\rangle \langle L_2 M_2 l_3 m_3 | L_3 M_3\rangle \cdot \ldots \right. \\ & \left. \cdot \langle L_{N-1} M_{N-1} l_N m_N | L_N M_N\rangle \prod_{j=1}^{N} Y_{l_j m_j}\left(\hat{\eta}_j\right)\right] \\ & \cdot \left[\prod_{j=2}^{N} \mathcal{N}(K_j; l_j K_{j-1}) (\sin\alpha_j)^{l_j} (\cos\alpha_j)^{K_{j-1}} \right. \\ & \left. \cdot P_{\mu_j}^{[l_j+1/2],[K_{j-1}+(3j-5)/2]}\left(\cos\left(2\alpha_j\right)\right)\right] \quad , \end{aligned} \tag{A.26}$$

which reads explicitly, in the five-body case,

$$\begin{aligned}&\mathcal{Y}_{[K]}\left(\Omega_N\right) = \\ &= \left[\sum_{m_1,\ldots,m_4} \langle l_1 m_1 l_2 m_2 | L_2 M_2\rangle \langle L_2 M_2 l_3 m_3 | L_3 M_3\rangle \right. \\ &\quad \left. \cdot \langle L_3 M_3 l_4 m_4 | L_4 M_4\rangle Y_{l_1 m_1}\left(\hat{\eta}_1\right) Y_{l_2 m_2}\left(\hat{\eta}_2\right) Y_{l_3 m_3}\left(\hat{\eta}_3\right) Y_{l_4 m_4}\left(\hat{\eta}_4\right)\right] \\ &\quad \cdot \left[\mathcal{N}(K_2; l_2 l_1) (\sin\alpha_2)^{l_2} (\cos\alpha_2)^{l_1} \cdot P_{\mu_2}^{[l_2+1/2],[l_1+1/2]}\left(\cos\left(2\alpha_2\right)\right)\right.\end{aligned}$$

$$\cdot\mathcal{N}(K_3;l_3K_2)(\sin\alpha_3)^{l_3}(\cos\alpha_3)^{K_2}\cdot P_{\mu_3}^{[l_3+1/2],[K_2+2]}\left(\cos\left(2\alpha_3\right)\right)$$
$$\cdot\mathcal{N}(K_4;l_4K_3)(\sin\alpha_4)^{l_4}(\cos\alpha_4)^{K_3}\cdot P_{\mu_4}^{[l_4+1/2],[K_3+7/2]}\left(\cos\left(2\alpha_4\right)\right)\Big] \quad . \quad \text{(A.27)}$$

The coupling described by the $N+1$ configuration is instead given by the following explicit form for the HH functions:

$$\begin{aligned}
\mathcal{Y}_{\left[K^{(A-1)}\right]}^{(A-1)}\left(\Omega_N^{(A-1)}\right) \;=\; & \Bigg[\sum_{m_2,\ldots,m_{N-1},m_1}\langle l_2m_2l_3m_3|L_2^{(A-1)}M_2^{(A-1)}\rangle \\
& \langle L_2^{(A-1)}M_2^{(A-1)}l_4m_4|L_3^{(A-1)}M_3^{(A-1)}\rangle\cdot\ldots \\
& \cdot\langle l_1m_1L_{N-1}M_{N-1}|L_NM_N\rangle\prod_{j=1}^{N}Y_{l_jm_j}\left(\hat{\eta}_j\right)\Bigg] \\
& \cdot\Bigg[\prod_{j=2}^{N-1}\mathcal{N}(K_j^{(A-1)};l_{j+1}K_{j-1}^{(A-1)})\left(\sin\alpha_j^{(A-1)}\right)^{l_{j+1}} \\
& \left(\cos\alpha_j^{(A-1)}\right)^{K_{j-1}^{(A-1)}}P_{\mu_j^{(A-1)}}^{[l_{j+1}+1/2],[K_{j-1}^{(A-1)}+(3j-5)/2]}\left(\cos\left(2\alpha_j^{(A-1)}\right)\right)\Bigg] \\
& \mathcal{N}(K_N^{(A-1)};K_{N-1}^{(A-1)}l_1)\left(\sin\alpha_N^{(A-1)}\right)^{K_{N-1}^{(A-1)}}\left(\cos\alpha_N^{(A-1)}\right)^{l_1} \\
& \cdot P_{\mu_N^{(A-1)}}^{[K_{N-1}^{(A-1)}+7/2],[l_1+1/2]}\left(\cos\left(2\alpha_N^{(A-1)}\right)\right) \quad , \qquad \text{(A.28)}
\end{aligned}$$

which, for the five-body case, is

$$\begin{aligned}
\mathcal{Y}_{[K^{\rm He}]}^{4+1}\left(\Omega_N^{\rm He}\right) \;=\; & \Bigg[\sum_{m_2,m_3,m_4,m_1}\langle l_2m_2l_3m_3|L_2^{\rm He}M_2^{\rm He}\rangle\,\langle L_2^{\rm He}M_2^{\rm He}l_4m_4|L_3^{\rm He}M_3^{\rm He}\rangle \\
& \cdot\langle l_1m_1L_3^{\rm He}M_3^{\rm He}|LM\rangle\,Y_{l_2m_2}\left(\hat{\eta}_2\right)Y_{l_3m_3}\left(\hat{\eta}_3\right)Y_{l_4m_4}\left(\hat{\eta}_4\right)Y_{l_1m_1}\left(\hat{\eta}_1\right)\Big] \\
& \cdot\Big[\mathcal{N}(K_2^{\rm He};l_3l_2)(\sin\alpha_2^{\rm He})^{l_3}(\cos\alpha_2^{\rm He})^{l_2} \\
& \cdot P_{\mu_2^{\rm He}}^{[l_3+1/2],[l_2+1/2]}\left(\cos\left(2\alpha_2^{\rm He}\right)\right) \\
& \mathcal{N}(K_3^{\rm He};l_4K_2^{\rm He})(\sin\alpha_3^{\rm He})^{l_4}(\cos\alpha_3^{\rm He})^{K_2^{\rm He}} \\
& \cdot P_{\mu_3^{\rm He}}^{[l_4+1/2],[K_2^{\rm He}+2]}\left(\cos\left(2\alpha_3^{\rm He}\right)\right) \\
& \mathcal{N}(K_4;K_3^{\rm He}l_1)(\sin\alpha_4^{\rm He})^{K_3^{\rm He}}(\cos\alpha_4^{\rm He})^{l_1} \\
& \cdot P_{\mu_4^{\rm He}}^{[K_3^{\rm He}+7/2],[l_1+1/2]}\left(\cos\left(2\alpha_4^{\rm He}\right)\right)\Big] \quad . \qquad \text{(A.29)}
\end{aligned}$$

The explicit form of the normalization coefficients is

$$\mathcal{N}(K_2; l_2 l_1) = \left[\frac{(2K_2+4)\mu_2!\Gamma[\mu_2+l_1+l_2+2]}{\Gamma\left[\mu_2+l_2+3/2\right]\Gamma[\mu_2+l_1+3/2]}\right]^{1/2} \tag{A.30}$$

$$\mathcal{N}(K_3; l_3 K_2) = \left[\frac{(2K_3+7)\mu_3!\Gamma[\mu_3+K_2+l_3+7/2]}{\Gamma\left[\mu_3+l_3+3/2\right]\Gamma[\mu_3+K_2+3]}\right]^{1/2} \tag{A.31}$$

$$\mathcal{N}(K_4; l_4 K_3) = \left[\frac{(2K_4+10)\mu_3!\Gamma[\mu_4+K_3+l_4+10/2]}{\Gamma\left[\mu_4+l_4+3/2\right]\Gamma[\mu_4+K_3+9/2]}\right]^{1/2} \tag{A.32}$$

$$\mathcal{N}(K_2^{\rm He}; l_3 l_2) = \left[\frac{(2K_2^{\rm He}+4)\mu_2^{\rm He}!\Gamma[\mu_2^{\rm He}+l_2+l_3+2]}{\Gamma\left[\mu_2^{\rm He}+l_3+3/2\right]\Gamma[\mu_2^{\rm He}+l_2+3/2]}\right]^{1/2} \tag{A.33}$$

$$\mathcal{N}(K_3^{\rm He}; l_4 K_2^{\rm He}) = \left[\frac{(2K_3^{\rm He}+7)\mu_3^{\rm He}!\Gamma[\mu_3^{\rm He}+K_2^{\rm He}+l_4+7/2]}{\Gamma\left[\mu_3^{\rm He}+l_4+3/2\right]\Gamma[\mu_3^{\rm He}+K_2^{\rm He}+3]}\right]^{1/2} \tag{A.34}$$

$$\mathcal{N}(K_4^{\rm He}; K_3^{\rm He} l_1) = \left[\frac{(2K_4^{\rm He}+10)\mu_4^{\rm He}!\Gamma[\mu_4^{\rm He}+K_3^{\rm He}+l_1+10/2]}{\Gamma[\mu_4^{\rm He}+K_3^{\rm He}+9/2]\Gamma\left[\mu_4^{\rm He}+l_1+3/2\right]}\right]^{1/2} \tag{A.35}$$

with

$$\mu_2 = \frac{K_2-l_2-l_1}{2} \quad ; \quad \mu_3 = \frac{K_3-l_3-K_2}{2} \quad ; \quad \mu_4 = \frac{K_4-l_4-K_3}{2} \tag{A.36}$$

$$\mu_2^{\rm He} = \frac{K_2^{\rm He}-l_3-l_2}{2} \quad ; \quad \mu_3^{\rm He} = \frac{K_3^{\rm He}-l_4-K_2^{\rm He}}{2} \quad ; \quad \mu_4^{\rm He} = \frac{K_4^{\rm He}-l_1-K_3^{\rm He}}{2} \quad . \tag{A.37}$$

The following relation holds:

$$\mathcal{Y}_{[K]}(\Omega_N) = \sum_{[K^{(A-1)}]} \langle \mathcal{Y}^{(A-1)}_{[K^{(A-1)}]}(\Omega_N^{(A-1)}) | \mathcal{Y}_{[K]}(\Omega_N) \rangle \, \mathcal{Y}^{(A-1)}_{[K^{(A-1)}]} \quad . \tag{A.38}$$

where the coefficients of the transformation are given by the tree coefficients and the 6-j coefficients for the recoupling of the orbital angular momenta. It has to be noted that the hyperradial part of the spatial wave function is not affected by this kind of hyperspherical recoupling.

The spin and isospin recoupling coefficients, as well as the ones for the orbital

angular momenta, can be deduced using the following relation:

$$\left\langle \left[\left[j_1, j_2 \right]_{j_{12}}, j_3 \right]_J \middle| \left[j_1, \left[j_2, j_3 \right]_{j_{23}} \right]_J \right\rangle = \\ = \sqrt{(2j_{12}+1)(2j_{23}+1)}\,(-)^{j_1+j_2+j_3+J} \cdot \left\{ \begin{array}{ccc} j_1 & j_2 & j_{12} \\ j_3 & J & j_{23} \end{array} \right\} \quad . \tag{A.39}$$

In general, the total () basis state function can be expressed as

$$\phi_i = \sum_{[K^{(A-1)}]_j} \sum_{[S^{(A-1)}]_j} \sum_{[T^{(A-1)}]_j} \langle \phi_j^{(A-1)} | \phi_i \rangle \, \phi_j^{(A-1)} \quad . \tag{A.40}$$

In the five-body case, the explicit form of the recoupling coefficients is given by

$$\langle \phi_j^{(4+1)} | \phi_i \rangle = \\ = T_{l_1,l_2,l_3,l_4}(K_2, K_3, K_4, K_2^{\mathrm{He}}, K_3^{\mathrm{He}}, K_4^{\mathrm{He}}, L_1, L_2, L_3, L_4, L_1^{\mathrm{He}}, L_2^{\mathrm{He}}, L_3^{\mathrm{He}}, L_4^{\mathrm{He}}) \\ \cdot C_S(S_2, S_3, S_4, S_2^{\mathrm{He}}, S_3^{\mathrm{He}}, S_4^{\mathrm{He}}) C_T(T_2, T_3, T_4, T_2^{\mathrm{He}}, T_3^{\mathrm{He}}, T_4^{\mathrm{He}}) \tag{A.41}$$

with

$$C_S(S_2, S_3, S_4, S_2^{\mathrm{He}}, S_3^{\mathrm{He}}, S_4^{\mathrm{He}}) = \\ = \sqrt{(2S_2^{\mathrm{He}}+1)(2S_2+1)}\sqrt{(2S_3+1)(2S_3^{\mathrm{He}}+1)} \\ \cdot\sqrt{(2S_4+1)(2S_4^{\mathrm{He}}+1)}\,(-)^{7/2+S_2^{\mathrm{He}}+S_3^{\mathrm{He}}+S_3+S_4+S} \\ \cdot \left\{ \begin{array}{ccc} \frac{1}{2} & \frac{1}{2} & S_2^{\mathrm{He}} \\ \frac{1}{2} & S_3 & S_2 \end{array} \right\} \cdot \left\{ \begin{array}{ccc} \frac{1}{2} & S_2^{\mathrm{He}} & S_3 \\ \frac{1}{2} & S_4 & S_3^{\mathrm{He}} \end{array} \right\} \cdot \left\{ \begin{array}{ccc} \frac{1}{2} & S_3^{\mathrm{He}} & S_4 \\ \frac{1}{2} & S & S_4^{\mathrm{He}} \end{array} \right\} \quad , \tag{A.42}$$

$$C_T(T_2, T_3, T_4, T_2^{\mathrm{He}}, T_3^{\mathrm{He}}, T_4^{\mathrm{He}}) = \\ = \sqrt{(2S_2^{\mathrm{He}}+1)(2S_2+1)}\sqrt{(2S_3+1)(2S_3^{\mathrm{He}}+1)} \\ \cdot\sqrt{(2S_4+1)(2S_4^{\mathrm{He}}+1)}\,(-)^{7/2+T_2^{\mathrm{He}}+T_3^{\mathrm{He}}+T_3+T_4+T} \\ \cdot \left\{ \begin{array}{ccc} \frac{1}{2} & \frac{1}{2} & T_2^{\mathrm{He}} \\ \frac{1}{2} & T_3 & T_2 \end{array} \right\} \cdot \left\{ \begin{array}{ccc} \frac{1}{2} & T_2^{\mathrm{He}} & T_3 \\ \frac{1}{2} & T_4 & T_3^{\mathrm{He}} \end{array} \right\} \cdot \left\{ \begin{array}{ccc} \frac{1}{2} & T_3^{\mathrm{He}} & T_4 \\ \frac{1}{2} & T & T_4^{\mathrm{He}} \end{array} \right\} \quad , \tag{A.43}$$

and

$$
\begin{aligned}
T_{l_1,l_2,l_3,l_4}(K_2,K_3,K_4,K_2^{\mathrm{He}},K_3^{\mathrm{He}},K_4^{\mathrm{He}},L_1,L_2,L_3,L_4,L_1^{\mathrm{He}},L_2^{\mathrm{He}},L_3^{\mathrm{He}},L_4^{\mathrm{He}}) = \\
= \sqrt{((2L_2^{\mathrm{He}}+1)\,(2L_2+1)}\sqrt{(2L_3+1)\,(2L_3^{\mathrm{He}}+1)} \\
\cdot(-)^{2l_1+l_2+l_3+L_2^{\mathrm{He}}+L_3+L} \\
\cdot\left\{\begin{array}{ccc} l_1 & l_2 & L_2 \\ l_3 & L_3 & L_2^{\mathrm{He}} \end{array}\right\}\cdot\left\{\begin{array}{ccc} l_1 & L_2^{\mathrm{He}} & L_3 \\ l_4 & L & L_3^{\mathrm{He}} \end{array}\right\} \\
\cdot T^{K_3;l_2l_1l_3}_{K_2K_2^{\mathrm{He}}} T^{K_4;K_2^{\mathrm{He}}l_1l_4}_{K_3K_3^{\mathrm{He}}} \quad .
\end{aligned} \tag{A.44}
$$

The symbols $T^{K;K_2K_1K_3}_{K_{12}K_{23}}$ denote the tree coefficients, whose form, although rather complicated, depends only on the quantum numbers appearing as labels, and can be calculated quite easily (see for example [38]).

A.3 Calculation of the integrals

For the implementation of the Kohn Variational Principle as described in Chapter 3.3, we define the Ω functions analogously to what has been done in Eq. (3.55) and Eq. (3.56):

$$
\Omega^\lambda = \frac{1}{\sqrt{A}}\sum_{p=1}^{A}\sigma_p\Omega_p^\lambda(\boldsymbol{\eta}_{1,p},\ldots,\boldsymbol{\eta}_{N,p}) \quad , \quad \lambda = R, I \quad , \tag{A.45}
$$

where

$$
\Omega_p^\lambda = \left[\Phi^{nucleus}(\boldsymbol{\eta}_{1,p},\ldots,\boldsymbol{\eta}_{N-1,p})G_L^\lambda(q\eta_{N,p})Y_L^M(\hat{\eta}_{N,p})\chi_{s_p}\chi_{t_p}\right]_{JJ_zTT_z} \tag{A.46}
$$

Since the A-nucleon wave function $\Psi^{(A)}$ is antisymmetric, as Ω^λ is, the following relation holds:

$$
\langle\Psi^{(A)}|H-E|\Omega^\lambda\rangle = \frac{A}{\sqrt{A}}\langle\Psi^{(A)}|H-E|\Omega_A^\lambda\rangle \quad , \tag{A.47}
$$

where Ω_A^λ in our choice of coordinates is given by the product of the antisymmetric $(A-1)$-nucleus wave function and the scattering wave function expressed in the coordinates of section A.1.
The $(A-1)$-nucleus is an eigenstate of the Hamiltonian, so that

$$(H-E)\,|\Omega_A^\lambda\rangle = (T_{rel} - E_{sc} + \sum_{i=1}^{A-1} V_{iA} + \cancel{H_{(A-1)} - E_{(A-1)}}\,|\Omega_A^\lambda\rangle \quad , \qquad \text{(A.48)}$$

where T_{rel} is the relative kinetic energy of the scattering nucleon.
Since the potential V is short-range, we may act on the left with V_{iA}. The wave function $\Psi^{(A)}$ is antisymmetric, so

$$\langle\Psi^{(A)}|\sum_{i=1}^{A-1} V_{iA}|\Omega_A^\lambda\rangle = (A-1)\,\langle\Psi^{(A)}|V_{1A}|\Omega_A^\lambda\rangle \quad . \qquad \text{(A.49)}$$

The integrals to be calculated are then of the kind

$$\langle\phi_i^{(A)}|\Omega_A^\lambda\rangle \quad ; \quad \langle\phi_i^{(A)}|T_{rel}|\Omega_A^\lambda\rangle \quad , \qquad \text{(A.50)}$$

which are relatively easy to calculate. The operator T_{rel} is acting on Ω_A^λ and does not affect the $(A-1)$-nucleus part, while V_{1A} can act on the left on $\phi_i^{(A)}$: it is simpler to make it act on the left, since in this way the permutation matrices can be used to calculate the action of V_{1A} (see Chapter 4.3.2); acting on the right would involve more complicated calculations, while acting on the A-body vector with V_{1A} on the left produces another vector expressed in terms of the same basis functions.
The former integrals are easily calculated by changing the A-body basis states $\phi_i^{(A)}$ into the $(N+1)$ basis using tree coefficients and 6-j symbols, as discussed in the previous section. In this new set, it is only necessary to calculate two-dimensional integrals. In fact, all the hyperangular quantum numbers of the A-body basis functions, up to the $(A-1)$-th particle are orthonormal with the $(A-1)$-nucleus part of the asymptotic wave function Ω_A^λ. All spin and isospin quantum numbers contribute with delta functions. The only parts of the functions which are not orthonormal are the hyperradial and the Bessel

function which appears in the definition of $\Omega^{\lambda}_{(A)}$, which involve only coordinates ρ and $\alpha_N^{(A-1)}$.
The explicit expression in the five-body case is

$$\begin{aligned}
&\langle \phi_i^{(4+1)}(\rho,\Omega_4^{\rm He})|\phi_j^{\rm He}(\rho\sin\alpha_4^{\rm He},\Omega_3^{\rm He})g_{l_1}(\rho\cos\alpha_4^{\rm He})Y_{l_1}(\hat{\eta}_1)\rangle = \\
&= \int \delta_{[K_3^{\rm He}]_i[K_3^{\rm He}]_j}\mathcal{N}(K_4^{\rm He};K_3^{\rm He}l_{1i})(\sin\alpha_4^{\rm He})^{K_3^{\rm He}}(\cos\alpha_4^{\rm He})^{l_{1i}} \\
&\quad P_{\mu_4^{\rm He}}^{[K_3^{\rm He}+7/2],[l_{1i}+1/2]}(\cos(2\alpha_4^{\rm He}))\sum_{m_1}\langle l_{1i}m_1L_3^{\rm He}M_3^{\rm He}|LM\rangle\,\delta_{l_{1i}l_{1j}} \\
&\quad R^5_{N_5}(\rho)R^4_{N_4}(\rho\sin\alpha_4^{\rm He})g_{l_1}(\rho\cos\alpha_4^{\rm He})d\rho\rho^{11}d\alpha_4^{\rm He}\cos^2(\alpha_4^{\rm He})\sin^8(\alpha_4^{\rm He}) \qquad \text{(A.51)}
\end{aligned}$$

while all the quantum numbers relative to spin and isospin give Kronecker deltas.
The functions $R^5_{N_5}(\rho)$ and $R^4_{N_4}(\rho\sin\alpha_4^{\rm He})$ are the hyperradial functions respectively of the five-body state and of the Helium basis functions. The function $g_{l_1}(\rho\cos\alpha_4^{\rm He})$ can denote the Bessel (or Coulomb) wave function for the scattering nucleon with respect to the Helium nucleus or its derivatives.
Despite the complicated form of the previous formula, the fact that only two-dimensional integrals are needed shows how the calculation may be performed easily with standard quadrature methods, and how it an be carried out without much computational effort.

Acknowledgements

I want to thank kindly my advisor for this work, prof. Winfried Leidemann, who has followed me in this three years with great patience, in particular in these last months, and with constant supervision and advice. His help has been determinant. I wish to thank also prof. Giuseppina Orlandini, for the useful discussions and her advice.
A thank you goes also to prof. Victor Efros, who has helped me with the understanding of the formalism as well as with the development of the code for the calculations, and to prof. Alejandro Kievsky, who provided the reference for some of the calculations and has been very helpful; I wish also to thank prof. Nir Barnea, who has helped with the NSHH code as well as with the discussions for new ideas.
I want to say thanks to my office-mates, Giulia, Lorenzo and Fabrizio, who have made me feel at home when I was working at the university.
A special thank you goes to Nadia, who has been infinitely patient, tolerant and supportive with me in these months.
I want also to thank all the people with whom I had the pleasure to sing and play during these years: Walter, Cristian, Luca, Andrew, Ceci, Nic, Frenko, il Cova, il Luz, Carla, Cami, José, Ric, Danilo, Ale, Zac, Tommy. The time spent playing with you will always be unforgettable.
Another special thank you to my dear friend Nicola, whose wisdom and strength is beyond doubt.
I want to thank also Marco, Luca and Paola for their friendship, which is very precious to me.
I have also to remember and thank Ana and Mario of "ai Castelli Romani", which have given me lots of psychological, and nutritional, support, more

times than I can remember.
Finally, I want to thank my family, my sister and my parents, which have been extremely supportive and helpful during these years.

Bibliography

[1] E. Epelbaum and U. G. Meissner, "Chiral Dynamics of Few- and Many-Nucleon Systems", *Ann. Rev. Nucl. Part. Sci.* **62**, 159 (2012)

[2] R. Machleidt and D. R. Entem, "Chiral effective field theory and nuclear forces", *Phys. Rep.* **503**, 1 (2011)

[3] W. Leidemann and G. Orlandini, "Modern ab initio approaches and applications in few-nucleon physics with $A \geq 4$", *Prog. Part. Nucl. Phys.* **68**, 158 (2013)

[4] M. Viviani, A. Deltuva, R. Lazauskas, J. Carbonell, A. C. Fonseca, A. Kievsky, L. E. Marcucci and S. Rosati, "Benchmark calculation of n-^{3}H and p-^{3}He scattering", *Phys. Rev. C* **84**, 54010 (2011)

[5] S.C. Pieper, "Quantum Monte Carlo calculations of light nuclei", *Rivista Nuovo Cim.* **31**, 709 (2008)

[6] P. Navrátil, J. P. Vary and B. R. Barrett, "Properties of ^{12}C in the Ab Initio Nuclear Shell Model", *Phys. Rev. Lett.* **84**, 5728 (2000)

[7] P. Navrátil, J. P. Vary and B. R. Barrett, "Large-basis ab initio no-core shell model and its application to ^{12}C", *Phys. Rev. C* **62**, 54311 (2000)

[8] V. D. Efros, W. Leidemann, G. Orlandini and N. Barnea, "The Lorentz integral transform (LIT) method and its applications to perturbation-induced reactions", *Journal of Physics G: Nuclear and Particle Physics* **12**, R459 (2007)

[9] C. Ciofi degli Atti, "Electron Scattering by Nuclei", *Prog. Part. Nucl. Phys.* **3**, 163 (1978)

[10] E. G. Adelberger, S. M. Austin, J. N. Bahcall, A. B. Balantekin, G. Bogaert, L. S. Brown, L. Buchmann, F. E. Cecil, A. E. Champagne, L. de Braeckeleer, C. A. Duba, S. R. Elliott, S. J. Freedman, M. Gai, G. Goldring, C. R. Gould, A. Gruzinov, W. C. Haxton, K. M. Heeger, E. Henley, C. W. Johnson, M. Kamionkowski, R. W. Kavanagh, S. E. Koonin, K. Kubodera, K. Langanke, T. Motobayashi, V. Pandharipande, P. Parker, R. G. H. Robertson, C. Rolfs, R. F. Sawyer, N. Shaviv, T. D. Shoppa, K. A. Snover, E. Swanson, R. E. Tribble, S. Turck-Chièze and J. F. Wilkerson, "Solar fusion cross sections", *Rev. Mod. Phys.* **70**, 1265 (1998)

[11] E. G. Adelberger, A. García, R. G. Hamish Robertson, K. A. Snover, A. B. Balantekin, K. Heeger, M. J. Ramsey-Musolf, D. Bemmerer, A. Junghans, C. A. Bertulani, J. W. Chen, H. Costantini, P. Prati, M. Couder, E. Uberseder, M. Wiescher, R. Cyburt, B. Davids, S. J. Freedman, M. Gai, D. Gazit, L. Gialanella, G. Imbriani, U. Greife, M. Hass, W. C. Haxton, T. Itahashi, K. Kubodera, K. Langanke, D. Leitner, M. Leitner, P. Vetter, L. Winslow, L. E. Marcucci, T. Motobayashi, A. Mukhamedzhanov, R. E. Tribble, K. M. Nollett, F. M. Nunes, T. S. Park, P. D. Parker, R. Schiavilla, E. C. Simpson, C. Spitaleri, F. Strieder, H. P. Trautvetter, K. Suemmerer and S. Typel, "Solar fusion cross sections II. The *pp* chain and CNO cycles", *Rev. Mod. Phys.* **83**, 195 (2011)

[12] A. Kievsky, M. Viviani and L.E. Marcucci, "Theoretical description of three- and four-nucleon scattering states using bound-state-like wave functions", *Phys. Rev. C* **85**, 14001 (2012)

[13] A. Kievsky, M. Viviani and S. Rosati, "Study of bound and scattering states in three-nucleon systems", *Nucl. Phys. A* **577**, 511 (1994)

[14] A. Kievsky, S. Rosati, M. Viviani, C. R. Brune, H. J. Karwowski, E. J. Ludwig, and M. H. Wood, "The three-nucleon system near the N-d threshold", *Phys. Lett. B* **406**, 292 (1997)

[15] A. Kievsky, "The complex Kohn variational method applied to N-d scattering", *Nucl. Phys. A* **624**, 125 (1997)

[16] A. Kievsky, "Variational study of 3N scattering", *Nucl. Phys. A* **631**, 668 (1998)

[17] A. Kievsky, S. Rosati, M. Viviani, L. E. Marcucci and L. Girlanda, "A high-precision variational approach to three- and four-nucleon bound and zero-energy scattering states", *J. Phys. G: Nucl. Part. Phys.* **35**, 63101 (2008)

[18] A. Kievsky, "The scattering matrix from bound state solutions", *J. Phys.: Conf. Ser.* **336**, 12005 (2011)

[19] C. Romero-Redondo, E. Garrido, P. Barletta, A. Kievsky and M. Viviani, "General integral relations for the description of scattering states using the hyperspherical adiabatic basis", *Phys. Rev. A* **83**, 22705 (2011)

[20] L. E. Marcucci, K. M. Nollett, R. Schiavilla and R. B. Wiringa, "Modern theories of low-energy astrophysical reactions", *Nucl. Phys. A* **777**, 111 (2006)

[21] A. Mengoni, "Neutron capture cross sections: from theory to experiments and back", *arXiv*:nucl-th/0501082 (2005)

[22] J. Golak, R. Skibiński, W. Glöckle, H. Kamada, A. Nogga, H. Witała, V. D. Efros, W. Leidemann, G. Orlandini and E. L. Tomusiak, "Benchmark calculation of the three-nucleon photodisintegration", *Nucl. Phys. A* **707**, 365 (2002)

[23] A. R. Edmonds, "Angular momentum in quantum mechanics", Princeton, Princeton University Press, 1970

[24] W. Greiner, and J. Maruhn, "Nuclear models", Berlin, Springer, 1996

[25] W. Kohn, "Variational methods in nuclear collision problems", *Phys. Rev.* **74**, 1763 (1948)

[26] B. N. Zakharyev, V. V. Pustovalov and V. D. Efros, "The three body problem. The K-harmonics method in problems involving the continuum spectrum", *Yad. Fiz.* **8**, 406 (1968)

[27] V. P. Permyakov, V. V. Pustovalov, Y. I. Fenin and V. D. Efros, "System of four nucleons. Neutron scattering by tritium", *Yad. Fiz.* **14**, 567 (1971)

[28] A. Messiah, "Quantum mechanics", New York, John Wiley & Sons, 1958

[29] R. A. Malfliet and J. A. Tjon, "Solution of the Faddeev equations for the triton problem using local two-particle interactions", *Nucl. Phys. A* **127**, 161 (1969)

[30] M. Abramowitz and I. A. Stegun, "Handbook of mathematical functions with formulas, graphs, and mathematical tables", New York, Dover Publications, 1964

[31] D. Andreasi, W. Leidemann, C. Reiss and M. Schwamb, "New inversion methods for the Lorentz Integral Transform", *Eur. Phys. J. A* **24**, 361 (2005)

[32] N. Barnea, V. D. Efros, W. Leidemann and G. Orlandini, "The Lorentz Integral Transform and its Inversion", *Few-Body Syst.* **47**, 201 (2010)

[33] S. Bacca, N. Barnea, W. Leidemann and G. Orlandini, "Isoscalar monopole resonance of the alpha particle: a prism to nuclear Hamiltonians", *Phys. Rev. Lett.* **110**, 42503 (2013)

[34] S. Gandolfi, A. Lovato, J. Carlson and K. E. Schmidt, "From the lightest nuclei to the equation of state of asymmetric nuclear matter with realistic nuclear interactions", *Phys. Rev. C* **90**, 61306 (2014)

[35] D. J. Dean and M. Hjorth-Jensen, "Coupled-cluster approach to nuclear physics", *Phys. Rev. C* **69**, 54320 (2004)

[36] A .Novoselsky and N. Barnea, "Matrix elements of two-body operators between many-body symmetrized hyperspherical states", *Phys. Rev. A* **51**, 2777 (1995)

[37] J. Raynal and J. Revai, "Transformation coefficients in the hyperspherical approach to the three-body problem", *Nuovo Cimento* **A68**, 612 (1970)

[38] N. Barnea, "Exact Solution of the Schrodinger and Faddeev Equations for Few Body Systems", *Ph.D. Thesis*, Hebrew University, 1997

[39] M. Gattobigio, A. Kievsky, M. Viviani and P. Barletta, "Harmonic hyperspherical basis for identical particles without permutational symmetry", *Phys. Rev. A* **79**, 32513 (2009)

[40] M. Gattobigio, A. Kievsky and M. Viviani, "Nonsymmetrized hyperspherical harmonic basis for an A-body system", *Phys. Rev. C* **83**, 24001 (2011)

[41] S. Deflorian, N. Barnea, W. Leidemann and G. Orlandini, "Nonsymmetrized Hyperspherical Harmonics with realistic potentials", *Few-Body Syst.* **55**, 831 (2014)

[42] S. Deflorian, N. Barnea, W. Leidemann and G. Orlandini, "Ab initio calculations with non-symmetrized Hyperspherical Harmonics for realistic NN potential models", *EPJ Web of Conferences* **66**, 2025 (2014)

[43] V. D. Efros, W. Leidemann and G. Orlandini, "Accurate Four-Body Response Function with Full Final State Interaction: Application to Electron Scattering off ^{4}He", *Phys. Rev. Lett.* **78**, 432 (1997)

[44] A. B. Volkov, "Equilibrium deformation calculations of the ground state energies of 1p shell nuclei", *Nuclear Physics* **74**, 33 (1965)

[45] A. Kievsky, Private communication

[46] S. Quaglioni and P. Navrátil, "Ab Initio Many-Body Calculations of n$-^3$H, n$-^4$He, p$-^{3,4}$He, and n$-^{10}$Be Scattering", *Phys. Rev. Lett.* **78**, 432 (1997)